UNIVERSITY OF CALIFORNIA SAN DIEGO

Assembly of a model cheese rind microbiome

A dissertation submitted in partial satisfaction of the requirements for
the degree Doctor of Philosophy

in

Biology

by

Brooke Anderson

Committee in Charge:

Professor Rachel J. Dutton, Chair
Professor Elsa Cleland
Professor Matthew Daugherty
Professor Paul Jensen
Professor Gürol M. Süel

2021

The dissertation of Brooke Anderson is approved, and it is acceptable in quality and form for publication on microfilm and electronically.

University of California San Diego

2021

DEDICATION

To Scott and Candyce Anderson, who I lucked out to be born to and raised by.

EPIGRAPH

Nothing in biology makes sense except in the light of evolution *and ecology*.

–Theodosius Dobzhansky, appendum by Moselio Schaechter

TABLE OF CONTENTS

LIST OF FIGURES

LIST OF SUPPLEMENTAL FIGURES

LIST OF TABLES

ACKNOWLEDGMENTS

Basic biological research was far from my own natural forté when I first entered graduate school. So my development as a capable scientist is thanks almost entirely to a number of influential fellows who took time to engage with my work and give constructive criticism. In particular, I want to thank Dr. Christina Saak, a post-doctorate fellow and now also a friend, who took the time to teach me the nuts and bolts of designing and executing good science. Much of the meat of this dissertation, and my corresponding metal health that came from producing good science, would not have happened without her.

I must also thank my PI and chair of my committee, Dr. Rachel Dutton, for assembling such a wonderful group of colleagues and for supporting me financially and with her time for more than 5 years. While graduate school can often be an emotionally trying time, the security of having such a conscientious and kind work environment to fall back is not taken for granted.

A warm thank you as well to my doctoral committee, for being a set of diverse and fresh voices to give feedback on my scientific progress. Annual meetings often served as transformational moments – almost entirely, in retrospect, in very beneficial ways. Thank you to Drs. Paul Jensen and Matt Daugherty for asking tough questions that I needed to think about, to Dr. Gürol Süel for being a gold mine of relevant information and smart ideas for me to consider, and to Dr. Elsa Cleland for being my advocate both inside and outside of meetings, both scientifically and personally.

Outside of the lab, I was fortunate to develop a previously unfathomable number of close relationships that I relied upon for times of both fun or commiseration. In particular, I want to acknowledge an incredibly accomplished group of female scientists with whom, if I had my way,

I would work alongside and make waves with far into the future. I want to especially thank Dr. Emily Pierce for always continuing to remind me of my value.

I would also like to acknowledge scientific contributions to this dissertation. Chapter 2 consists of unpublished material, currently being prepared for submission for publication. The following individuals are also authors on this work: Julie E. Button (Harvard FAS Center for Systems Biology), Collin Edwards (Tufts), Elizabeth Brown (UCSD), Benjamin E. Wolfe (Tufts), Rachel J. Dutton (UCSD). The dissertation author is the primary author of this manuscript.

Chapter 3 consists of unpublished material. The following individuals are also authors on this work: Cong Dinh (UCSD), Galilea Guererro (UCSC) and Rachel Dutton (UCSD). The dissertation author is the primary author of this material.

Chapter 4 consists of unpublished material. The following individuals are also authors on this work: Section 4.2 - Rachel Dutton (UCSD); Section 4.3 - Jessica Mark-Welch (Marine Biological Laboratory), Rachel Dutton (UCSD). The dissertation author is the primary author of this material.

VITA

Education

University of California San Diego — San Diego, CA
Ph.D. in Biology — 2015-2021
Graduate research in the laboratory of Dr. Rachel Dutton
"Assembly of a model cheese rind microbiome"
Micro-MBA, Rady School of Management

The Ohio State University — Columbus, OH
B.S. with honors research distinction in Biochemistry — 2011-2015
Undergraduate research thesis with Dr. Ana Paula Alonso
"^{13}C labeling of the tricarboxylic acid cycle and carbon conversion efficiency in Lesquerella (*Physaria fendleri*) embryos."
Minor in French Language
cum laude

Publications

Aksenov, Alexander A.,… **Brooke Anderson**,… Pieter C. Dorrestein, and Kirill Veselkov (2021). *Auto-deconvolution and molecular networking of gas chromatography–mass spectrometry data*. Nature Biotechnology 39, 169–173.

Taton, Arnaud,… **Brooke Anderson**,… William H. Gerwick, and James W. Golden (2020). *Heterologous expression of cryptomaldamide in a cyanobacterial host*. ACS Synthetic Biology 9(12), 3364-3376.

Anderson, Brooke (2015). ^{13}C labeling of the tricarboxylic acid cycle and carbon conversion efficiency in Lesquerella (Physaria fendleri) embryos. The Ohio State University. Department of Biochemistry Honors Theses.

[Blog article] **Anderson, Brooke**. "Standing on the Shoulders of a Tiny Giant." *Small Things Considered*. Amer. Soc. Microbiol. 22 Aug. 2016.

Cocuron, Jean-Christophe, **Brooke Anderson**, Alison Boyd, and Ana Paula Alonso (2014). *Targeted Metabolomics of Physaria fendleri, an Industrial Crop Producing Hydroxy Fatty Acids.* Plant and Cell Phys. 55(3), 620-633.

Awards, Honors, and Grants

NSF Graduate Research Fellowship	2017–2020
Cell and Molecular Genetics Training Program Grant	2016
Bertram Thomas Memorial Scholarship	2014
College of Arts and Sciences Undergraduate Research Scholarship	2013, 2014

Teaching Experience

University of California San Diego
San Diego, CA
Instructional Assistant 2016, 2018, 2019
Microbiology Lab, Metabolic Biochemistry, Microbiology Lecture

Research Mentor to Undergraduate Researchers 2017–2020

Piano Studio 2010–2015
Medina, OH | Columbus, OH
Beginning to Advanced Piano Lessons

Activities

Leadership team member of the Biotech Group at UCSD	2021
Content Development Head & Teacher for Science Class program in San Diego Jails	2018–2021
Mentor, UCSD Biology Undergraduate and Master's Mentorship Program.	2020
Admissions committee for Biological Sciences' Ph.D. recruitment	2018, 2020
Guest Lectures and Lab Courses at Coronado High School	2018, 2019
BioEASI volunteer: Fleet Science Center, La Jolla Riford Library, & E3 Civic High	2017–2018
Principle Chair of San Diego Microbiology Group, Seminar Series	2017–2018
Event Organizer for San Diego Microbiology Group Symposium	2017
Organizer of CMG Training Program Symposium	2017
Graduate student chair for Biological Sciences' Ph.D. recruitment	2017
Volunteer for Fleet Science Center, San Diego	2016
Mentor for Women Organization for Research Mentoring in STEM	2016

Select Presentations

American Society for Microbiology Microbe 2020 cancelled
Anderson B, Button JE, Dutton RJ. A Cheese Rind Model for 2020
Microbial Interactions and Their Ecology. Oral presentation accepted.

American Society for Microbiology 8th Conference on Biofilms Washington, D.C.
Anderson B and Dutton RJ. Effect of pH on Microbial Interaction 2018
in a Model Cheese Rind Community. Poster presentation.

Center for Microbiome Innovation's California Microbiome Meeting San Diego, CA
Anderson B and Dutton RJ. Probing the Microbial Structure 2017
of a Cheese Rind Biofilm. Oral presentation.

Cell and Molecular Genetics Training Program Colloquium San Diego, CA
Anderson B and Dutton RJ. Probing the Microbial Structure 2017
of a Cheese Rind Biofilm. Oral presentation.

ASM Mechanisms of Interbacterial Cooperation and Competition Washington, D.C
Anderson B, Mark-Welch J, Dutton RJ. Imaging the Spatiotemporal 2017
Organizatio of the Cheese Rind. Poster presentation.

Denman Undergraduate Research Forum Columbus, OH
Anderson B, Cocuron JC, Alonso AP. Carbon conversion efficiency and ^{13}C 2015
^{13}C labeling of the Tricarboxylic acid cycle in lesquerella (Physaria fendleri) embryos.
1st place poster presentation.

American Society for Plant Biologists Midwestern Conference Columbus, OH
Anderson B, Cocuron JC, Alonso AP. Identifying in vitro culture conditions 2014
for Lesquerella (Physaria fendleri), a promising alternative crop.
Undergraduate poster award.

ABSTRACT OF THE DISSERTATION

Assembly of a model cheese rind microbiome

by

Brooke Anderson

Doctor of Philosophy in Biology

University of California San Diego, 2021

Professor Rachel J. Dutton, Chair

Many aged cheeses consistently develop a bloom of microbes at their surface, called a rind. Proper development of the rind and the underlying cheese's defining characteristics depends on the specific assembly of a community of microbes at the rind. Oftentimes, the assembly process of rind microbiomes as well as other relevant microbiomes is quite dynamic and results in a series of different dominant community members, called a pattern of ecological succession. The specific factors that shape a specific pattern of succession are only superficially understood. While microbial communities serve as useful study models because of their rapid development in comparison to, for example, a forest, the drivers of their successional patterns are primarily studied observationally or theoretically using sequencing datasets. This dissertation explores the drivers

underlying the pattern of succession that occurs during the aging of a natural rind cheese, through both metagenomic investigations of rind microbiome development as well as *in vitro* experimentation using a model community assembled from the cave-aged rind. We first find that the overarching pattern of succession is driven primarily by two fungal species who modulate the pH of the environment or inhibit population size. I further explore the mechanisms underlying these activities and identify potentially novel mechanisms involved in both stimulation and inhibition of community neighbors. We also show how segregated spatial organization of the rind biofilm may explain why the effects of fungal species are stronger than those of bacteria. And finally, we start to consider how bacteriophage might contribute to rind assembly dynamics, by contributing genetic functions or by generating dynamic patterns at the strain level. I conclude these studies with advice on how our findings can be followed up to further explore and identify mechanisms involved in community assembly both of a cheese rind and potentially of other medicinally-, environmentally-, and industrially-relevant microbiomes.

CHAPTER 1. Introduction

1.1 Patterns of community assembly and underlying driving processes

Microbiomes exist in nearly every ecosystem on earth, from relatively quotidian microbial consortia in the soil or in our guts to those associated with extreme environments like deep-sea hydrothermal vents (Dick, 2019; Thompson et al., 2017). Many microbiomes impact the greater ecosystem in which they exist and can be central to ecosystem functioning. After all, cyanobacteria are predicted to be responsible for the Great Oxygenation Event, during which Earth's atmosphere accumulated sufficient oxygen to support respiring organisms like ourselves (Olejarz et al., 2021). Even today, microorganisms living in the ocean and soil are key players in balancing atmospheric and oceanic carbon, nitrogen, and oxygen levels (Bardgett et al., 2008; Fuchsman et al., 2019).

Communities of microbes assemble through a complex set of processes that unfold to create myriad unique ecosystem characteristics. Microbiomes that interact with a host may develop into a form that improves host health through the production of nutrients or vitamins or through protection from disease; alternately, they may take on a form that contributes to a disease state, for example by creating a favorable environment for pathogenic microbes (Akin and Borneman, 1990; Kim and Kim, 2019; Lozupone et al., 2012; Vannier et al., 2019). Since it's of medicinal and environmental interest to support healthy microbiome-containing ecosystems, scientists are devoting considerable effort to understanding how microbial communities assemble.

The dominant processes underlying assembly can be simplified into: 1) dispersal of organisms into the ecosystem, 2) selection by the environment, and 3) interactions with neighboring community members. In many communities, these processes are dynamic and thus result in a temporal progression of dominant species within the environment, called a pattern of succession. Primary ecological succession is a pervasive phenomenon in community assembly that

occurs when a new environment is first colonized by organisms. Microbial communities, commonly assembling on experimentally-friendly time scales, provide a new frontier for studying ecological succession.

Temporal changes occur in diverse microbiomes, such as in newborn and juvenile animal guts (Burns et al., 2016; Koenig et al., 2011) and in fermented foods (Bertuzzi et al., 2018; Ercolini et al., 2013; Spitaels et al., 2014; Wolfe et al., 2014), and over a wide range of time scales from hours in the fermented milk product called kefir (Walsh et al., 2016), days in nectar microbiomes (Herrera et al., 2008; Pozo et al., 2012), a summer's worth of leaf and phyllosphere development on trees (Redford and Fierer, 2009), and over seasons in aquatic microbiomes (Gilbert et al., 2012). Many of these temporal patterns of community assembly have been revealed in detail through sequencing studies that measure relative abundance of all community members at varying taxonomic resolutions. However, due to the observational nature of most sequencing-based studies, we lack an understanding of the drivers underlying these temporal patterns of community assembly.

The microbiome that forms on the surface of an aged cheese, called the rind, is a model for studying patterns of community assembly and its underlying driving processes, including environmental selection and biotic interactions between microbes (Wolfe et al., 2014). For example, a world-wide survey of cheese rind communities and their physicochemical environment found that moisture was the most influential determinant of community composition, even more so than pH or salt (Wolfe et al., 2014). Furthermore, culturing representative rind isolates *in vitro* identified extensive interactions between rind microbes (Wolfe et al., 2014). Remarkably, reproducing a cheese rind community by combining representative isolates on laboratory cheese curd-based agar was able to mimic the pattern of succession that is observed in the rind of the

cave-aged cheese from which the model community was derived (Wolfe et al., 2014). This indicates that the *in vitro* model community incorporates the components driving community assembly and can facilitate investigations of its temporal pattern. Below I present a brief summary of selected factors that are known to contribute to the assembly of a cheese rind microbial community.

Abiotic environment dynamics. Cheese rind microbiomes are known to undergo reproducible patterns of succession, often characterized by an early abundance of yeast species and later abundance of coryneform bacteria and molds (Bertuzzi et al., 2018; Marcellino and Benson, 1992; Petersen et al., 2002; Rea et al., 2007; Wolfe et al., 2014). Abiotic drivers of this succession at the rind have been discussed before (Bertuzzi et al., 2018; McSweeney, 2004; Purko et al., 1951). Fresh cheeses are typically acidic (around pH 5) due to the conversion of lactose into lactate by microbes added to the milk. Upon cave aging, as early-colonizing, acid-tolerant microbes form the nascent rind, lactate is consumed and macromolecular casein proteins are broken down into amino acids, which are further metabolized to release ammonium. Thus as a cheese ages, the pH rises to neutral or even alkaline conditions. So while the acidity of a fresh cheese initially selects for acid-tolerant microbes, the metabolic activity of these early colonizers raises the pH of the environment to allow acid-sensitive species to bloom.

Bacterial-fungal interactions. One valuable feature of many model cheese communities is their inclusion of fungal species. Fungal members of microbiomes are likely to play important roles in shaping complex communities (Abrego et al., 2020; Filion et al., 1999; Xu et al., 2021) and have been recently shown to have the potential to influence community succession patterns (Rao et al., 2021). Fungi are frequently identified members of animal- and plant-associated microbiomes, and much attention has focused on mitigating the fungi in those systems that act as

pathogens. However, fungi are known to play far more complex roles in terrestrial biological communities, including acting as mediators of nutrient transfer from plants or detritus to soil microbes (Gorka et al., 2019; Kaiser et al., 2015; Kramer et al., 2016). More recently, studies have revealed a diversity of mechanisms by which fungi can affect the growth of neighboring bacterial species in the cheese rind environment, including cell dispersal along fungal filaments (Zhang et al., 2018), amino acid cross-feeding (Morin et al., 2018; Pierce et al., 2021), siderophore sharing that aids in iron acquisition (Kastman et al., 2016; Pierce et al., 2021), growth-impacting volatile emissions (Cosetta et al., 2020), and antibiotic production (Morin et al., 2018; Pierce et al., 2021).

Bacteriophage. Viruses that infect bacteria, called bacteriophage, are a ubiquitous and integral component of microbiomes. Through their various reproductive cycles, bacteriophage are capable of shaping microbial community composition and function. Viral predation leading to cell lysis selects for bacterial populations that encode resistance mechanisms or for cells with immunity through super-infection (Hampton et al., 2020; Knowles et al., 2016). This understanding of lytic selection has paved the way for phage therapy treatments of pathogenic bacterial infection (Gurney et al., 2020; Kortright et al., 2019). Phage infection can also interfere with host gene sequence or gene expression, resulting in metabolic reprogramming of cells that may additionally affect the surrounding ecosystem (De Smet et al., 2016; Feiner et al., 2015; Hendrix et al., 2019; Howard-Varona et al., 2020). Finally, temperate phage are often vectors for horizontal gene transfer, enabling the spread of diverse functional genes among infected bacteria (Labrie and Moineau, 2007; Menouni et al., 2015; Zeidner et al., 2005).

While phage are found to be part of cheese rind microbial communities (Dugat-Bony et al., 2020; de Melo et al., 2020), their diversity and dynamics in this environment have yet to be studied. Fundamentally, how phage integrate into the process of community assembly, including both their

maintenance in a community by hosts as well as their role in the selection for certain microbial strains over others, is still an open question in microbiology. This question is well suited for the cheese rind microbiome system, combining characterization work to identify the distribution of phage and their hosts in native, cave-aged cheese rinds as well as experimental work in *in vitro* models to identify and predict host outcomes when challenged with phages.

A model system for studying community assembly. The following dissertation continues with the previously introduced cheese rind from which an *in vitro* model was built to mimic its pattern of succession (Wolfe et al., 2014). The cave-aged cheese is made in the natural rind style, meaning that no microbes were introduced to the rind for maturation and the cheese is left mostly undisturbed over its aging process. The model community derived from this cheese consists of seven microbes: four bacteria and three fungi. Much of the *in vitro* experimentation using this and other model cheese rind communities has considered how interactions unfold at single time points, with minimal exploration into how interactions contribute to temporal patterns in a community. This particular model community provides a system in which to dissect the factors that drive patterns and processes underlying the assembly of a mixed-species community.

CHAPTER 2. Fungi play prominent roles in ecological succession of a model cheese rind microbiome

2.1 Chapter Summary

Our lab previously developed a tractable model microbial community that demonstrates a pattern of succession mimicking the native microbiome on which it is modeled (Wolfe et al., 2014). Presumably, this means that the key drivers of this pattern of succession are also modeled in this *in vitro* system, and so we set out to identify these drivers. We first assessed the contribution of interactions between community members to the characteristic features of succession. From there, we broke down the complete community into its simplest interacting parts. Pairwise co-culturing identified a large number of strong interactions, where a neighboring community member altered the growth of another species. Thirdly, we reconstructed the community and strategically removed impactful neighbors to assess their importance to shaping succession in the community context. We found that two fungal species in particular drive the characteristic pattern of succession and can hypothesize their mechanisms of interaction within the community. Lastly, we used a modeling approach, incorporating pairwise co-cultures, that quantitatively highlights how useful our reconstruction approach is when considering how pairwise interactions behave in a community context; while pairwise interactions can reveal the scope of possible interactions between microbes in a community, as a whole they were shown to be poor predictors of community composition.

2.2 Deconstructing and reconstructing interactions in an *in vitro* model cheese rind community

Introduction

In Chapter 1, I introduced the concept of succession, a temporal community assembly phenomenon characterized by a series of different microbes dominating a microbial community. There are likely many interacting factors underlying the succession of microbiomes, including both stochastic and deterministic processes. Stochastic processes, including random fluctuations in dispersal, growth, and death can contribute to temporal community dynamics (Brislawn et al., 2019; Liu et al., 2020; Vass et al., 2020). These processes lead to ecological drift, wherein the culmination of small random changes can drive unpredictable shifts in community composition. However, many studies find that communities show highly reproducible assembly patterns, suggesting that deterministic interactions between species and the environment as well as interactions directly between species are likely to play an important role in shaping community composition (Brislawn et al., 2019; Jackrel et al., 2020; Mönnich et al., 2020). For example, the composition of a flower's nectar microbiome, affecting pollination success, is dependent on the first microbes deposited by flower visitors (Morris et al., 2020; Toju et al., 2018). These early microbial colonizers alter nectar biochemistry and compete with microbes that disperse into the nectar later on (Tucker and Fukami, 2014).

Further investigation of what drives temporal patterns of microbiome assembly is important in order to better predict, manipulate, or completely engineer microbiomes towards desirable outcomes. It is often hard to measure the contributions of microbial interactions to succession because microbiomes that exhibit such temporal dynamics are difficult to model and manipulate *in vivo* (Cadotte et al., 2005). Cheese rind microbiomes are a model for studying microbial interactions in a realistic *in vitro* ecosystem, and work in these systems has uncovered extensive interactions between species (Wolfe et al., 2014). The reproduction of these microbiomes *in vitro* has allowed for the study of interactions at different scales, from pairwise to

more complex communities, and thus has enabled the identification of important interaction mechanisms including amino acid crossfeeding and iron acquisition (Kastman et al., 2016; Morin et al., 2018; Pierce et al., 2021). Moreover, these studies have consistently revealed that fungi play a large role in species interactions and shaping community structure.

Cheese rind microbiomes have been shown to undergo reproducible patterns of succession (Bertuzzi et al., 2018; Marcellino and Benson, 1992; Petersen et al., 2002; Rea et al., 2007; Wolfe et al., 2014). Previous work with a seven-member model community from the rind of a cave-aged cheese found that, remarkably, the *in vitro* community exhibited a reproducible pattern of succession that mimics the ecological succession observed in the native rind of the cave-aged cheese from which the community was isolated (Wolfe et al., 2014). Much of the *in vitro* experimentation using this and other model cheese rind communities has considered how interactions unfold at single time points, with minimal exploration into how interactions contribute to temporal patterns in a community. This model community provides a system in which to dissect the factors that drive succession of a mixed-species community.

In this study, we systematically deconstruct and reconstruct a model rind community, assessing the growth of individuals or pairs of microbes or more complex communities, to identify the scope and role of interactions occurring in the community. In doing so, we are able to show how both growth-stimulating and -inhibiting effects from a subset of species contribute dramatically to the temporal dynamics of the complete community. In particular, we find that two fungal members are dominant drivers of succession, emphasizing the importance of giving more consideration to fungi in microbiome studies. Lastly, we use a modeling approach to quantify how well pairwise interactions can predict the community composition and find that interactions not

accounted for by pairwise interactions alone contribute to community formation. This highlights the necessity of studying microbial interactions in the context of more complex ecosystems.

Results

Ecological succession is shaped by microbial interactions. A seven-member model community was previously isolated from the rind of a cave-aged, natural-rind cheese (Wolfe et al. 2014). This model consists of representatives of the dominant (>1% abundance) bacterial and fungal genera found in the rind. Of the four total bacterial representatives, two are of the genus *Staphylococcus* (*S. xylosus* and *S. equorum*) and two are of the phylum Actinobacteria (*Brevibacterium* and *Brachybacterium*). Of the three total fungal representatives, two are filamentous fungi (*Penicillium* and *Scopulariopsis*) and one is a yeast (*Diutina catenulata*, formerly classified as *Candida catenulata*).

The model community, inoculated all together in equal starting proportions on cheese curd-based agar media (CCA), exhibits a reproducible pattern of succession that mimics the ecological succession observed in the native rind of the cave-aged cheese from which the community was isolated (Wolfe et al., 2014). The model community's dynamics are also consistent with the reproducible pattern of succession previously reported using a nearly identical *in vitro* community model in (Wolfe et al., 2014). This pattern of succession is characterized by two phases: the first phase is dominated by early colonizing species (both *Staphylococcus* bacteria and the yeast *Diutina*) which reach their maximum population size in the first three days of growth, then the second phase includes membership by the late colonizing species (the Actinobacteria and the filamentous fungi) which become significant or majority members of the community between 3 and 21 days of growth (Figure 1A, C, "community"). The growth dynamics underlying this pattern of succession in the community includes a decline in viable cell counts of the early colonizers after

they reach their maximum population size, and the slow growth of the late colonizers, who continue to grow or maintain their population by 21 days.

The pattern of succession observed could either be due to differences in the intrinsic growth rates of individual species populations, or the specific pattern could arise from interactions between species. Here we are defining interactions as changes in viable cell counts resulting from the presence of other community members. To determine the importance of intrinsic growth rates versus microbial interactions in shaping the characteristic pattern of succession during community assembly, we compared the pattern of succession of the in vitro community to the expected pattern of succession if there were no microbial interactions altering species growth in the community, based on growth in isolation. The interaction-free succession was estimated by adding up the viable cell counts of each species grown as a monoculture, then calculating the relative abundance of each bacteria and fungus for each harvest time point. Our comparison revealed that interactions contributed significantly to key features of the pattern of succession based on PERMANOVA (pseudo-$F_{1,23} = 25.973$, $p < 0.01$). Without microbial interactions, the second phase of succession would be markedly different: the late-colonizing bacteria would not become abundant members and early-colonizing *Diutina* and *Staphylococcus* species, plus *Scopulariopsis*, would remain more abundant than what is observed in the community (Figure 1C). Microbial interactions thus significantly contribute to the characteristic two-phased pattern of succession in the community.

Community interactions impose both net stimulatory and inhibitory effects. To assess the scale at which community growth dynamics are affected by interactions, we compared the number of colony forming units (CFUs) of each species grown in monoculture to their number in the community. The community impacts the growth of each species at nearly every time point measured (Figure 1B, D). Presence of a community alters the growth of each species differently,

resulting in diverse interaction phenotypes that vary in direction, magnitude, and temporal dynamics. The changes in viable cell counts when grown in the community versus in monoculture can be over 10,000-fold. Overall, two species exclusively exhibit growth stimulation by the community (viable cell counts at any given time point are higher when grown with the community than at the same time point when grown as a monoculture), 4 species exhibit only growth inhibition by the community (viable cell counts at any given time point are lower when grown with the community than at the same time when grown as a monoculture), and a single species exhibits both net stimulation and inhibition at different stages of community assembly.

The species that are most dramatically stimulated by the community are the late-colonizing bacteria, *Brevibacterium* and *Brachybacterium*. While neither of these species grow particularly well, if at all, in monoculture on cheese curd agar, in the community *Brachybacterium* is stimulated to high cell counts by 21 days and *Brevibacterium* reaches peak cell counts much earlier, around day 10 (Figure 1A). Dynamics of inhibition are extremely variable; even the most closely related community members (two *Staphylococcus* species) show different changes in dynamics in the presence of the community. The population size of *S. xylosus* is significantly inhibited at all time points. *S. equorum*, on the other hand, is initially stimulated to a higher cell count in the community condition compared to alone (Figure 1A, B). However, the community then imposes an inhibitory effect on *S. equorum*, as by day 21 the viable cell count significantly declines by a factor of five. This results in a smaller population size in the community as compared to monoculture.

While the growth of all three fungal species (measured as viable spore formation for filamentous fungi) is reduced in the community as compared to monoculture, *Penicillium* is impacted the least, with the community having no net effect on spore count by day 21 (Figure 1B). In contrast, *Scopulariopsis* has a much slower rate of growth due to sustained inhibition of

sporulation throughout community development, with viable spore counts reduced by 5- to nearly 900-fold over time. Most notably among inhibitory interactions in the community, *Diutina* exhibits a particularly dramatic decline in viable cell counts after three days of growth in the community, but maintains its carrying capacity in monoculture (Figure 1A). This implies that the community kills off *Diutina*, either directly (i.e. antibiotic production) or indirectly (modulation of the environment).

Many positive & negative interactions among pairwise co-cultures, and a subset of community members are particularly strong interactors. Given the differences between growth patterns in the community versus alone, we next aimed to identify the underlying interactions. We grew co-cultures of all pairwise combinations of the seven species and calculated the fold-change of population size in co-culture to population size in monoculture at the same time points (Figure 2). In 19/21 co-cultures, at least one interacting partner affected the growth dynamics of the other, and from the 42 total species growth curves obtained in these pairwise co-culture experiments, 27 showed growth dynamics that were significantly different from alone (from Wilcoxon Rank-Sum test of pairwise co-culture versus monoculture for each time point, for at least one time point a test $p < 0.05$; see Methods for more on interpreting our statistical tests). There are equal numbers of stimulatory and inhibitory interactions: out of those 27 cases where one species significantly affected the population size of the other, 13 were stimulatory and 13 were inhibitory, as measured by a significant change in total colony-forming units alone versus with the partner (Wilcoxon rank-sum test, considered significant if test $p < 0.05$). Only one interaction was mixed, where a species' population size was either stimulated or inhibited by its partner depending on the time point measured.

The complete set of pairwise interactions reveal fungi to be prolific interactors. Among the 28 interactions that are significantly stimulatory (where each measured time point is considered an individual interaction), 18 scenarios were a fungus stimulating another species (Figure 2B, top). Similarly for the 20 total interaction phenotypes demonstrating significant inhibition of population size, 15 scenarios were a fungus inhibiting growth of another species (Figure 2B, bottom).

While the network plots in Figure 2A might suggest that interactions tend to get stronger over time, it should be noted that interpretation of these results sometimes shows the net effect of a pairwise interaction over time; for example, since *Brachybacterium* does not grow at in monoculture, even small additions to population size between days 10 to 21 will appear as a bigger fold-change at day 21 compared to day 10. In contrast, when assessing how growth rates change between pairwise co-cultures and monocultures, the magnitude of growth effects tended to be strongest between days 0-3. Only for *Penicillium* is the magnitude of its effects on partner species growth maximized later in succession, between days 10-21 (Suppl. Fig. 3). It should be noted that, due to the uncertain relationship between fungal vegetative cell growth and sporulation, growth rates of filamentous fungi (measured here by spore production) were not included in this analysis.

The three fungi together with the bacterium *S. xylosus* are the community members that most frequently affect the population size of other species (Suppl. Fig. 1). The majority of interactions in which *Diutina*, *Scopulariopsis*, or *S. xylosus* have a strong significant effect are stimulatory. In contrast, nearly all interactions with *Penicillium* as a partner are inhibitory. In fact, *Penicillium* inhibits five out of six fellow community members. Only *Brachybacterium* is uninhibited, and instead is variably stimulated by *Penicillium* (Suppl. Fig. 2).

Stimulation is predominantly driven by deacidification. Among all stimulatory pairwise interactions, *Brevibacterium* and *Brachybacterium* are the most frequently and strongly affected

by growth with a partner. Interestingly, both *Brevibacterium* and *Brachybacterium* are stimulated by the same three species: *Diutina*, *S. xylosus*, and *Scopulariopsis* (Figure 2C, Figure 2A top). The stimulation of these Actinobacteria is extreme: *Diutina* can stimulate *Brevibacterium* growth rate up to 140,000-fold, and *Brachybacterium* growth 19-million-fold. To a lesser but still significant extent, *S. equorum* is also stimulated by *Diutina* and *Scopulariopsis* (up to 10-fold increase in viable cell counts), but not by the other *Staphylococcus* species.

The stimulation of *Brevibacterium*, *Brachybacterium*, and *S. equorum* by these species is correlated with these partners' activity towards deacidifying the cheese medium (Suppl. Fig. 4). pH is known to be an important selective force in cheese rind aging (McSweeney, 2004). Fresh cheeses are typically acidic (around pH 5) due to the conversion of lactose into lactate by microbes in or added to the milk (Bintsis, 2018; Fox et al., 1990). Upon cave aging, as early-colonizing, acid-tolerant microbes form the nascent rind, lactate is consumed and macromolecular casein proteins are broken down into amino acids, which are further metabolized to release ammonium (Bonaïti et al., 2004; Fox and Wallace, 1997; Karahadian and Lindsay, 1987). Thus, as a cheese ages, the pH rises to neutral or even alkaline conditions. So while the acidity of a fresh cheese initially selects for acid-tolerant microbes, the metabolic activity of these early colonizers raises the pH of the environment to allow acid-sensitive species to bloom.

Early-colonizing cheese yeasts have been found previously to deacidify media and correspondingly stimulate growth of Actinobacteria like *Brevibacterium* (Mounier et al., 2008; Purko et al., 1951). In line with these earlier findings, the Actinobacteria in our model community exhibit slow or no growth in monoculture on CCA at pH 5, but both grow rapidly on CCA adjusted to pH 7, confirming that they are both sensitive to the acidic conditions of fresh cheese (Figure 3A). pH dynamics of pairwise co-cultures show further correlation between medium

deacidification Actinobacterial stimulation. These pairwise co-culture show that not only the yeast *Diutina* but also the bacterial early colonizer *S. xylosus* as well as the late-colonizing filamentous fungus *Scopulariopsis* are able to deacidify the media and stimulate growth of acid-sensitive species. *Penicillium* also deacidifies the media but does not result in stimulation of these Actinobacteria, suggesting that additional inhibitory mechanisms are in effect. Consistent with the observations of stimulatory interactions being related to acid sensitivity, these same pairwise co-cultures at pH7 showed a dramatic reduction in stimulatory interactions (Figure 2B).

To investigate the role of each of the early-colonizing deacidifying species (*Diutina* and *S. xylosus*) in stimulating the acid-sensitive Actinobacteria, we repeated the community growth experiments (a) without *Diutina*, (b) without *S. xylosus*, and (c) without either. Overall, exclusion of the yeast *Diutina* had a much more dramatic effect than exclusion of just *S. xylosus* (Figure 3B). Exclusion of *Diutina* reduced the population size of Actinobacteria through day 10, correlating with reduced deacidification in the early community. However, both the pH and Actinobacterial colony counts reached the same as in the complete community by day 21, suggesting that other community members may have compensated for the stimulatory role of *Diutina* by the end of the experiment. In contrast, excluding *S. xylosus* from the community either had no effect or slightly increased Actinobacterial growth, suggesting that the stimulatory role indicated by pairwise co-cultures is completely compensated by others in a community throughout the experiment.

Excluding both *Diutina* and *S. xylosus* from the community had longer-lasting effects, especially for *Brevibacterium* which exhibited thousand-fold decrease in viable cell counts in the modified community when compared to the complete community, even at day 21 (Figure 3B). The apparent compensation in the single-species dropout communities compared to the far more dramatic change in the double-dropout community suggests that *Diutina* and *S. xylosus* may have

partially redundant roles in stimulating late colonizing Actinobacteria. The difference in pH between a community excluding *Diutina* versus a community excluding both early deacidifiers is not significant at any time point ($p > 0.05$), suggesting either that timing of deacidification matters or that mechanisms other than acidity prevent *Brevibacterium* from reaching a larger population size in the double drop-out community. Altogether, results from pairwise co-cultures and these drop-out communities indicate that deacidification early in succession is the dominant mechanism for stimulating late colonizers in the community.

pH-independent processes are predominantly inhibitory and reflect numerous pairwise interactions. In contrast to stimulatory interactions, of which were largely eliminated at pH 7, most of the strongest (10-fold or more decrease in co-culture compared to alone) inhibitory pairwise interactions at pH 5 are also strongly inhibitory at pH 7 (Table 1). *Penicillium* was revealed to be a strong and prolific growth inhibitor in pairwise co-cultures at both pH 5 and pH 7, and complete community effects on species growth frequently mimics the growth seen in these co-cultures (Figure 2A, Figure 2B bottom). The inhibitory effects can be even more clearly seen in the double dropout community that lacks stimulation by early deacidifiers *Diutina* and *S. xylosus*: in this condition, both *Scopulariopsis* and *Brevibacterium* may be inhibited in a way that is similar to when grown in pairwise co-culture with *Penicillium* (Figure 3B & Suppl. Fig. 5).

To assess whether inhibition by *Penicillium* was contributing to growth suppression in the complete community, model communities were grown with or without *Penicillium*. Each other member grew significantly better when *Penicillium* was left out of the community, particularly at day 10, with a range of 1.5- to 15-fold increases in growth as compared to when grown in the complete 7-member community that includes *Penicillium* (Figure 3B, Suppl. Fig. 6).

Together, deacidification by early colonizers and inhibition by *Penicillium* constitute dramatic growth effects in shaping community assembly. To assess whether any additional growth effects, unrelated to these dominant drivers, occur in the community, a model community without *Penicillium* was inoculated on pH 7 medium. In contrast to the community effects seen in Figure 1D, where the complete community at pH 5 imposed strong inhibitory or stimulatory effects on constituent members, the *Penicillium* drop-out community at pH 7 resulted in non-significant and relatively minor effects on member growth (<10-fold change compared to monoculture growth at pH 7) (Figure 3C). Overall, many members growing in this community grew more similarly to their monoculture growth at pH 7, consistent with our findings from pairwise co-cultures that deacidification dynamics and inhibition by *Penicillium* are the dominant drivers of community succession. While not quantitatively significant, this pH 7 *Penicillium* dropout experiment still revealed changes in CFUs that were up to 10-fold higher or lower than in monocultures. Qualitatively, these remaining interactions may reflect more subtle but still significant growth effects that occurred in pairwise co-cultures at pH 5 or pH 7: for example, numerous small interactions stimulating *Brachybacterium* in late community growth, and inhibition of *S. equorum* by *S. xylosus* (Figures 2A, 2B).

Discussion

Our foundational understanding of the processes that drive succession has been almost exclusively laid down by macroecologists studying forest and field plant communities (Chapin et al., 1994; Cooper, 1923). Such studies have highlighted the importance of environmental factors driving community changes: selection for a set of organisms who modify the environment which then selects for a new set of organisms. Microbiologists pursuing drivers of microbial community succession have often worked off of this idea of succession being driven by environmental

remodeling and selection. For example, (Enke et al., 2019) reframes this in terms of assembly modules, where primary specialist degraders produce nutrients that can be metabolized by secondary generalists.

By breaking down the model community in this study, we also identify that environmental modulation in the form of deacidification to be a critical mechanism for stimulating late-colonizing, acid-sensitive Actinobacteria. Abiotic drivers of cheese rind succession – including deacidification of the rind through consumption of lactate and amino acid breakdown – have been reported previously (Bertuzzi et al., 2018; McSweeney, 2004; Purko et al., 1951). While the yeast *Diutina* predominantly serves in this role as an early deacidifier, other species are capable of slower deacidification and stimulation of Actinobacteria; therefore, community succession is slowed down but not completely derailed by even the most significantly stimulating community member. While this supports the theory that deacidification is the predominant driver of stimulation in the community, interestingly, a double drop-out community lacking early colonizers revealed a conditionally important role for *S. xylosus* in stimulating *Brevibacterium* that is unrelated to deacidification.

The additional important driver of succession that we identified is inhibition by a late colonizer. Despite extensive pairwise interactions among community members, a late colonizing *Penicillium* fungus was found to be the most impactful driver of the second phase of succession. The *Penicillium* strain used in this model community is a prolific inhibitor, and community growth effects on *Staphylococci* and fungal members qualitatively reflect the inhibitory effects seen with *Penicillium* in pairwise co-cultures. The dominance of *Penicillium* inhibitory interactions over the pairwise growth effects of other community partners makes sense whether this inhibition is caused by nutrient limitation or antibiosis.

By deconstructing the model cheese rind community to survey the scope of interaction phenotypes, we have learned fundamental principles that allow us to better predict its assembly dynamics. For example, filamentous fungal species take a number of days to start spore production, which is particularly notable since sporulation is often correlated with secondary metabolite production (Calvo et al., 2002; Kosalková et al., 2009). This delay allows species that are sensitive to fungal antibiotics a chance to grow up in early community formation. Such a feature is particularly important in this cheese rind community, where *Diutina* plays an outsized role in stimulating late colonizing bacteria before it is killed off by *Penicillium*. Early arrival of *Penicillium*, which additionally inhibits the growth of most other community members, could impair characteristic microbiome succession. This potential example of priority effects is worth exploring, if experimental difficulties regarding sequential inoculation of microbial species to an established solid-surface biofilm could be addressed.

While microbial interactions are often portrayed as intrinsically stimulatory or inhibitory, the reality is that interaction phenotypes can be extremely variable depending on ecosystem parameters such as nutrient availability or strain ratio (Gao et al., 2021; Hoek et al., 2016; Pacheco et al., 2019). Further, myriad interaction mechanisms can occur simultaneously between two species, but our growth assays only report the net outcome of various mechanisms of interaction. In the case of *Penicillium* interacting with *Brevibacterium*, variability in growth dynamics between replicate cultures seems to indicate a knife's-edge balance between negative and positive interactions. When cultured with *Penicillium*, *Brevibacterium* either may be killed off or may recover, as seen in Suppl. Fig. 5. We can trace this to pairwise co-culture phenotypes, where *Penicillium* may or may not stimulate the growth of *Brachybacterium* depending on the replicate (Suppl. Fig. 2). These net growth phenotypes seem to reflect the deacidification potential of

Penicillium coupled with its inhibitory capacity, where stimulation often wins out for *Brachybacterium* but inhibition wins out in interactions with *Brevibacterium*. Fungi have been found to interact with bacteria through multiple mechanisms of interaction that can be either positive or negative (Pierce et al., 2021). The extensive range of growth phenotypes that we observe here is telling of how much more there is to learn about the parameters that determine the ultimate impact of fungi on neighboring species.

Our community reconstruction approach is a useful complement to pairwise growth assays by highlighting how pairwise interactions frequently fail to predict community growth phenotypes. The two-phase assembly dynamics of this community are largely determined by two fungi: a yeast that stimulates late-colonizing bacteria through environmental deacidification and a filamentous fungus that imposes potent inhibition later in community development. Fungi have previously been found to serve as impactful chemical engineers of their environment (Akin and Borneman, 1990; Dutton and Evans, 1996; Whiteside et al., 2019; Worrich et al., 2017) and their dominant role here in driving succession underlines the importance of addressing the role of fungal members in other microbiomes, such as the human gut (Rao et al., 2021). The specific inter-microbial phenotypes we demonstrated may be relevant not just to solid fermented foods like cheese rinds or aged meats (Capouya et al., 2020; Dordet-Frisoni et al., 2007); skin is another acidic, protein-rich, and solid-substrate environment, where *Brevibacterium*, *Staphylococcus*, *Diutina*, and other genera also found in cheese rinds may coexist and interact (Grice and Segre, 2011; Ming et al., 2019). Filamentous fungi closely related to those in this model are also relevant as human or plant pathogens (Cuenca-Estrella et al., 2003; Luciano-Rosario et al., 2020). Further investigation into the mechanisms of interaction between members of the cheese rind experimental model system

may elucidate more widely-applicable processes underlying microbial interactions and microbiome formation.

Methods

Media preparation. Cheese curd agar (CCA) medium was prepared as previously described (Cosetta and Wolfe, 2020), except pH of the medium was adjusted before autoclaving. For preparation of CCA at pH 5, pH was adjusted with a hydrochloric acid solution. For CCA at pH 7, the medium was adjusted using a sodium hydroxide solution.

For counting colonies in petri dishes, plate count agar with milk powder and salt (PCAMS) was prepared as previously described (Cosetta and Wolfe, 2020). Fungal species were selected for by supplementing PCAMS with chloramphenicol at a final concentration of 20 ng/mL. Bacterial species were selected for by supplementing PCAMS with cycloheximide after autoclaving for a final concentration of 200 ng/mL. All plates were stored at 4 degC in dark.

Strain selection and preparation. All bacterial and fungal strains were isolated from a natural rind cheese as described previously (Wolfe et al., 2014). Representative isolates of each abundant bacterial and fungal genera (>1%) were selected for the *in vitro* model. Since there were regularly at least two clearly distinguishable species of *Staphylococcus* isolated from different batches of this natural rind cheese, isolates of the two most commonly present species, *S. equorum* and *S. xylosus*, were selected.

In preparation for culturing, each bacterial and yeast strain was precultured to late log phase in liquid LB medium, shaking. Cells were pelleted, washed with PBS supplemented with 20% glycerol, then resuspended in fresh PBS-20% glycerol. Filamentous fungal isolates were streaked on CCA medium and grown in the dark at 15 degC for 7 days. Spore mats were scraped up using PBS-20% glycerol. All cell stocks were distributed into aliquots and stored at -80 degC. To

quantify cell stocks, aliquots frozen for at least 24 hours were thawed, serially diluted, and plated on PCAMS medium to measure colony-forming units per milliliter of strain stock.

In vitro culturing. Strain stocks with quantified densities were thawed and serially diluted to 200 CFUs per 1 uL. For each culture inoculum, 1 uL of each required diluted strain was added to a master mix then PBS was added to bring the final volume of each inoculum to 10 uL. 96-well plates of CCA were inoculated using 10 uL of master mix. For a single replicate, 3 separate wells were each inoculated with 10 uL of the same master mix for harvest after 3, 10, and 21 days. 10 uL of master mix was mixed with 190 uL PBS, and 100 uL was plated on both PCAMS-cycloheximide and PCAMS-chloramphenicol and then stored at 23 degC in the dark to for "day zero" quantification of each species in a master mix. Once day zero plates were grown and counted, day zero CFUs for each species were multiplied by two to account for the plating dilution.

Inoculated 96-well plates were left at room temperature in a dark closet overnight so that inocula dried completely. The following day (day 1), plates were covered with a sterile [Aeraseal film] (to maintain moisture and reduce inter-well contamination) and then plates without their lid were placed inside a plastic bag made humid with a damp towel. On day 2, the humid bag containing plates was transferred to a 15˚C incubator. Coplating effects have been observed where volatiles from some species, trapped in the humid bag, can affect the growth of others. To avoid this, *Penicillium* was never inoculated in the same plate with *Brevibacterium* or *Brachybacterium* unless as part of a community.

Destructive sampling of biofilms to monitor species abundance was performed on days 3, 10, and 21 after inoculation. Aeraseal film over samples to be harvested was aseptically cut and removed. A sterile toothpick was used to remove each biofilm along with its medium and then each sample was homogenized in 1 mL PBS using a microtube pestle. Resuspended samples were

serially diluted in PBS and then plated on either nonselective PCAMS or on two selective PCAMS, supplemented with either cycloheximide or chloramphenicol, if the sample contained a mix of both bacteria and fungi. Plates were grown in the dark in a 23 degC incubator for 3 days and then moved to a benchtop exposed to light so that *Brevibacterium* and *Brachybacterium* could develop distinguishing pigmentation. Colonies of each species were counted once all species were grown enough to be distinguished, and CFUs per sample were back-calculated using the dilution factor and the ratio of resuspended sample volume to plating volume.

Measuring pH of in vitro cultures. Pairwise co-cultures were sampled destructively as detailed before. For the pairwise coculturing experiment, the relative pH of each sample, homogenized in PBS, was measured using a MI-410 pH probe (Microelectrodes, Inc.). To assess the pH trend over time for each culture, the pH of an uninoculated agar well was homogenized in PBS and measured and then each resuspended sample pH was subtracted for "ΔpH" as shown in Supplemental Figure 4. For a direct measurement of sample pH in the community reconstruction culturing experiment shown in Figure 3B, pH was measured prior to harvest and homogenization of samples, as follows: the pH probe was sterilized with 70% ethanol, then the bulb of the probe was just submerged under the surface of the biofilm, approximately 1 mm deep, for sample pH measurement. Statistical comparisons of replicate community pH values displayed in Figure 3B were performed at each time point using ANOVA with post-hoc analysis by Tukey's Honest Significant Difference method, both tests run using the R 'stats' package (version 3.6.3).

Analysis of culture data. All analysis was performed using R version 3.6.3 (2010). For each culture, replicate experiments were clustered by constituent species and time point. Much of the data followed non-normal sampling distributions. As such, the non-parametric Wilcoxon Rank-Sums test (also known as the Mann–Whitney U test) as implemented in the R 'stats' package was

used to compare population sizes of species grown in different culture conditions at the same time point or in the same culture condition but at different time points. Samples were considered significantly different when the test $p < 0.05$. We note that such statistical tests are meant to be exploratory, and given the number of comparisons it is not reasonable to account for concerns of multiple testing. Our goal with this analysis is to identify potential trends, rather than strict hypothesis testing (for nuanced discussion of exploration versus hypothesis testing, see (Tredennick et al., 2021)). However, as a simple heuristic, we make 6 tests per co-culture, meaning that for a threshold of $p < 0.05$, we expect about a 25% chance of one or more false positives per co-culture, and so we might expect 5 or 6 co-cultures to present one or more false positive interactions; this is far less than the 19 co-cultures that show interactions.

Dropout communities on CCA pH 5 were performed in an experiment separate from pairwise co-cultures. The population size of each species in these communities was compared using Kruskal Wallis tests at each time point, as implemented in the R 'stats' package. For tests that reject the null hypothesis that population sizes at a time point were equivalent across the communities structures tested, post-hoc analysis was performed using Dunn's Test as implemented in the R package 'dunn.test' v. 1.3.5 (Dinno, 2015), with correction for multiple comparisons using the Benamini-Hochberg adjustment.

Species data for each time point in each culture was summarized using median CFUs. Relative abundance of species grown in a community was summarized as the median of relative abundances within an experimental replicate. Fold-change in population size was calculated by taking the median of ratios taken between two conditions that were part of the same experimental replicate. Growth rates were calculated assuming exponential growth between two adjacent time points within a replicate. Networks of pairwise effects, with edges scaled by median fold-change

in population size between pairwise co-culture and monoculture (transformed for edge width by formula $2*\log_{10}$(fold-change)), were constructed in Cytoscape (Shannon et al., 2003). Data to reproduce these networks is available on github. The full reproducible code is available on Github at https://github.com/DuttonLab/Anderson_et_al_Succession.

Figures

Figure 2.2-1. Community- versus alone-growth patterns.
(A) Experimental schematic demonstrating monocultures and complete community cultures, with each circle representing a well in a 96-well plate. 200 CFUs of each species were inoculated in triplicate either alone or, for the community, in equal proportions. After 3, 10, and 21 days, one replicate well was harvested. Experiment was repeated for n = 5. (B) Growth dynamics of each community member grown as monocultures or in the complete community. Points represent replicate measurements and the lines connect median values for each time point. (C) Median relative abundance of all seven Bayley members grown together in vitro (left) or of the interaction-free community predicted from summing monoculture data (right). (D) Fold-change in growth of each species in the community versus as monoculture for each collected time point. Fold-change of *Diutina* at day 21 is negative infinity due to division by zero, and is marked by a non-finite bar. Asterisks denote significance according to Wilcoxon rank-sum tests comparing community to alone CFUs of each species at each time point (* $p < 0.05$; ** $p < 0.01$; *** $p < 0.001$; n = 4 - 5).

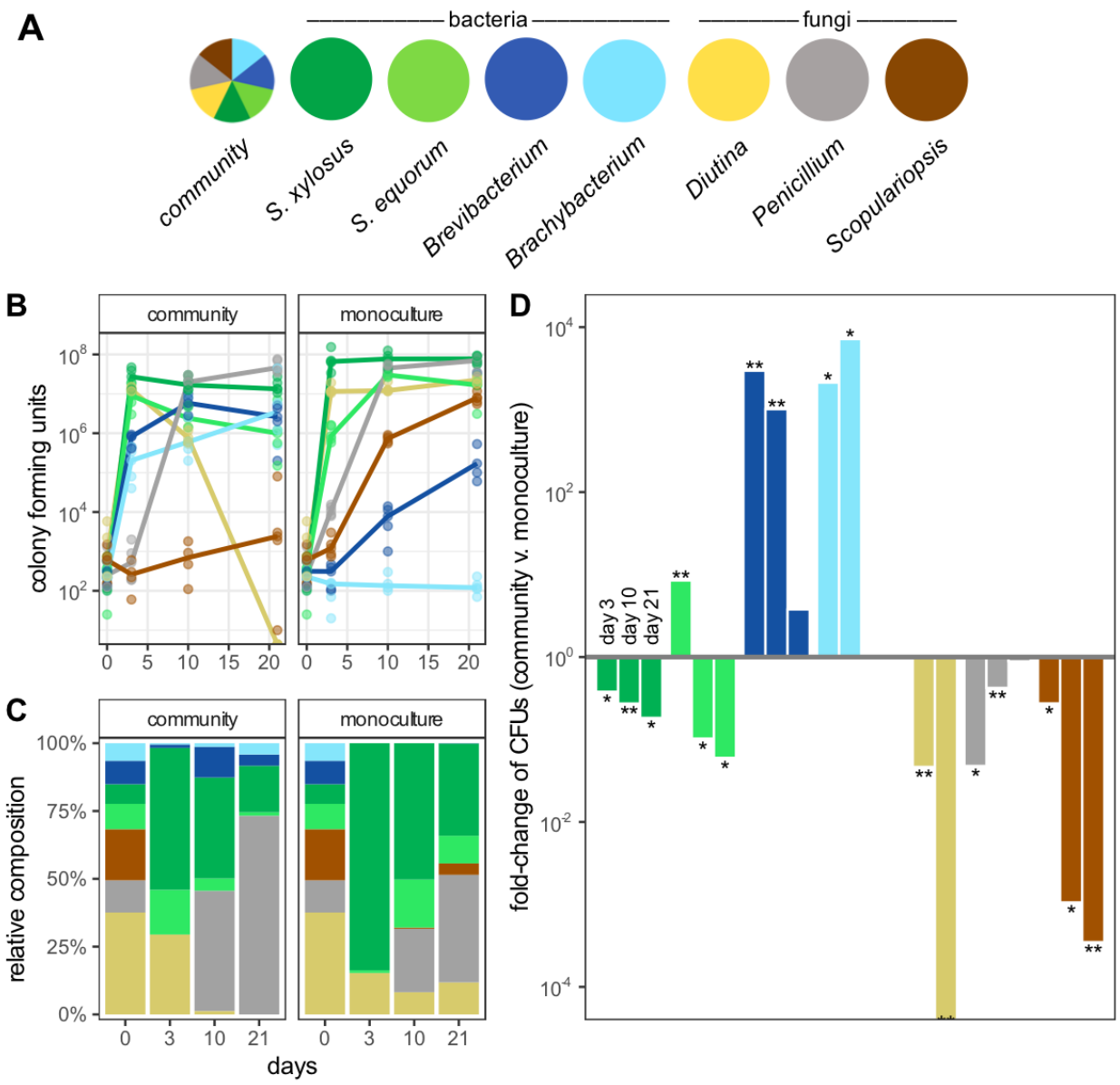
A
bacteria
fungi
community
S. xylosus
S. equorum
Brevibacterium
Brachybacterium
Diutina
Penicillium
Scopulariopsis
B
community
monoculture
colony forming units
C
relative composition
days
D
fold-change of CFUs (community v. monoculture)
day 3
day 10
day 21

Figure 2.2-2. Interaction effects in pairwise co-cultures.
(A-B) Network display of significant stimulatory (top) or inhibitory (bottom) pairwise interactions at all measured time points on CCA pH 5 (A) or CCA pH 7 (B). Arrows show the impact of the start-arrow "neighbor" species on the end-arrow "target" species, with the width of the connecting edge scaled by the log-fold-change in growth with a partner versus in monoculture at a given time point. ND = no detectable colonies of the end-arrow species in co-culture. (C) Fold-change comparing growth in co-culture with one partner or with the complete community to growth in monoculture on CCA pH 5. Each cluster of 3 bars show the growth impacts at day 3, 10, and 21, left to right. Asterisks denote significance according to Wilcoxon rank-sum tests comparing co-culture CFUs to alone CFUs of each species at each time point (* $p < 0.05$; ** $p < 0.01$; *** $p < 0.001$; n = 4 - 5).

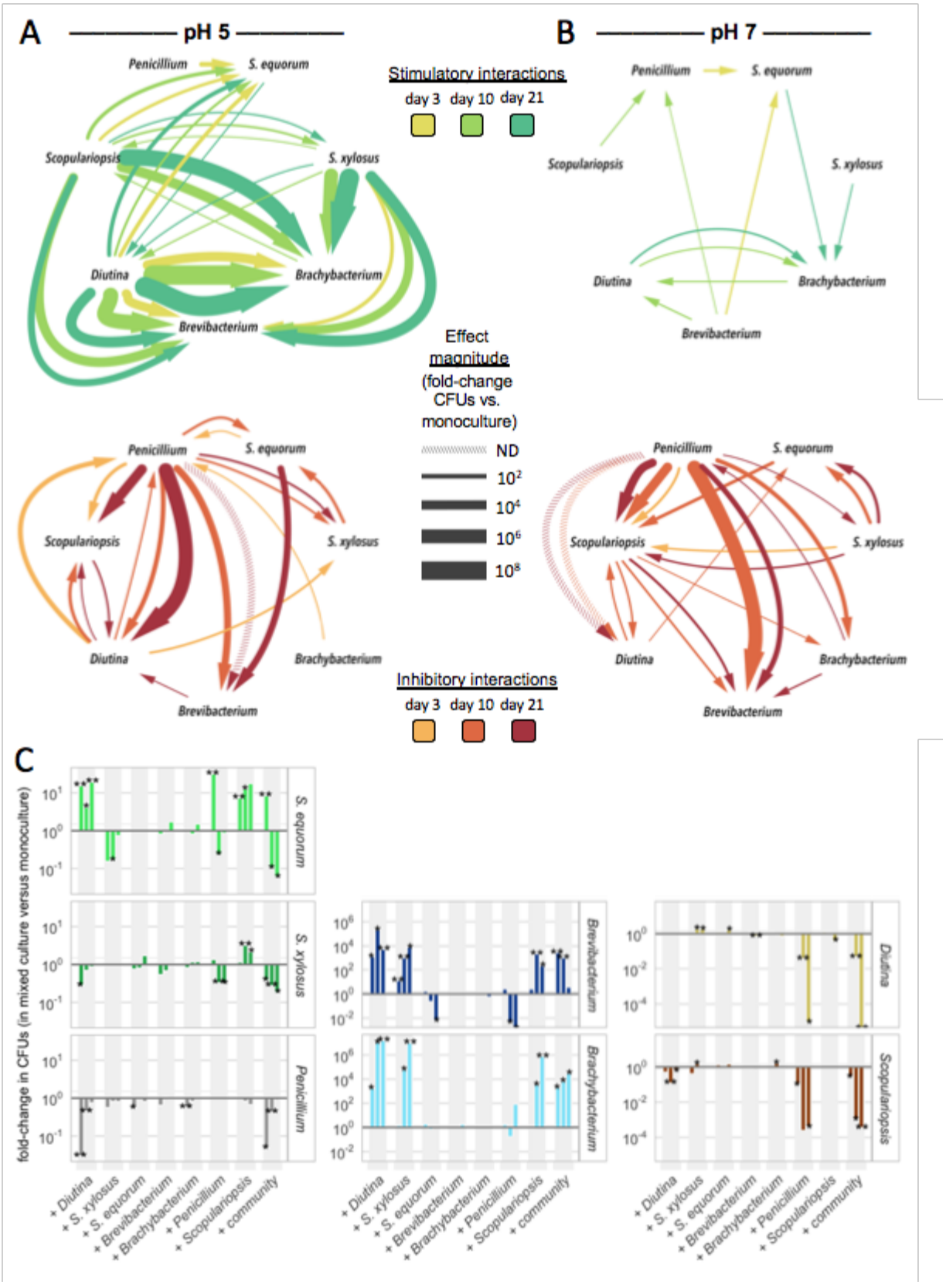
A
pH 5
B
pH 7
Penicillium
S. equorum
Scopulariopsis
S. xylosus
Diutina
Brachybacterium
Brevibacterium
Stimulatory interactions
day 3 day 10 day 21
Effect magnitude (fold-change CFUs vs. monoculture)
ND
10²
10⁴
10⁶
10⁸
Inhibitory interactions
day 3 day 10 day 21
C
fold-change in CFUs (in mixed culture versus monoculture)
S. equorum
S. xylosus
Penicillium
Brevibacterium
Brachybacterium
Diutina
Scopulariopsis
+ Diutina
+ S. xylosus
+ S. equorum
+ Brevibacterium
+ Brachybacterium
+ Penicillium
+ Scopulariopsis
+ community

Figure 2.2-3. Growth effects in community reconstruction.
(A) *Brevibacterium* and *Brachybacterium* growth on CCA pH 5 or CCA pH 7. (B) *Brevibacterium* and *Brachybacterium* growth in the complete community consortium or in communities that lack one or two model species, all grown on CCA pH 5. Large points show the median colony-forming units in a drop-out community, calculated from n=3 replicates plotted in surrounding small points. (C) Fold change in growth in a community without *Penicillium* on CCA pH 7 compared to growth alone on CCA pH 7. Each cluster of 3 bars show the growth impacts at day 3, 10, and 21, left to right. Lack of asterisks indicates no significant ($p < 0.05$) difference in population size between the two conditions, according to Wilcoxon rank-sum tests comparing community to alone CFUs of each species at each time point.

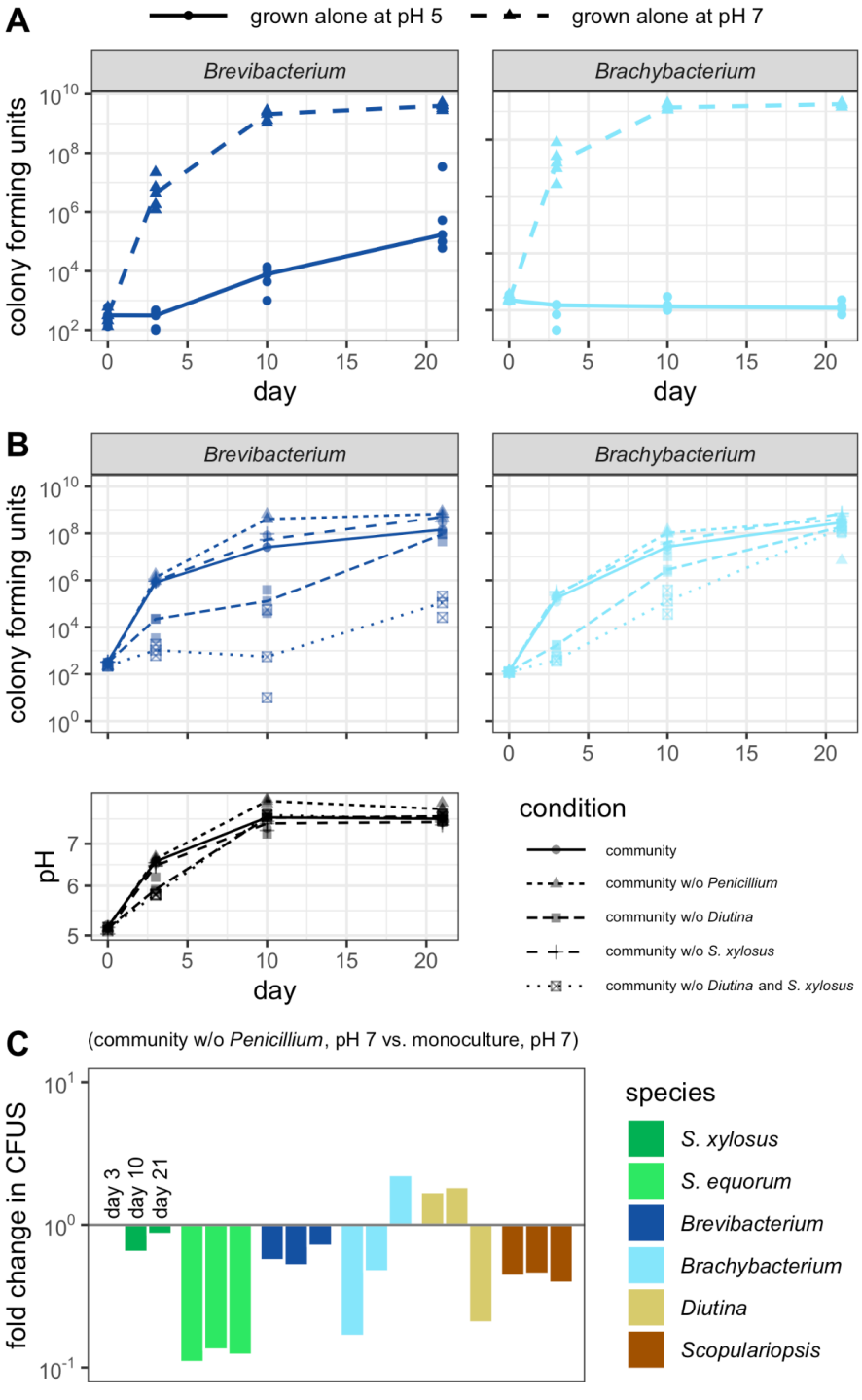
A
grown alone at pH 5
grown alone at pH 7
Brevibacterium
Brachybacterium
colony forming units
day
B
pH
condition
community
community w/o Penicillium
community w/o Diutina
community w/o S. xylosus
community w/o Diutina and S. xylosus
C
(community w/o Penicillium, pH 7 vs. monoculture, pH 7)
fold change in CFUS
day 3
day 10
day 21
species
S. xylosus
S. equorum
Brevibacterium
Brachybacterium
Diutina
Scopulariopsis

Supplemental Figures

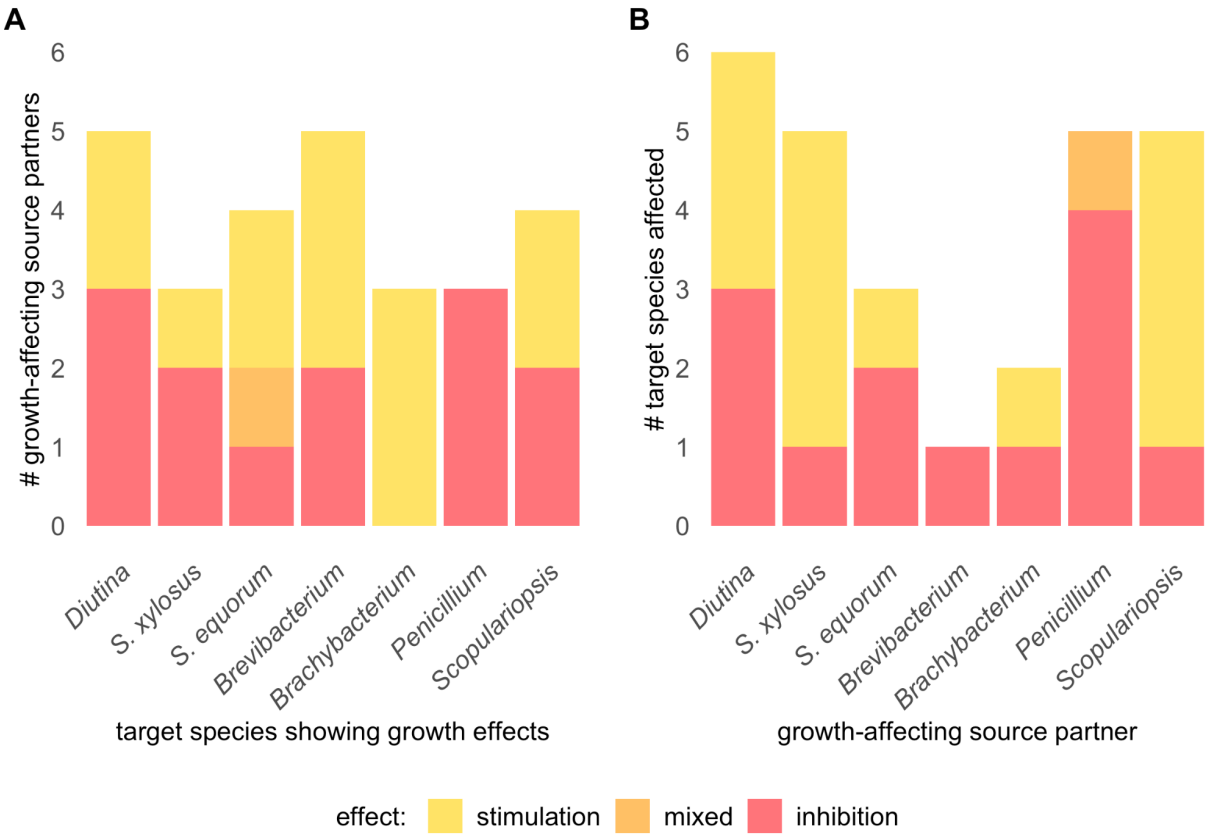

Supplemental Figure 2.2-1. Summary of pairwise interaction phenotypes affecting the target species (A) or caused by each neighbor species (B).
For each species in a co-culture, if the ratio between its co-culture and monoculture population sizes is greater than 1 at all significant time points, it counts as the co-culture neighbor species having a stimulation effect on the target species. If the ratio between co-culture and monoculture population sizes is less than 1 at all significant time points, it counts as the neighbor species having an inhibitory effect on the target species. If the ratio between co-culture and monoculture population sizes is greater than 1 at one significant time point but less than 1 at another, it's assigned the mixed effect category. (A) The number of growth-affecting neighbors is determined by counting up co-cultures where the target species demonstrates any significant change in co-culture population size when compared to its monoculture population size at the same time point. (B) The number of target species showing growth effects is determined by counting up co-cultures where the neighbor species induces any significant change in the target species' co-culture population size when compared to monoculture at the same time point.

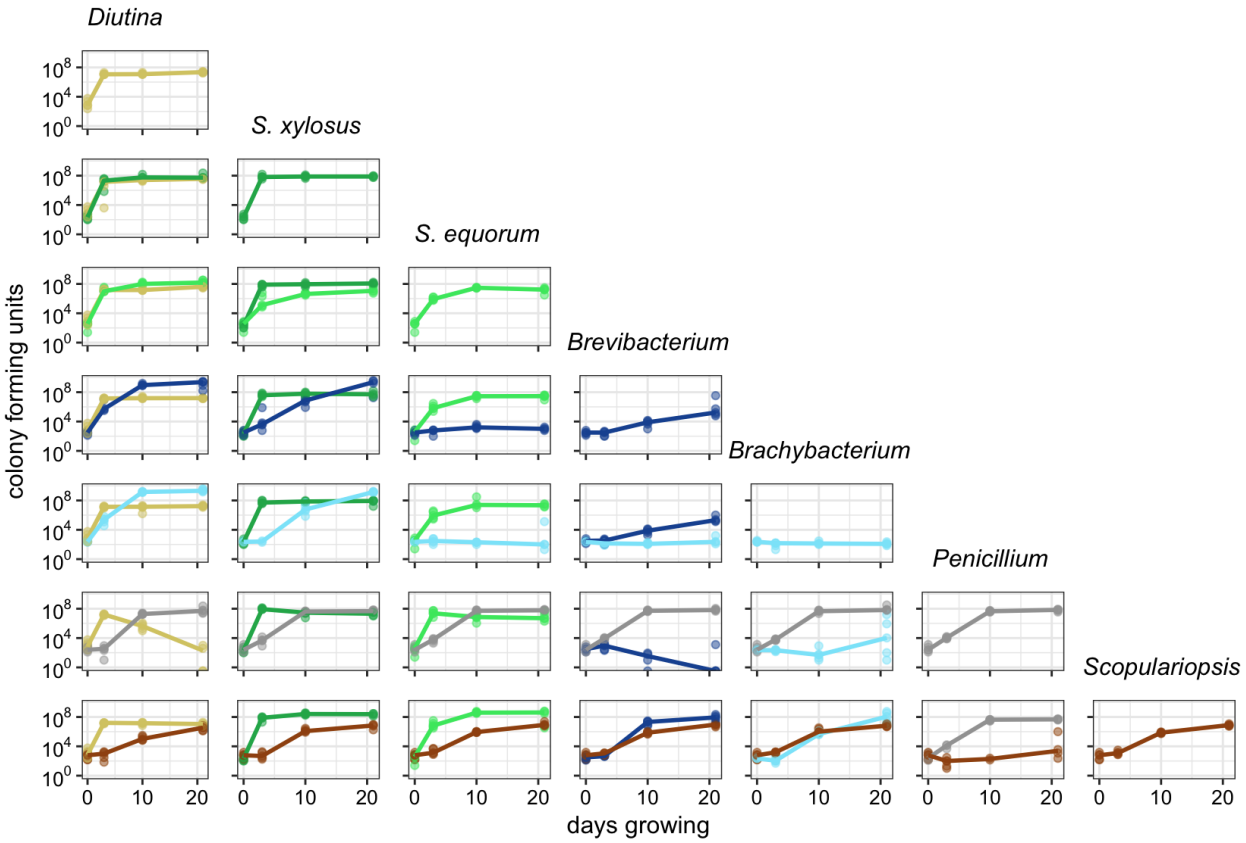

Supplemental Figure 2.2-2. Co-culture growth curves.
Growth curves (as measured by colony-forming units at days 3, 10, and 21 of growth) alone (outer diagonal of single curves under their corresponding genus-species name) or of both microbes when grown in co-culture (gridded crosses). Points show colony-forming units measured in 5 replicate pairwise co-culture experiments (actual replicate CFUs measurements for any species in culture, n = 3-5). Lines summarize median CFUs for a species at each time point.

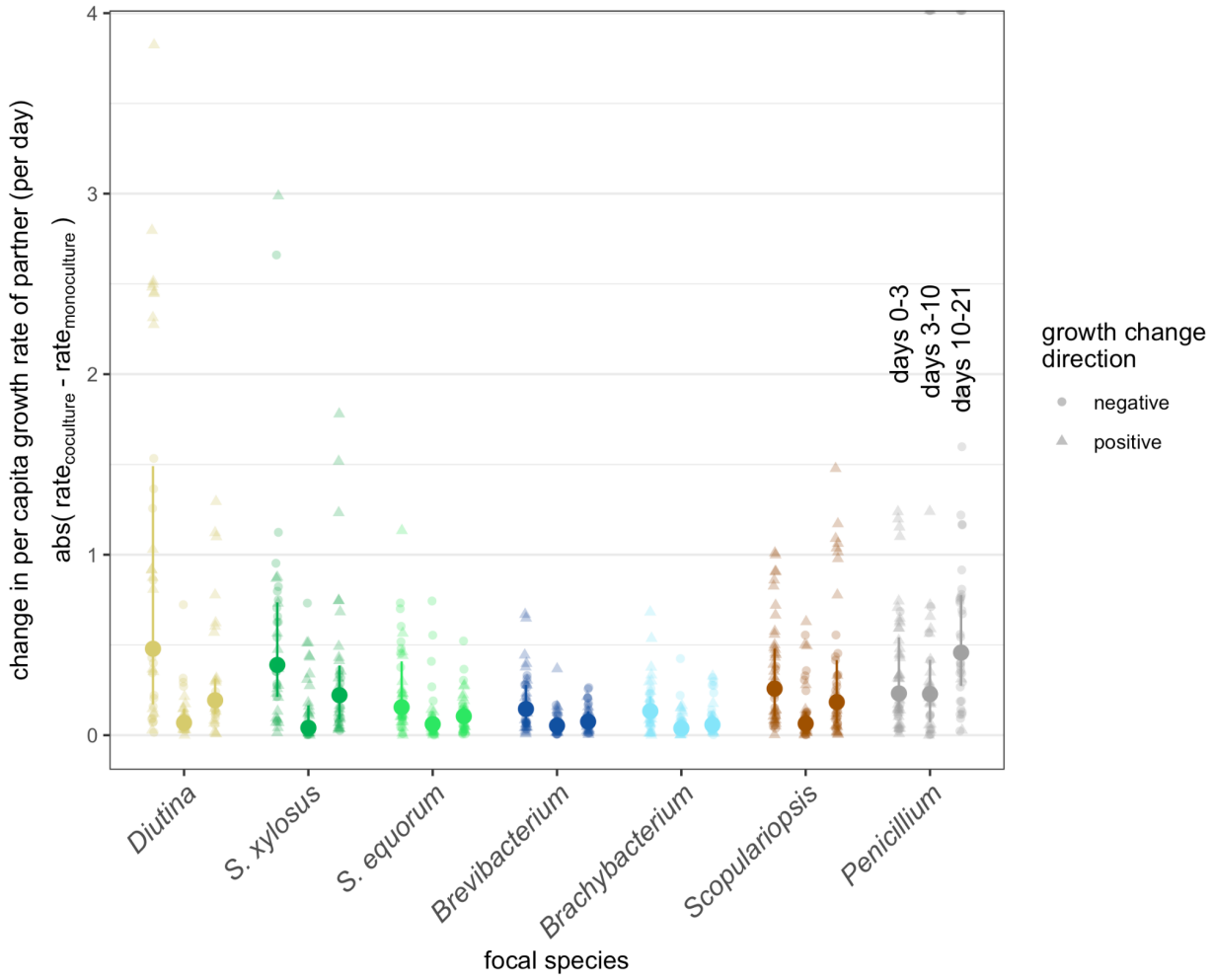

Supplemental Figure 2.2-3. Magnitude of focal species effects on growth of their co-culture partners for each measurable time frame.
Magnitude of effect on growth was determined using the absolute value of the difference between the growth rate of a partner species in co-culture with the focal species and its growth rate in monoculture, in the same replicate experiment and in the same time frame. Growth rates were calculated assuming exponential growth between adjacent time points within an experimental replicate (days 0, 3, 10, 21). If the calculated difference in growth rates was positive, then the species effect was considered stimulatory, marked by triangle-shaped points. Absolute differences in partner growth rates are plotted for each co-culture, organized by the species in co-culture with the partner and by each growth period between sample harvests.

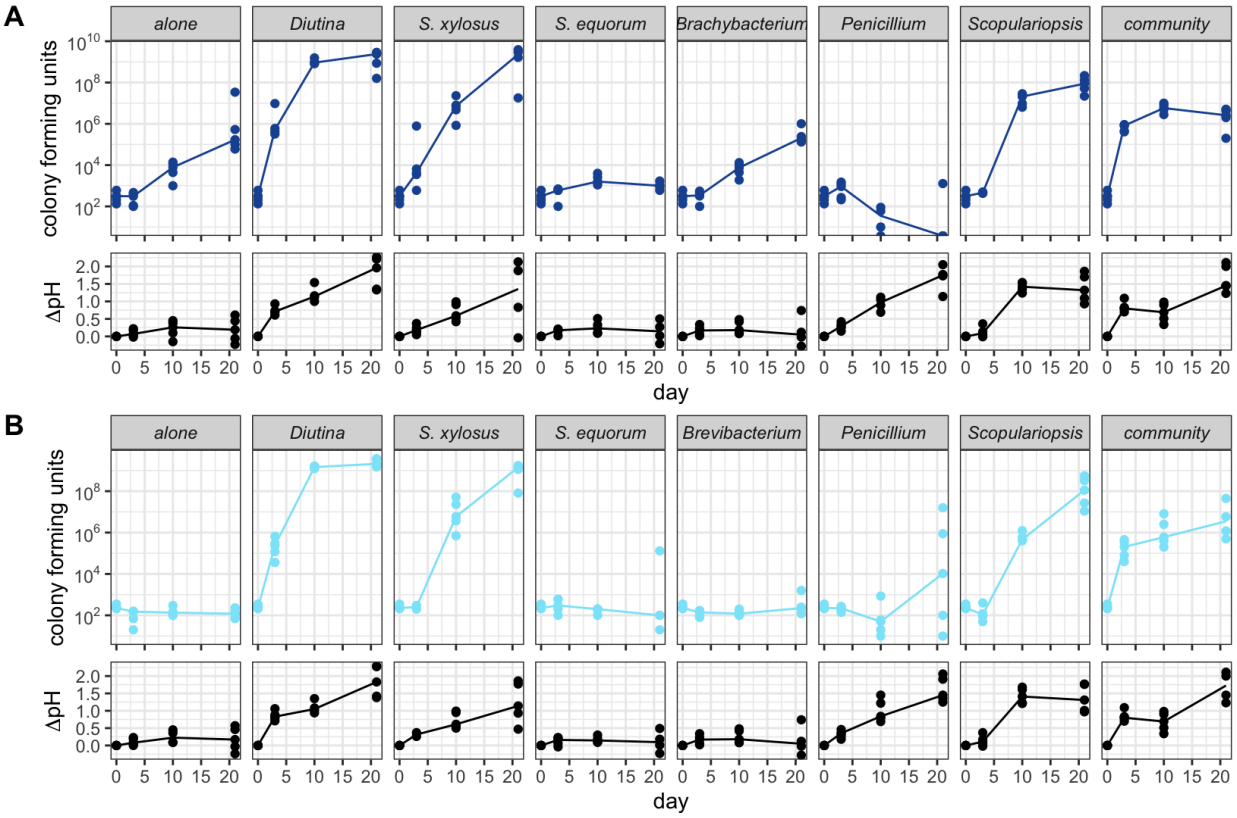

Supplemental Figure 2.2-4. Growth and pH curves of Actinobacteria grown with other community members.
Growth (top) in terms of colony forming units and change in measured pH from starting medium pH (bottom) of sample cultures of (A) Brevibacterium or (B) Brachybacterium grown alone, with a partner, or in the complete community on CCA pH 5.

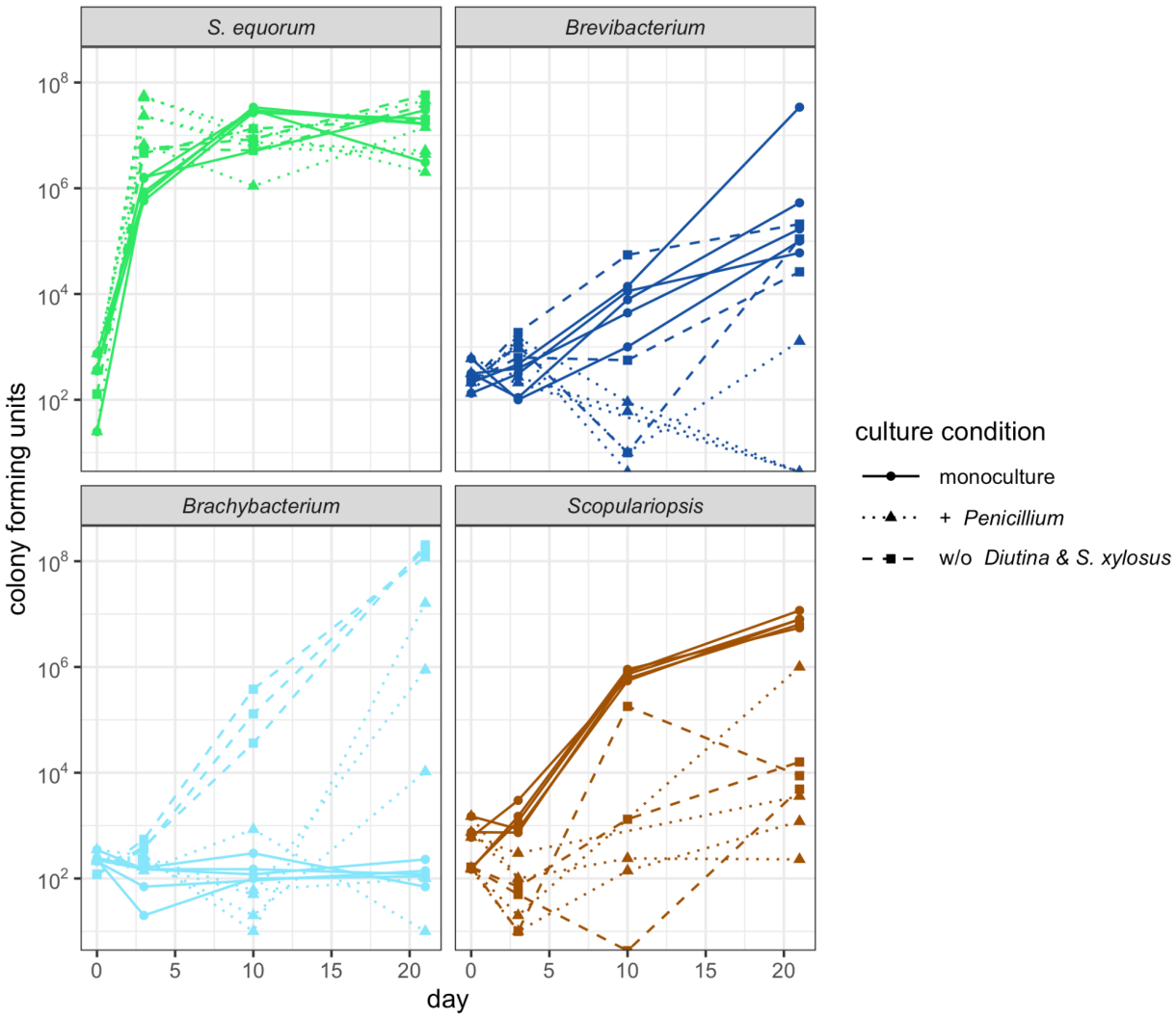

Supplemental Figure 2.2-5. Growth of model species on CCA pH 5 in monoculture, in co-culture with Penicillium, or in a double dropout community without early deacidifers.
Each line connects CFU counts from the same experimental replicate (n = 3 for pairwise co-culture and dropout community; n = 5 for monoculture).

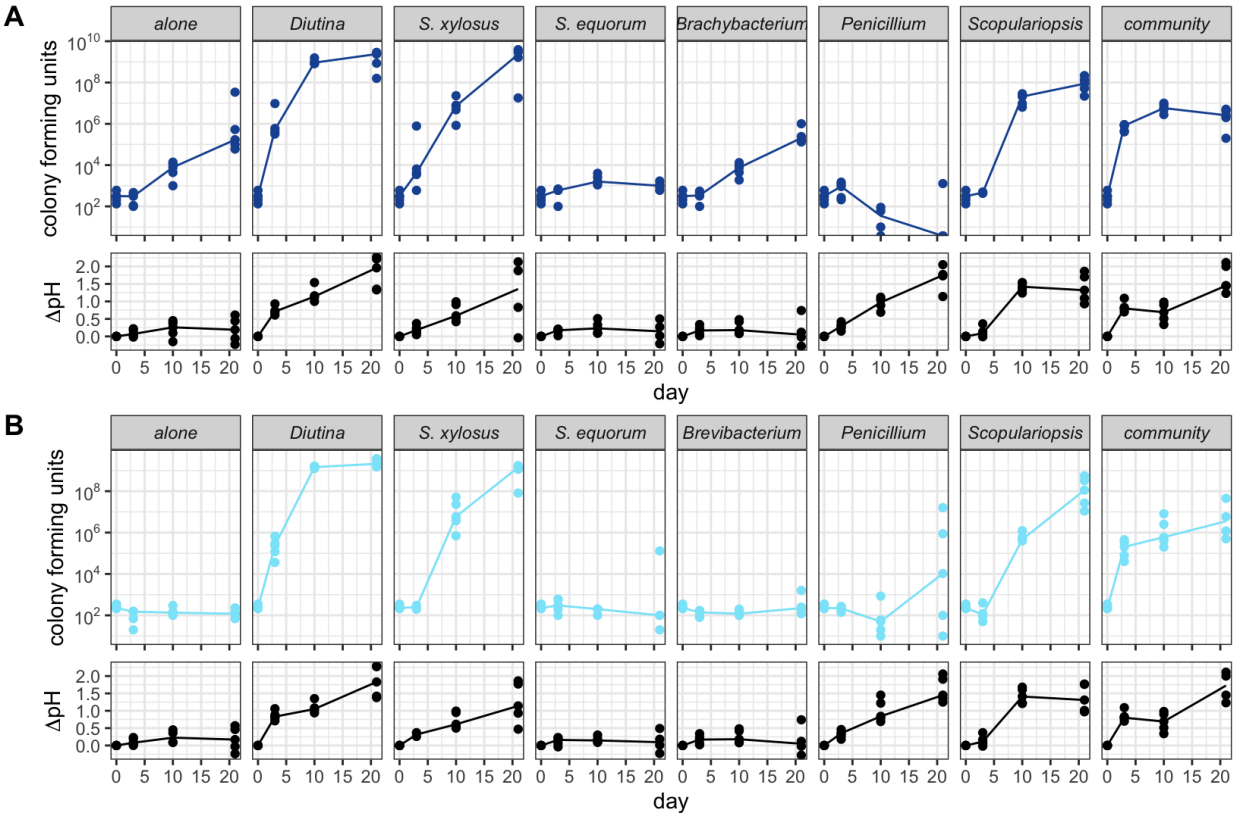

Supplemental Figure 2.2-6. Growth and pH curves of Actinobacteria grown with other community members.
Growth (top) in terms of colony forming units and change in measured pH from starting medium pH (bottom) of sample cultures of (A) Brevibacterium or (B) Brachybacterium grown alone, with a partner, or in the complete community on CCA pH 5.

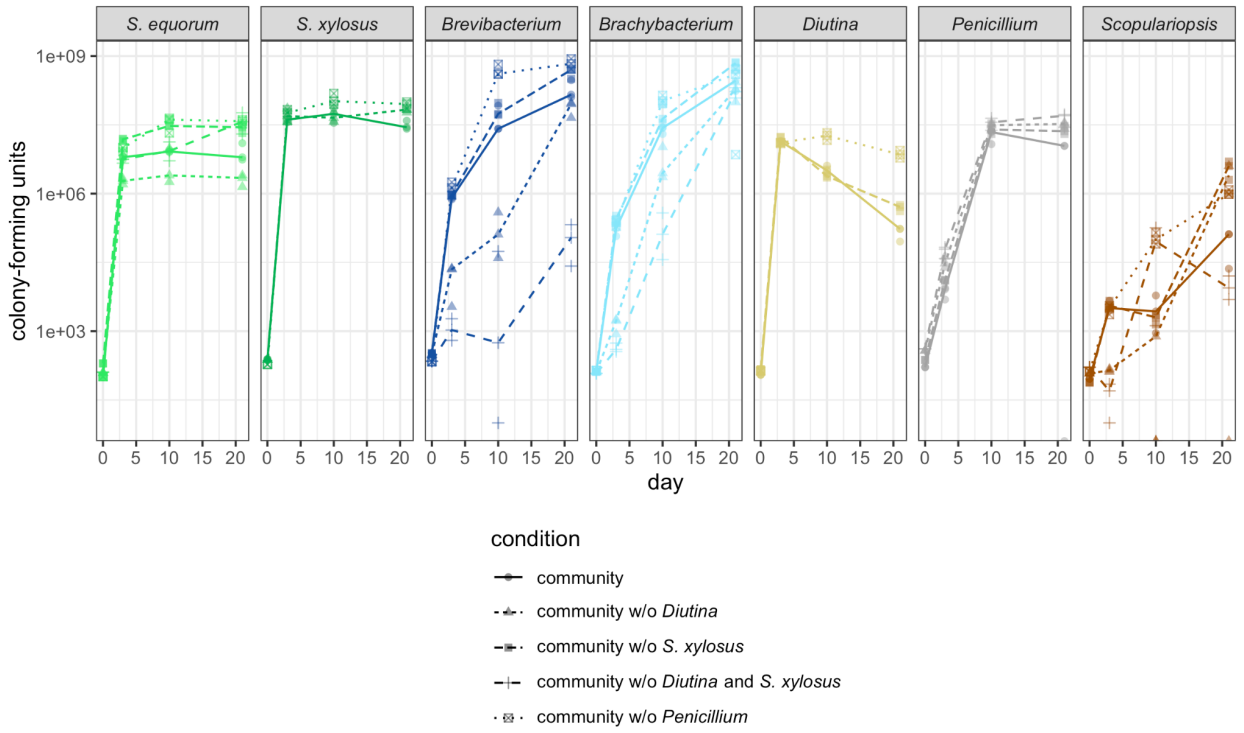

Supplemental Figure 2.2-7. Growth curves of each species in drop-out communities and in the complete community when grown on CCA pH 5.
Colony forming units of each species measured at inoculation (day 0) and from community harvests at day 3, 10, or 21. Points mark replicate growth measurements (n = 3) and lines connect median measurement.

Table

Table 2.2-1. Significant pairwise interactions at pH 5 and pH 7.
Significance was determined according to Wilcoxon ranked sums tests comparing community to alone CFUs of each species at each time point (* $p < 0.05$; ** $p < 0.01$; *** $p < 0.001$; n = 4 - 5). Fold-change compares species growth in the co-culture condition to species growth alone on media at the same pH.

target	source	day	level of signif. (pH5)	level of signif. (pH7)	intx direct. (pH5)	median fold-change (pH5)	intx direct. (pH7)	median fold-change (pH7)
Brevibacterium	*Penicillium*	21	*	*	neg	0	neg	0.01932241
Diutina	*Penicillium*	21	*	**	neg	8.93E-06	neg	0
Scopulariopsis	*Penicillium*	21	*	*	neg	3.90E-04	neg	0.001408105
Brevibacterium	*Penicillium*	10	*	**	neg	0.004342013	neg	9.75E-06
Brevibacterium	*S. equorum*	21	*		neg	0.006264706		
Penicillium	*Diutina*	3	**		neg	0.029323308		
Diutina	*Penicillium*	10	**	**	neg	0.036440678	neg	0
Scopulariopsis	*Penicillium*	3	*	*	neg	0.1	neg	0.214876033
Scopulariopsis	*Diutina*	10	**	**	neg	0.121818182	neg	0.430379747
S. equorum	*S. xylosus*	10	*	**	neg	0.164733581	neg	0.111538462
S. equorum	*Penicillium*	10	*		neg	0.232589016		
S. xylosus	*Diutina*	3	*		neg	0.276190476		
S. xylosus	*Penicillium*	21	*	*	neg	0.32	neg	0.7125
S. xylosus	*Penicillium*	10	**		neg	0.326086957		
Diutina	*Scopulariopsis*	21	*		neg	0.393501805		
Penicillium	*Diutina*	10	**		neg	0.444444444		
Penicillium	*S. equorum*	3	*		neg	0.551948052		
Penicillium	*Brachybacterium*	3	**		neg	0.563909774		
Scopulariopsis	*Diutina*	21	*		neg	0.609375		
Diutina	*Brevibacterium*	21	**		neg	0.709821429		
Scopulariopsis	*S. xylosus*	10	*		pos	1.545454545		
Scopulariopsis	*Brachybacterium*	10	*		pos	1.639344262		
Diutina	*S. equorum*	21	*		pos	1.708333333		
Diutina	*S. xylosus*	21	*		pos	1.851686508		
Diutina	*S. xylosus*	10	*		pos	1.909090909		
S. xylosus	*Scopulariopsis*	21	*		pos	2.177777778		
S. xylosus	*Scopulariopsis*	10	**		pos	3.231884058		
S. equorum	*Diutina*	10	*	**	pos	4.200928751	neg	0.763779528
S. equorum	*Scopulariopsis*	3	**		pos	7.361111111		
S. equorum	*Scopulariopsis*	10	*		pos	12.76394052		
Brevibacterium	*S. xylosus*	3	**		pos	13.5483871		
S. equorum	*Diutina*	3	**		pos	15.58441558		
S. equorum	*Diutina*	21	**		pos	19.34131737		
S. equorum	*Penicillium*	3	**	*	pos	31.80124224	pos	4.048846269
Brevibacterium	*Scopulariopsis*	21	*	**	pos	220	neg	0.221428571
Brevibacterium	*S. xylosus*	10	**		pos	1012.820513		
Brevibacterium	*Diutina*	3	*		pos	1285.359801		
Brachybacterium	*Diutina*	3	*		pos	1800		
Brevibacterium	*Scopulariopsis*	10	**	**	pos	2181.818182	neg	0.332129964
Brachybacterium	*Scopulariopsis*	10	*	*	pos	3633.333333	neg	0.713043478
Brevibacterium	*Diutina*	21	**		pos	5471.698113		
Brevibacterium	*S. xylosus*	21	*		pos	8532.186459		
Brachybacterium	*S. xylosus*	10	*		pos	62916.66667		
Brevibacterium	*Diutina*	10	*		pos	231118.8811		
Brachybacterium	*Scopulariopsis*	21	**		pos	800000		
Brachybacterium	*S. xylosus*	21	**	*	pos	10363636.36	pos	1.618811881
Brachybacterium	*Diutina*	10	*	*	pos	11333333.33	pos	1.783453957
Brachybacterium	*Diutina*	21	**	*	pos	16500000	pos	2.608391608
Diutina	*Brevibacterium*	10		*			pos	1.977777778
Diutina	*Brachybacterium*	10		*			pos	1.886792453
Diutina	*Scopulariopsis*	10		*			neg	0.396226415
S. equorum	*S. xylosus*	21		**			neg	0.153571429
S. equorum	*Brevibacterium*	3		*			pos	2.381148479
Brevibacterium	*Brachybacterium*	21		**			neg	0.492156863
Brachybacterium	*S. equorum*	21		*			pos	1.482517483
Brachybacterium	*Penicillium*	10		**			neg	0.051470588
Penicillium	*Brevibacterium*	10		*			pos	1.233333333
Penicillium	*Brachybacterium*	21		*			neg	0.661971831
Penicillium	*Scopulariopsis*	10		*			pos	1.672354949
Scopulariopsis	*S. xylosus*	3		*			neg	0.347107438
Scopulariopsis	*S. xylosus*	21		*			neg	0.385964912
Scopulariopsis	*S. equorum*	10		*			neg	0.117647059
Scopulariopsis	*Penicillium*	10		*			neg	6.35E-04

2.3 Acknowledgments

I would also like to acknowledge scientific contributions to this dissertation. Chapter 2 consists of unpublished material, currently being prepared for submission for publication. The following individuals are also authors on this work: Julie E. Button (Harvard FAS Center for Systems Biology), Collin Edwards (Tufts), Elizabeth Brown (UCSD), Benjamin E. Wolfe (Tufts), Rachel J. Dutton (UCSD). The dissertation author is the primary author of this manuscript.

CHAPTER 3. Phage dynamics and persistence in a cheese rind microbiome

3.1 Chapter Summary

In the previous chapter we showed how interactions between bacteria, fungi, and the cheese environment shape overarching patterns of microbial succession at the rind. Using the natural-rind, cave-aged cheese from which the *in vitro* community in Chapter 2 was built, in this chapter we use metagenomic sequencing to explore an additional component of the microbial community as yet ignored: bacterial viruses, called bacteriophage. This time course investigation into the diversity of rind bacteriophage during cave-aging reveals a reproducible succession of phage across three different batches, including phage sequences predicted to infect "wild" bacteria which are not added to cheeses as starters. Many of the phage sequences were found to persist not only between sequentially-prepared batches but even over years of the cheese's preparation, as found by comparing the phage in a metagenome from the mature cheese prepared six years after the initial time course study. Genetic diversity and composition of phage may reveal functional roles for bacteriophage in cheese rind microbiome succession.

3.2 Characterizing phage dynamics in cheese rind metagenomes

Introduction

Numerous modern sequencing studies have characterized the spatiotemporal distribution of bacteriophage (bacteriophage or phage) populations across different ecosystems. Many of these studies come from environments where communities are well-mixed and experience frequent disturbance. Despite the chaos of aquatic environments, many phage in bodies of water demonstrate seasonal trends matching the seasonal dynamics of their hosts (Arkhipova et al., 2018;

Chow and Fuhrman, 2012; Kavagutti et al., 2019; Luo et al., 2017). Phage population dynamics in human guts, while highly individual-specific, also match the stability of the bacterial microbiome composition (Draper et al., 2018; Shkoporov et al., 2019). It's unclear how findings about phage composition and dynamics in these high-disturbance environments are applicable to microbial communities that assemble on solid substrates with less disturbance, such as those in the soil or on living or nonliving surfaces.

Phage are rapidly-evolving microbes, with proliferate reproduction and an extraordinary capacity for genetic recombination. At least partly due to these features, shotgun metagenomic sequencing finds that a majority of bioinformatically-identified phage genomes are novel based on comparison to databases of sequenced phages (Luo et al., 2017). But despite the vast diversity of phage sequences, some extremely similar and even identical phage sequences can be identified even when sampling the same environment a year apart (Draper et al., 2018; Emerson et al., 2012; Kavagutti et al., 2019; Luo et al., 2017; Shkoporov et al., 2019). Understanding the extent to which phages are evolving in natural ecosystems is of vital importance to predicting microbiome composition and implementing phage therapy-based treatments.

During microbial colonization of a new ecosystem, microbiome composition often undergoes a pattern of succession as the environment is modified by metabolic processes of early colonizers and becomes selective for other microbial species. How phage are integrated into the process of community assembly, including both their maintenance in a community by hosts as well as their role in the selection for certain microbial strains over others, is an open question in microbiology. Approaching this question must combine characterization work to identify the distribution of phage and their hosts in existing microbiomes as well as experimental work to identify and predict host outcomes when challenged with phages.

The microbial biofilms that grow on the surface of aged cheeses, called cheese rind communities, provide a semi-natural microbiome system that is relatively controllable and demonstrates consistent taxonomic dynamics (Wolfe et al., 2014). While phage are found to be part of cheese rind microbial communities (Dugat-Bony et al., 2020; de Melo et al., 2020), their diversity and dynamics in this environment have yet to be studied. Here we characterize the phage community over a time series of cheese rind development for three batches of the same cheese. Our goals in this study are a) to assess the reproducibility of the phage community in this cheese rind across batches of the same cheese, b) assess how phage dynamics compare to bacterial host dynamics, c) to compare phage community composition from the same cheese produced six years apart, and to d) examine genetic changes in phage sequences, both during the course of rind succession and over six years of cheese production.

Results

Characterization of the phage population in a natural rind cheese. Cheese rind samples from 3 separate batches (batches A, B, and C) that were collected after 1, 21, 41, 61, and 81 days of aging were coassembled into contiguous sequences (hereafter referred to as "contigs") (see "Methods"). 224 total contigs were predicted to originate from bacteriophage genomes, up to 120 kbp (Figure 3.2.1A). A small portion of contigs were predicted to be full or nearly-full phage genomes, as indicated by CheckV's quality assessment (Figure 3.2.1B), and a total of 15 sequences are predicted to be prophage sequences integrated into a bacterial genome. Many contigs marked as low-quality are likely phage genome fragments. Eight phage sequences, from lengths 18-121 kilobase pairs, were marked as 95-100% complete: five predicted to infect *Staphylococci*, two predicted to infect *Klebsiella*, and one predicted to infect a *Lactococcus* bacterium.

Most of the phage sequences collected from the time series study were predicted to infect *Staphylococcus* bacteria, when measured as a summation of phage sequence lengths to eliminate bias based on contig size (Figure 3.2.1C). Many of these *Staphylococcus* phage sequences were found to have good matches in CheckV's reference database of high-quality phage sequences, and thus completeness could be assessed using an AAI-based method (Figure 3.2.1D).

Phage sequences that did not have a good database hit were assessed for completeness using a comparable HMM profile. The majority of predicted Actinobacteria phage sequences (72% of total Actinobacterial phage nucleotides) had to be assessed based on HMM profiles or couldn't be assessed at all (Figure 3.2.1D). This indicates that, despite searching against a reference database of high-quality virus sequences sourced from both NCBI Genbank and publicly available metagenomes, these Actinobacteria-infecting phage sequences lack quality representation in public datasets.

Reproducible phage succession across batches of a natural rind cheese. Relative abundance of phage, bacterial, and fungal metagenome-assembled genomes (hereafter, "MAGs") were determined as detailed in "Methods." Triplicate time series data allowed for a more careful curation of MAG binning according to coverage trends of each contig over time within a replicate. The relative composition of phage sequences at each time of aging was very similar across the three batches sampled, and phage community composition became more similar after 41 days (Supplemental Figure 3.2-1, Supplemental Figure 3.2-2). Phage dynamics follow closely with the dynamics of their putative hosts so that as the relative abundance of Lactobacillales decrease, so do phage infecting Lactobacillales, and as the relative abundance of Actinobacterial genera *Brevibacterium* and *Brachybacterium* increase, so do phage infecting Actinobacteria (Figure 3.2.2). Lactobacillales and Proteobacterial phage are notable in that their relative abundance

compared to other phage is greater than the relative abundance of Lactobacillales or Proteobacteria compared to other bacteria.

Persistent phage sequences in a natural rind cheese. The rind from the same cheese was sampled six years after the time series experiment. The sampled cheese rind was aged to maturity (and so hereafter referred to as the "mature sample") and therefore we expected it to be most comparable to late-stage (day 81) rind samples from the earlier time series study. Reads from the mature sample were mapped to the set of 224 curated phage contigs from the cheese rind time series, and 78 contigs were found to map with non-zero read depth, probability of wrong mapping <= 0.05 (mapQ >=13), and reads mapping across >= 50% of the contig (Figure 3.2.3). These 78 contigs were binned using the phage MAG assignments from the time series, and 11 out of the 16 MAGs containing persistent phage contigs were found to be more than 70% complete as measured by total nucleotides in the MAG (Figure 3.2.3D). Four of these 11 likely persistent phage MAGs are predicted to infect Actinobacteria, and six are predicted to infect *Staphylococci*, in concordance with proportions observed in day 81 rind phage communities.

Genetic changes in cheese rind phage. The dominant sequence variants for phage contigs present in each time series sample or in the mature sample were aligned and compared for changes in the genetic sequence. Multiple phage sequences showed a pattern of succession in the dominant sequence variant over the time series samples (data not shown). Overall, persistent phage sequences from the mature sample were very similar to the sequences from the time series (96.5%-100% identity), but many of the persistent phage sequences from the mature sample were more different from time series variants than the differences between sample variants from the time series (Supplemental Figure 3.2-3). Sequence variants from the mature sample tended to be slightly more similar to the sequence variants found after the start of succession (21+ days).

Discussion

The presented analysis establishes a population of phage sequences from a time series study of three batches of a natural rind cheese. 42 phage MAGs were identified over the course of rind community succession, with temporal relative abundances matching the relative abundance of predicted host bacteria. This curated set of phage sequences was then used to compare the phage community of the same cheese prepared six years after the initial time series, and 11 phage MAGs were found to be persistent phage in this rind microbiome.

Drawbacks of using short-read shotgun sequencing for identifying phage populations include fragmented phage genomes and uncertainty in phage-host pairing. Genome binning into MAGs was aided by time series trends of contig coverage, and increased sequencing depth would improve the utility of this technique. While host prediction is done very conservatively in this analysis, there are methods for more specifically matching phage sequences with potential bacterial hosts. For example, it is a common practice to improve upon phage-host pairing by matching host CRISPR spacers or tRNA integration sites with phage sequences (Arkhipova et al., 2018; Kavagutti et al., 2019; Somerville et al., 2019). An analysis of CRISPR spacers per bacterial MAG would be an appropriate method for assessing infectious history, though it cannot prove active cell infection during rind aging.

CheckV's algorithm for assessing phage completeness compares phage sequences to a modern and extensive database of high-quality, publicly available phage genomes. The method that CheckV must use for assessing sequence completeness depends on its ability to find a related phage sequence in its database; thus, the method used by the package can serve as a proxy for sequence novelty. From the curated set of phage from time series rind sampling, phage predicted to infect rind Actinobacteria, in particular, are under-represented among high-quality phage

genomes. This suggests that cheese rinds are a reservoir of novel phage sequences with potentially novel functions, and that Actinobacterial phage require more sequence-based exploration and characterization.

Our results show that, like in other dynamic microbiomes (Draper et al., 2018; Emerson et al., 2012; Kavagutti et al., 2019; Luo et al., 2017; Shkoporov et al., 2019), phage population dynamics closely track with those of their bacterial hosts. While the resolution of time-sampling in this study is not fine enough to detect boom-bust patterns of abundance expected from lytic phage lifecycles, the overall positive correlation trend between phage abundance and *Staphylococci* or Actinobacteria (encompassing genera *Brevibacterium* and *Brachybacterium*) suggests that the most abundant phage infecting these bacteria are not lytic. In contrast, the higher relative abundance of Lactobacillales- and Proteobacteria-infecting phage to host bacteria relative abundance may suggest more active lysis among these bacterial groups, though the relative nature of our sequenced samples make this a difficult point to prove. Some studies aim to build more evidence of lysis versus lysogeny by measuring the proportion of prophage marker genes in phage sequences or phage MAGs (Labonté et al., 2015; Luo et al., 2017). Recent tools also aim to distinguish between lytic versus lysogenic phages (Kieft and Anantharaman, 2021; Kieft et al., 2020).

Almost all phage MAGs (10/11) that persist in this community are not predicted to infect bacteria that are used as "starters" in the cheese-making process; rather, these bacteria and their phage likely arrive through cheese-cheese dispersal in the cave where cheeses age and develop their rind. This allows for a sort of passaging of phage and their hosts over time. Despite six years of this passaging, relatively few mutations were acquired by the persistent phage; the most divergent phage sequences from the mature sample shared 96.5% nucleotide identity with

dominant sequence variants in the time series samples. Further exploration of the sites of these mutations may provide insight into selective forces for phage within the cheese rind microbiome.

Methods

Metagenome processing and assembly. Raw fastq files from Illumina paired-end sequencing were quality controlled and adapters trimmed using FastQC v0.11.9 [Andrews S. (2010). FastQC: a quality control tool for high throughput sequence data. Available online at: http://www.bioinformatics.babraham.ac.uk/projects/fastqc] and Trimmomatic v0.39 (Bolger et al., 2014), respectively. All time series samples from 3 batches of cheese were coassembled using metaSPAdes v3.14.0 with k-mer sizes set to 33, 55, 77, 99, and 127 (Nurk et al., 2017). All contigs with length at least 3 kilobase pairs were used for downstream analysis.

Phage characterization. VirSorter2 v2.1 (Guo et al., 2021a) was used to predict phage sequences from the complete coassembly, using the dsDNAphage and ssDNA settings to select for bacteriophage. For curation, a modified version of the VirSorter2 SOP for viral identification was followed (Guo et al., 2021b). the 273 contigs identified by VirSorter2 were first run through a taxonomic classifier, Kraken 2 v2.0.8_beta (Wood et al., 2019), which was equipped with a custom database including cheese isolate genomes. 35, or just under 13% of the total predicted phage contigs, were classified as eukaryotes, a rate of error in phage prediction expected by VirSorter2 (Guo et al., 2021a).

After eliminating the eukaryotic sequences, the remaining 238 phage contigs were run through CheckV v0.7.0 (Nayfach et al., 2021) and contigs that are unlikely to be viral (i.e. many host genes identified but no viral genes identified by CheckV) were also removed from the phage set, leaving 224 total phage sequences for further investigation. CheckV also determines the length of phage sequences from prophage integrated into host contigs. These prophage sequence lengths

were used when considering prophage sequence lengths; otherwise, the length of the contigs from phage sequences not predicted to be integrated prophage was used.

Measuring abundance. Sequencing reads were mapped to the curated set of phage sequences using Bowtie2 v2.4.2 (Langmead and Salzberg, 2012). Coverage (average number of reads mapping across the length of a contig) tables for each contig were generated using SAMtools v1.12. Phage contigs were binned by coverage and kmer similarity using CONCOCT v1.1.0 (Alneberg et al., 2014) as implemented through Anvi'o v6.2 (Murat Eren et al., 2015). Bins were manually refined using temporal coverage trends and assessment of completeness by CheckV. Complete prophage or phage sequences with direct terminal repeats were assigned their own bin. A total of 42 phage MAGs were defined, 55% of which were classified by CheckV as "high-quality" or "complete." Abundance of each MAG at each timepoint in a batch was calculated by taking the mean coverage of all contigs in the MAG bin.

To measure abundances of all community microbes, sequencing reads were mapped to all coassembled contigs and all contigs binned into MAGs, all in the same manner as for the predicted phage set of contigs detailed before. To obtain abundances of only cellular microbes within the community, the 224 contigs predicted to be phage were removed from the dataset and then abundances of each cellular MAG was calculated by taking the mean coverage of all contigs in the MAG bin.

Taxonomic classification. All cellular contigs in the coassembly were assigned taxonomy using Kraken 2, equipped with a custom database containing genomes from cheese rind isolate bacteria and fungi. Phage contigs were classified by their putative host; those contigs that were unclassified by Kraken 2 were assigned their putative host using the top hit of a Blastx (Altschul

et al., 1990) search of the nucleotide sequence. All MAGs were assigned a taxonomy or putative host taxonomy by applying the most frequent taxonomic classification among classified contigs.

Identifying persistent phage. A sample of mature cheese rind from the same type used in the time series sequencing study, but six years later, was subject to shotgun sequencing. Illumina paired-end reads were mapped to the set of 224 phage contigs identified in the time series data using Bowtie2. A phage contig was considered present in the mature sample if reads mapped with non-zero average read depth, mapQ score >= 13, and if reads mapped along 50% or more of the contig length. The 78 phage sequences passing these thresholds make up the set of persistent phage.

Sequence variant analysis. The dominant sequence variant from each sequenced sample (individual time series samples and the mature sample) was called using simple variant calling with bcftools v1.12, with a max read depth of 5000 (Li, 2011). Low-quality calls < 20 were filtered out, text format of the calls were indexed, indels normalized and those within 5 basepairs of each other were filtered out, and then resulting consensus sequences were generated. Consensus sequences of the same contig across the samples were aligned using MAFFT v7.475 (Katoh and Standley, 2013). Alignments were imported into Geneious Prime 2010.2.6 for visualization, and percent identity matrices comparing sequence variants of each contig across samples were exported for summary visualization in R v3.6.3. Heatmap of sequence identity, comparing the mature sample persistent phage variant sequences to the time series sample sequences, was generated using the ggplot package (Wickham H (2016). ggplot2: Elegant Graphics for Data Analysis. Springer-Verlag New York. ISBN 978-3-319-24277-4, https://ggplot2.tidyverse.org).

Figures

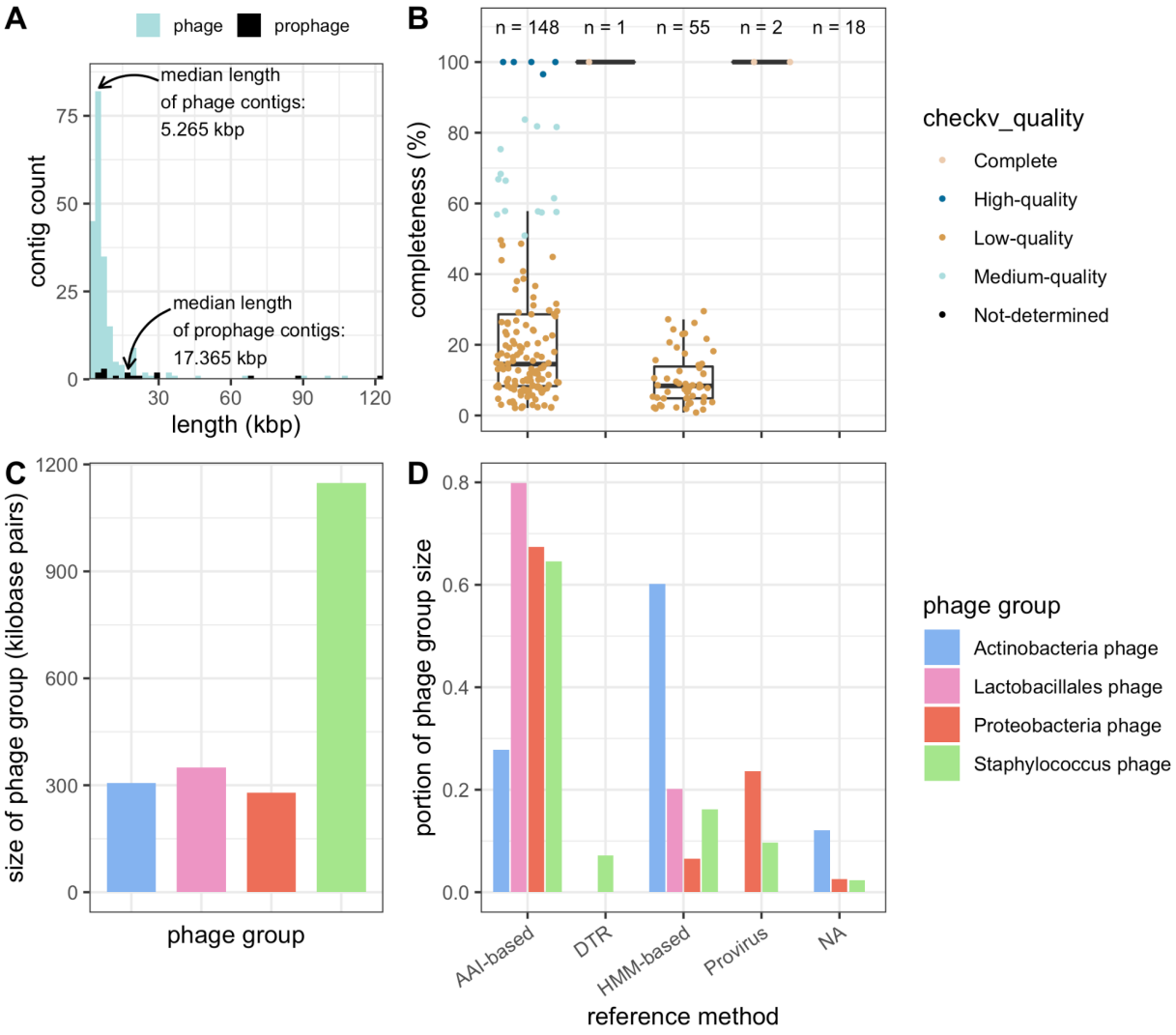

Figure 3.2-1. Curated phage contigs from time series cheese rind coassembly.
(A) distribution of predicted phage or prophage contig lengths from all 224 curated phage contigs. Prophage distinction predicted by CheckV. (B, D) Assessment of phage contig completeness (B) and portion of nucleotides per putative phage host (D) sorted by the method used by CheckV to assess sequence completeness. AAI-based assessment of completeness is used when a reasonable match to database viruses was found. HMM-based methods were used when no good database hit was identified for the phage sequence and instead compares contig length with the length of database viruses that contain a similar set of HMMs. DTR = direct terminal repeats, indicating a circular genome. (C) Sum total of nucleotides from curated phage contigs grouped by their predicted host.

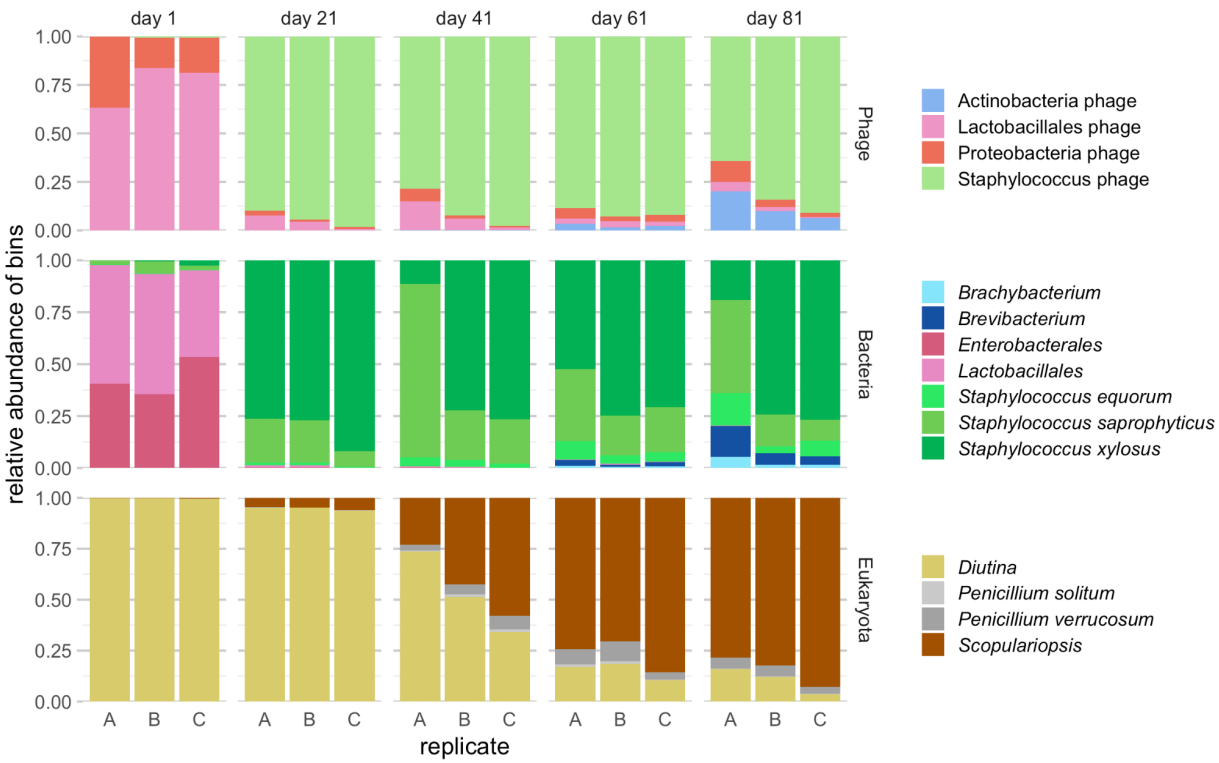

Figure 3.2-2. Abundance over time of microbial MAGs from 3 cheese batches.
Each row shows the relative abundance of contigs contained in phage, bacterial, or fungal MAGs within each replicate batch (A, B, or C) of cheese rind sampled at different times in the cheese aging process.

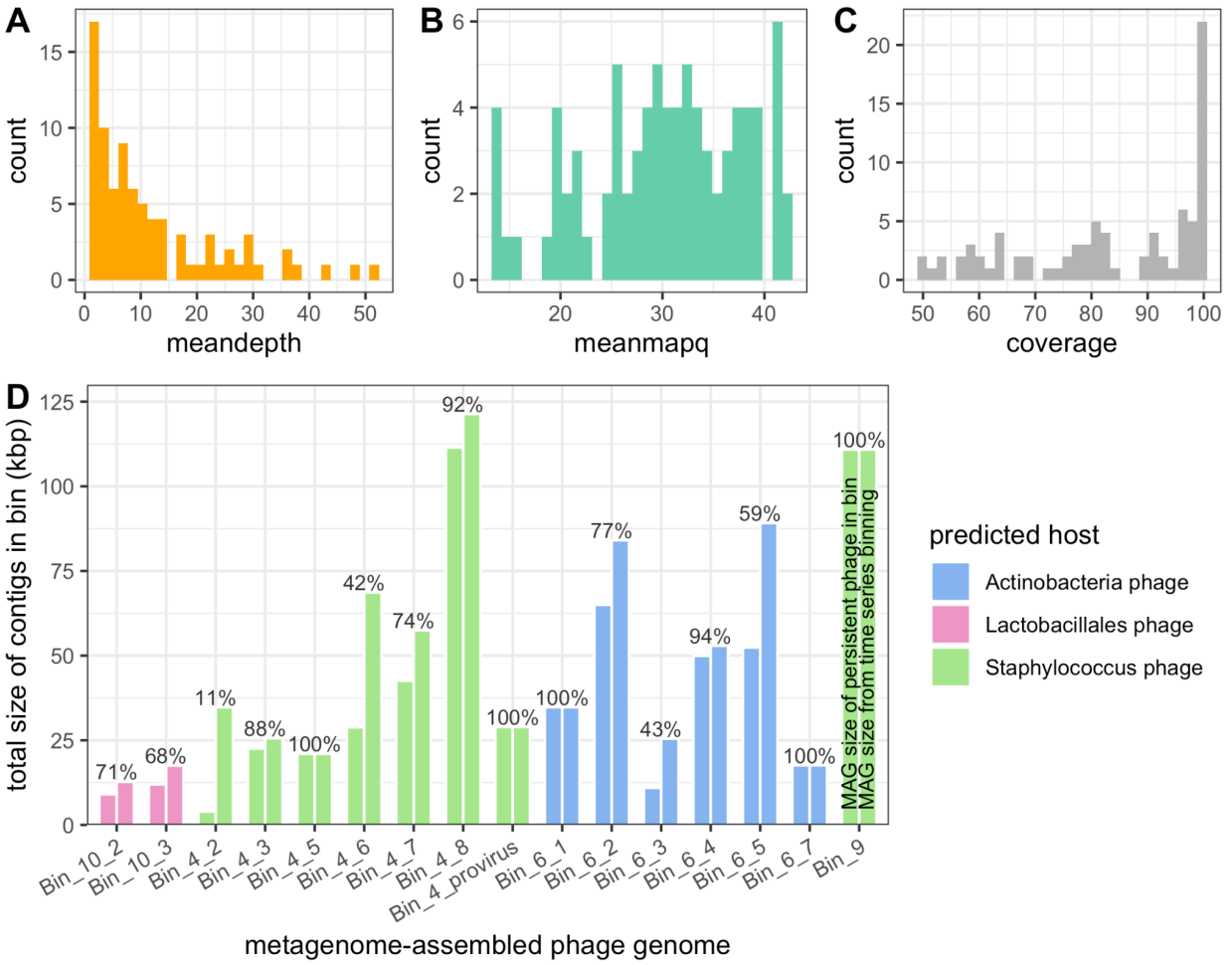

Figure 3.2-3. Persistent phage in a natural cheese rind.
(A-C) Mapping characteristics of the curated set of 83 persistent phage contigs, showing (A) average number of reads and (B) average quality of read mapping across each contig and (C) percentage of each contig's base pairs that have non-zero mapped reads. (D) Persistent MAGs assessed by comparing MAG size from time series phage bins (right clustered bars, sum of binned contig lengths) to the cumulative length of the persistent contigs in each bin (left clustered bars). Predicted host assigned using the most common classification among phage contigs in a bin.

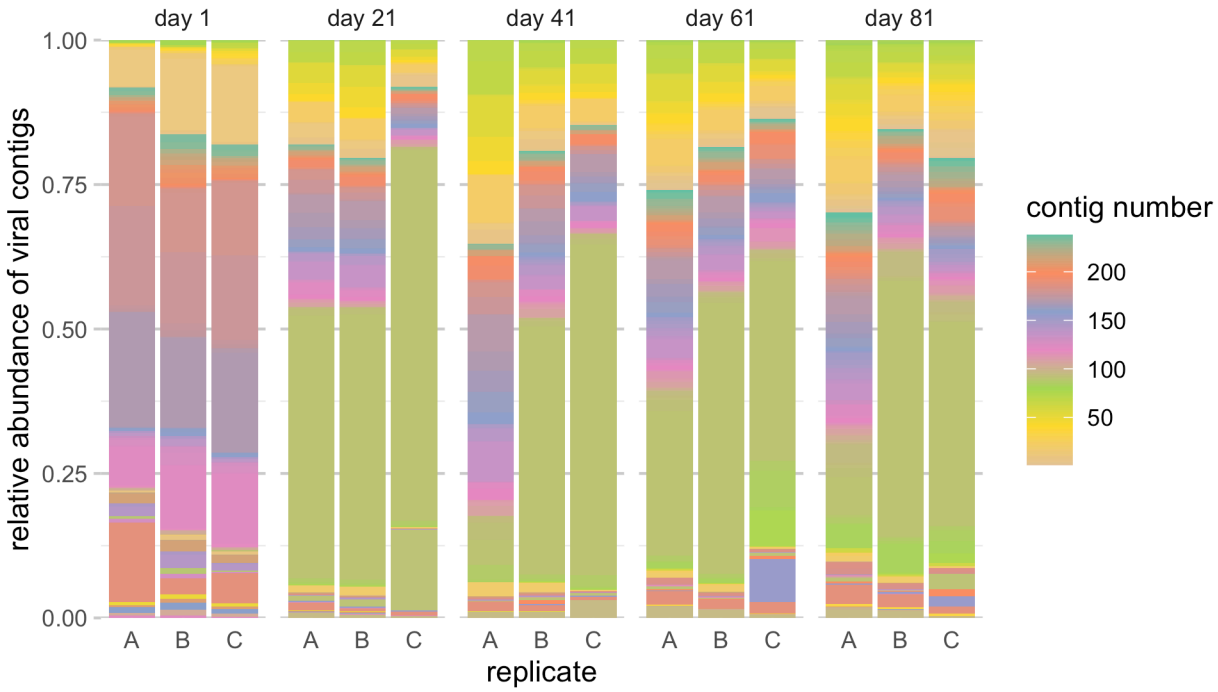

Supplemental Figure 3.2-1. Abundance over time of predicted phage contigs from 3 cheese batches.
Each of 224 curated phage sequences is shown in rainbow colors, scaled by relative read coverage of contigs at each time point in each replicate batch.

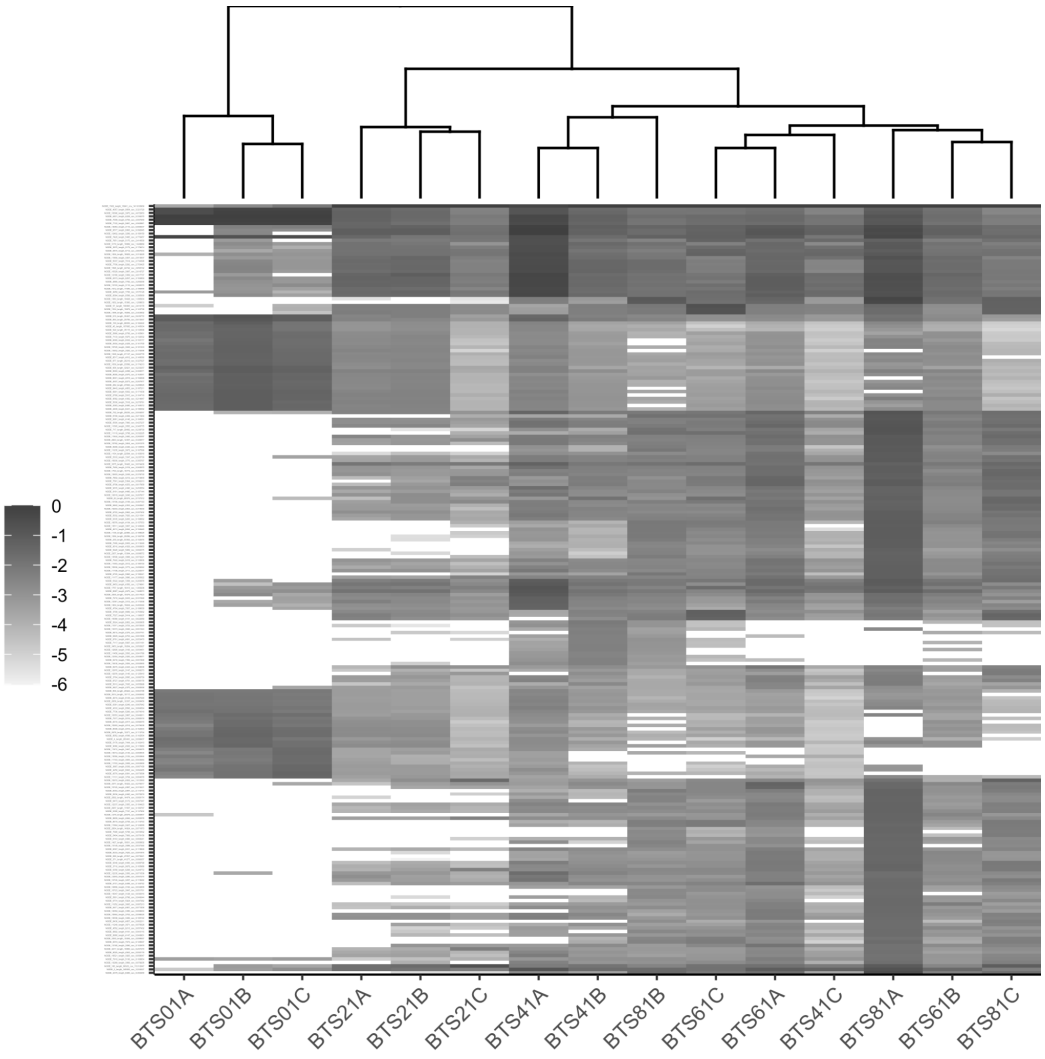

Supplemental Figure 3.2-2. Clustering phage contigs by presence/absence in each sample. Each of 224 curated phage sequences represented in rows is shaded by their mean coverage in each sample, coverage values normalized by sample and non-zero values log10-transformed. Time series sample names under each column are encoded as "BTS" followed by two numbers representing days of rind aging and letter "A", "B", or "C" denoting replicate batches. Clustering of cheese samples was done using a matrix of presence or absence of phage contigs in each sample. Heatmap was made using heatmaply version 1.2.1.

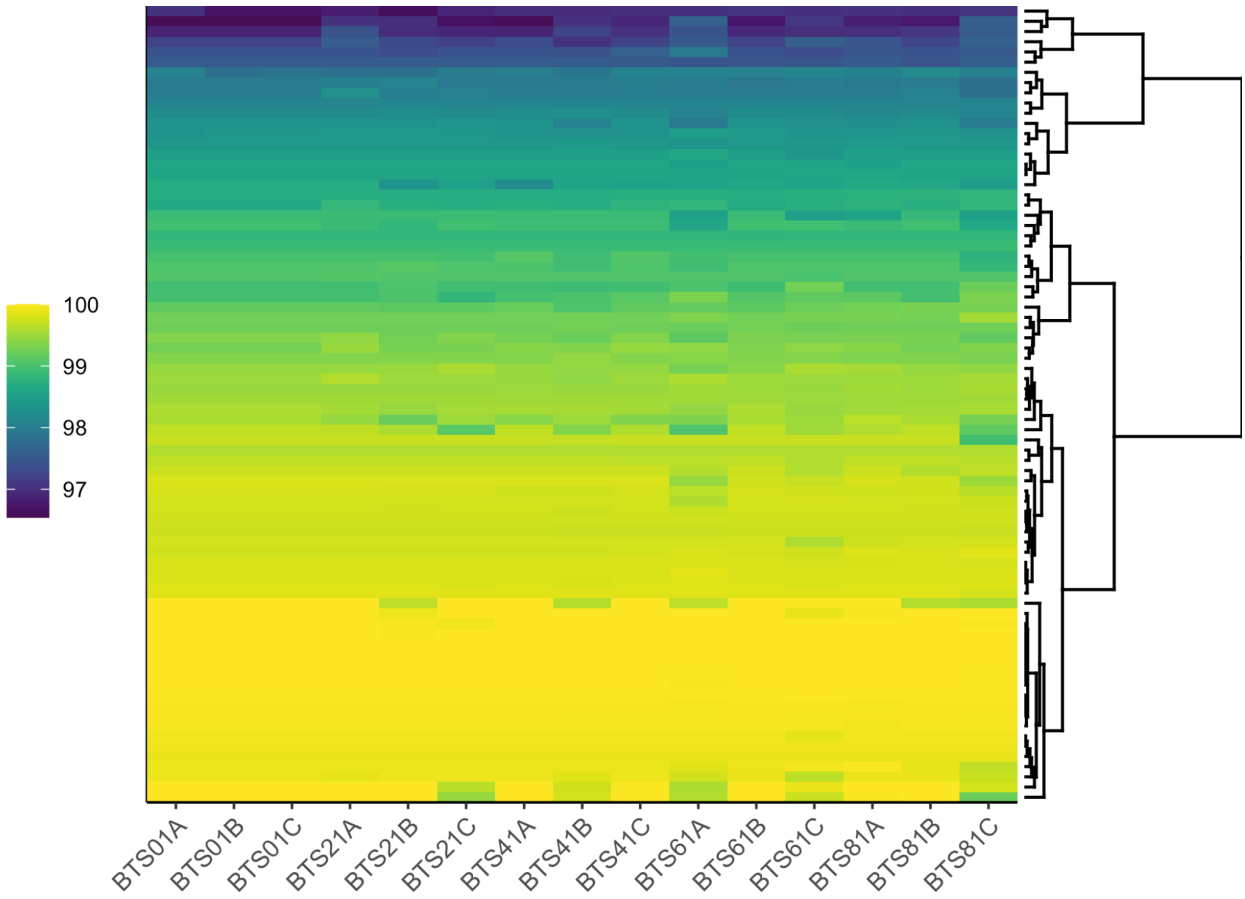

Supplemental Figure 3.2-3. Percent identity between dominant sequence variant of persistent phage contig versus time series sequence variants.
78 curated persistent phage sequences represented in rows are colored by their percent identity to the dominant sequence variant of the same contig in each time series sample. Time series sample names under each column are encoded as "BTS" followed by two numbers representing days of rind aging and letter "A", "B", or "C" denoting replicate batches. Heatmap was made using heatmaply version 1.2.1.

3.3 Acknowledgments

Chapter 3 consists of unpublished material. The following individuals are also authors on this work: Cong Dinh (UCSD), Galilea Guererro (UCSC) and Rachel Dutton (UCSD). The dissertation author is the primary author of this material.

CHAPTER 4. Zooming in and out on community assembly processes

4.1 Chapter Summary

We have so far characterized the succession of bacteria, fungi, and bacteriophage in a cheese rind microbiome. Using an *in vitro* model of this cheese rind, in Chapter 2 we showed that deacidification of the cheese by community members stimulates the growth of late-colonizing bacteria, and that inhibition by *Penicillium* is responsible for the loss of the yeast *Diutina*. In Section 4.2, we further explore these influential pairwise interactions that shape the pattern of succession, with the future goal of identifying mechanisms. Recognizing that these interactions are occurring in a spatially-structured biofilm, in Section 4.3 we lay a technical groundwork for examining the organization of microbes within the cheese rind biofilm. Preliminary images indicate that non-filamentous microbes are largely unmixed and spatially segregated from each other, suggesting that some community members may not co-exist closely enough in space for their interactions with each other to occur in the community.

4.2 Interaction mechanisms between microbes in a cheese rind microbiome

Introduction

While environmental pH modulation has been neatly shown to drive interactions outside of cheese microbiomes, the understanding of how such dynamics affect complex community assembly is still minimal (Herschend et al., 2018; Ilhan et al., 2017; Ratzke and Gore, 2018; Ratzke et al., 2020; Tripathi et al., 2018). The change in cheese rind community pH over cheese aging, rising from pH 5 to almost pH 8, is possible due to the nutrient environment of fresh curd consisting of high protein and low fermentable carbon. The metabolic contributions to deacidification of the

cheese rind have been minimally explored, and is commonly attributed to consumption of lactate (McSweeney, 2004). Also likely to contribute to rind deacidification is production of ammonium as a byproduct of amino acid catabolism (Curtin and McSweeney, 2004; Fröhlich-Wyder et al., 2019). Here I present an initial investigation into the contributions of a volatile-mediated mechanism of cheese rind deacidification towards stimulating cheese rind community members.

Even as neutralization of rind pH works to stimulate species growth and increase rind microbiome diversity, *Penicillium* sp. strain JBC was shown to broadly inhibit the population size of community members. Species of the fungus *Penicillium* are well-known for products of their secondary metabolism, including the antibiotic penicillin (Kumar et al., 2018). Here we pursue possible antibiotic-mediated community interactions involving *Penicillium*, particularly the mechanism of inhibition against *Diutina catenulata* strain 135E, and consider the scope of its antibiotic capabilities against other cheese rind-associated fungi.

Results

Cheese rind deacidification through volatile organic compounds. The model cheese rind system uses 96-well plate-based growth assays for a relatively high-throughput assessment of the growth of cheese rind microbial communities. While some level of variability is to be expected among non-laboratory adapted microbes, there came a point at which years of growing the bacterium *Brevibacterium* sp. strain JB5 in monoculture revealed two distinct alternate growth patterns: one in which the growth rate was slow and relatively constant over the 21-day experiment, and a second in which rapid exponential growth occurred between days 3 and 10 and a population maximum was reached between days 10 and 21.

I noticed that the second, rapid growth phenotype was correlated with growing *Brevibacterium* monocultures in the same 96-well plate with *Penicillium* sp. strain JBC. Given

previous work using a cheese rind microbiome system showing that fungal volatiles can shape community composition (Cosetta et al., 2020), I wondered whether *Penicillium* volatiles were sufficient to stimulate rapid growth of *Brevibacterium*. After 10 days of sharing airspace, I found that *Penicillium* volatiles were capable of stimulating *Brevibacterium* growth, where cheese medium alone could not (Figures 4.2.1A, 4.2.1B). Interestingly, when I measured the pH of the medium, it was apparent that these *Penicillium* volatiles had increased the pH of the neighboring medium. Furthermore, I noticed that our positive control for *Brevibacterium* growth, on CCA pH 7 medium, had increased the pH of its neighbor medium as much as it had increased medium pH *in situ* (Figure 4.2.1C).

Since deacidification was shown to be an impactful driver of rind community development (Chapter 2), I tested all community members for their ability to increase medium pH through volatile production with the experimental set-up shown in Figure 4.2.1D. *Penicillium*, *Brevibacterium*, and *Scopulariopsis* were all capable of significantly raising the pH of CCA pH 5 through volatile compounds within 5 days of growth (Figure 4.2.1E). Additional mechanisms of deacidification, other than through basic volatile compounds, are apparently at play: some of the largest *in situ* pH increases derive from species that don't produce deacidifying volatiles, including *Staphylococcus* species and *Brachybacterium* (Figure 4.2.1F). Also notable is that while *Diutina* was found to be a rapid *in situ* deacidifier of pH 5 CCA media, it is apparently not contributing to volatile-based deacidification nor deacidification much beyond pH 7 (Figure 4.2.1E-F).

Inhibition of *Diutina catenulata* strain 135E by *Penicillium* sp. strain JBC. Culturing *Diutina* with *Penicillium* results in a die-off of *Diutina catenulata* strain 135E (Supplemental Figure 2.2-2). Plate-based assays show that *Penicillium* creates a diffusible molecule that can prevent *Diutina* growth (Figure 4.2.2A). Production of this molecule is approximately correlated

with *Penicillium* sporulation, as a zone of inhibition in *Diutina* growth is strongest when *Diutina* is plated at the onset of *Penicillium* spore production (Figure 4.2.2A). Furthermore, fluorescence *in situ* hybridization of *Penicillium-Diutina* co-cultures show deformed and fragmented *Dituina* cells at the top of biofilms, with the affected region increasing over time (Supplemental Figure 4.2-1).

The *Penicillium* sp. strain JBC genome, assembled from Oxford Nanopore sequencing reads using Canu (Koren et al., 2017), was annotated using the fungal version of the secondary metabolite predictor antiSMASH (Blin et al., 2019). 46 biosynthetic gene clusters (BGCs) were predicted, but few were good matches to known gene clusters. One of these good matches is a gene predicted to synthesize naphthopyrone, a family of molecules that includes fungal pigments (Xu et al., 2019). Another gene, with the closest match to database genes (86% nucleotide identity), is predicted to synthesize a cyclic depsipeptide called fungisporin. Fungisporins have previously been extracted from *Penicillium* strains with activity against yeasts (Oppong-Danquah et al., 2020), but antifungal activity has not been directly attributed to this family of mycotoxins.

Without any clear molecular targets, we attempted a crude extraction of the active compound responsible for killing *Diutina* using a number of culturing (liquid mat vs. agar) and extraction (filtration vs. chemical extraction) methods. Extract activity was evaluated by applying extract to antibiotic discs on top of a freshly inoculated lawn of *Diutina* (for small volumes of concentrated extracts) or by soaking agar plates with 0.1-1 mL of extract before inoculating a dilute lawn of *Diutina* (for unconcentrated culture filtrates). Only fresh (unfrozen) liquid culture filtrate was able to inhibit *Diutina* growth, though this result is difficult to reproduce (Figure 4.2.2C). It should be noted that while zones of inhibition on PCAMS are visible, preliminary pairwise

cocultures of *Dituina* and *Penicillium* on PCAMS do not exhibit the same level of *Diutina* death as when grown on cheese curd-based agar medium (data not shown).

Interactions between cheese rind-associated fungal strains. In light of widespread inhibition by *Penicillium* revealed by *in vitro* pairwise cocultures (Chapter 2), we further explored the scope of inhibition between fungal species at the cheese rind. In addition to preventing the growth of *Diutina*, *Penicillium* was found to inhibit the growth of the other cheese rind-associated yeast in the screen, *Debaryomyces* sp. strain 135B (Figure 4.2.2B). Despite also inhibiting the growth of *Scopulariopsis* sp. strain JB370 in pairwise coculture (Figure 2.2.2), no clear zone of inhibition was visible in these assays.

In vitro streak inhibition assays were performed to look at the effect of other cheese rind-associated fungal species on *Diutina*. The growth-inhibiting phenotype by *Penicillium* sp. strain JBC may not be common to other *Penicillium* species; *Penicillium* sp. strain SAM created no zone of inhibition greater than can be expected from competition alone, and *Penicillium* sp. strain #12, while possibly inhibiting *Diutina* in the 5-day preculture, does not inhibit to the same scale nor follow the same pattern of inhibition over preculture time. This assay also revealed that growth of *Diutina* is inhibited when plated against *Scopulariopsis* sp. strain JB370 that had been precultured for 5 days, but not when this *Scopulariopsis* had been precultured for 0 or 2 days (Supplemental Figure 4.2-2). This may reflect the small inhibitory phenotype observed in pairwise coculture (Figure 2.2.2).

These *in vitro* streak assays were further expanded to assess the effects of many of our cheese rind-associated fungal isolates against each other. Interestingly, among all other streak pairs, *Geotrichum* species were the most frequently and strongly affected by other fungi, after *Diutina* and *Debaryomyces* (Supplemental Figure 4.2-3). *Geotrichum*, while considered

filamentous fungal molds, share biological features with yeasts (Morel et al., 2015). All of these target species were affected by the same set of fungi: two *Penicillium* strains, JBC and #12, and two *Scopulariopsis* strains, JB370 and 165-5.

From this expanded all-versus-all interactions panel, *Debaryomyces* was often found to produce colonies that resisted inhibition by other fungi (Supplemental Figure 4.2-4A). To assess whether this might be due to a polyclonal glycerol stock of *Debaryomyces*, cells from resistant colonies and cells from the surrounding lawn were both streaked out to select for isolate clones. These isolate clone strains, called "pRes" and "pWT," along with a single isolate colony from the original glycerol stock of *Debaryomyces*, were tested as targets for a streak assay against all fungal sources. The pRes strain grew much better in the vicinity of fungal source precultures than the pWT strain, reinforcing that the pRes strain is resistant to fungal growth inhibition (Supplemental Figure 4.2-4B). That pRes is globally more resistant, regardless of the source fungus, suggests a non-specific mechanism of improved resistance. Furthermore, multiple target streaks of pWT, specifically against *Geotrichum* or *Penicillium* sp. strain JBC or #12, eventually grew resistant colonies, indicating a high rate of mutation for resistance (Supplemental Figure 4.2-4B, right).

Discussion

In this section we pursued mechanisms of stimulation and inhibition identified to be influential in the pattern of succession of a cheese rind. We identified an unexpected method of stimulation through deacidifying volatile compounds, and further exploration of inhibition by *Penicillium* indicates that this cheese rind isolate may be synthesizing novel antifungal compounds under specific conditions.

Our discovery that volatile compounds, produced by a subset of cheese rind bacteria and fungi, are capable of deacidifying cheese sets up an additional role for microbial volatiles in

directing community assembly. While the study by (Cosetta et al., 2020) found that primarily *Vibrio* was stimulated by fungal volatiles, and in fact through acidic volatiles, the experiments presented in this section reveals a stimulative role for fungal volatiles that is presumably mediated by alkaline volatiles. Work in other systems has identified pH-increasing volatile compounds with biological effects, such as triethylamine and ammonia (Jones et al., 2017; Vylkova et al., 2011). While these studies identified deacidifying volatiles from yeast strains, the cheese rind-associated yeast *Diutina* was not found to produce deacidifying VOCs, despite its central role in early *in situ* deacidification of the cheese rind community model as presented in section 2.2.

Despite 46 predicted BGCs in the *Penicillium* sp. strain JBC genome, few were annotated and even fewer matched well to known gene clusters. There is increasing interest in exploring fungal secondary metabolites (Keller, 2019) and cheese rind-associated species may be a vast source of bioactive molecules (Pierce et al., 2021). The antifungal activity against *Diutina* and *Debaryomyces* is of particular interest since to the best of our knowledge there are no antifungals identified that are specifically active against yeast.

Methods

Volatile-based deacidification assay. Two 35-cm petri dishes were placed within a larger 90-mm petri dish. 1 cm^2 squares of CCA medium were cut out using a sterile exacto knife and placed into the smaller petri dishes. 10 uL of diluted frozen glycerol stocks was spread evenly across a CCA square to plate 2,000-10,000 CFUs, then agar was dried under a flame. Small petri dish lids were discarded, large petri dish lids were parafilmed on, and then experiments were incubated at 21 °C in the dark. pH was measured with an ethanol-sterilized micro pH probe, submerging just the glass bulb of the probe into the medium.

In vitro streak assay. Source species being tested for activity were inoculated from glycerol stocks at the top of PCAMS "OmniTray" plates, unless otherwise noted. Glycerol stocks were diluted 1/10X with 1X PBS, then 30 uL of source stock was spread in a ~1 cm band along the long edge of the plate using a sterile toothpick. If co-inoculating the target species being tested for susceptibility, source streaks were let to dry before proceeding. For source preculturing, plates were lidded and stored in the dark at room temperature (~23 °C). To add target species, 10-uL streaks of target species glycerol stocks (diluted 1/10X with 1X PBS) were added perpendicular to the source species using a sterile toothpick, taking care to get close to but not touch the source species. Plates were lidded and grown at room temperature in the dark.

Metabolite extraction techniques. For liquid cultures of *Penicillium*, spores from a glycerol stock were added to a 250-mL flask with 40 mL 0.5X LB + 1% skim milk and grown at room temperature in the dark, without shaking, for 4 to 6 days (after onset of sporulation). Optionally, a target species was precultured in the medium for 1-2 days with shaking before adding *Penicillium* spores along with a supplemental 5 mL 2% sterile skim milk solution. To obtain the culture filtrate, the culture was strained through a sieve to remove the mycelial mat. For sterile raw culture filtrate, the liquid medium was transferred to a 50-mL falcon tube, centrifuged to pellet any remaining cells, then the aqueous layer was filtered through a 0.22 μm filter. To perform extractions, strained culture medium was transferred to a flask and an equal volume of organic solvent (ethyl acetate: EtOAc; acetonitrile: AcN) added and mixed on a rotary shaker for 10 minutes. The organic layer was transferred to a fresh flask, and the organic extraction repeated. The organic layer was dehydrated over sodium sulfate and then dried under air and resuspended in methanol.

For agar-based extractions, *Penicillium* spores were spread on PCAMS plates and grown into a fungal for 4 to 6 days. For extractions, fungal mats were removed by scraping with 1 mL of 1X PBS. For "freeze-and-squeeze" agar extractions, plates were stored at -20 °C overnight then thawed the following day and liquid filtered through a 0.22 μm filter. For chemical extraction, scraped agar was cut up using an exacto knife and transferred into a 50-mL tube. A scraper was used to further break up the agar. 20 mL of organic solvent or 1X PBS was added to agar and samples placed in an ultrasonic bath for 30 minutes to extract. Tubes were centrifuged to pellet agar and then the liquid layer was transferred to a new tube. Fresh solvent was added to the agar and the extraction process repeated. The PBS-based extracts were filtered through a series of 0.45 μm then 0.22 μm filters. The organic extracts were dehydrated over sodium sulfate then dried under air and resuspended in methanol.

Figures

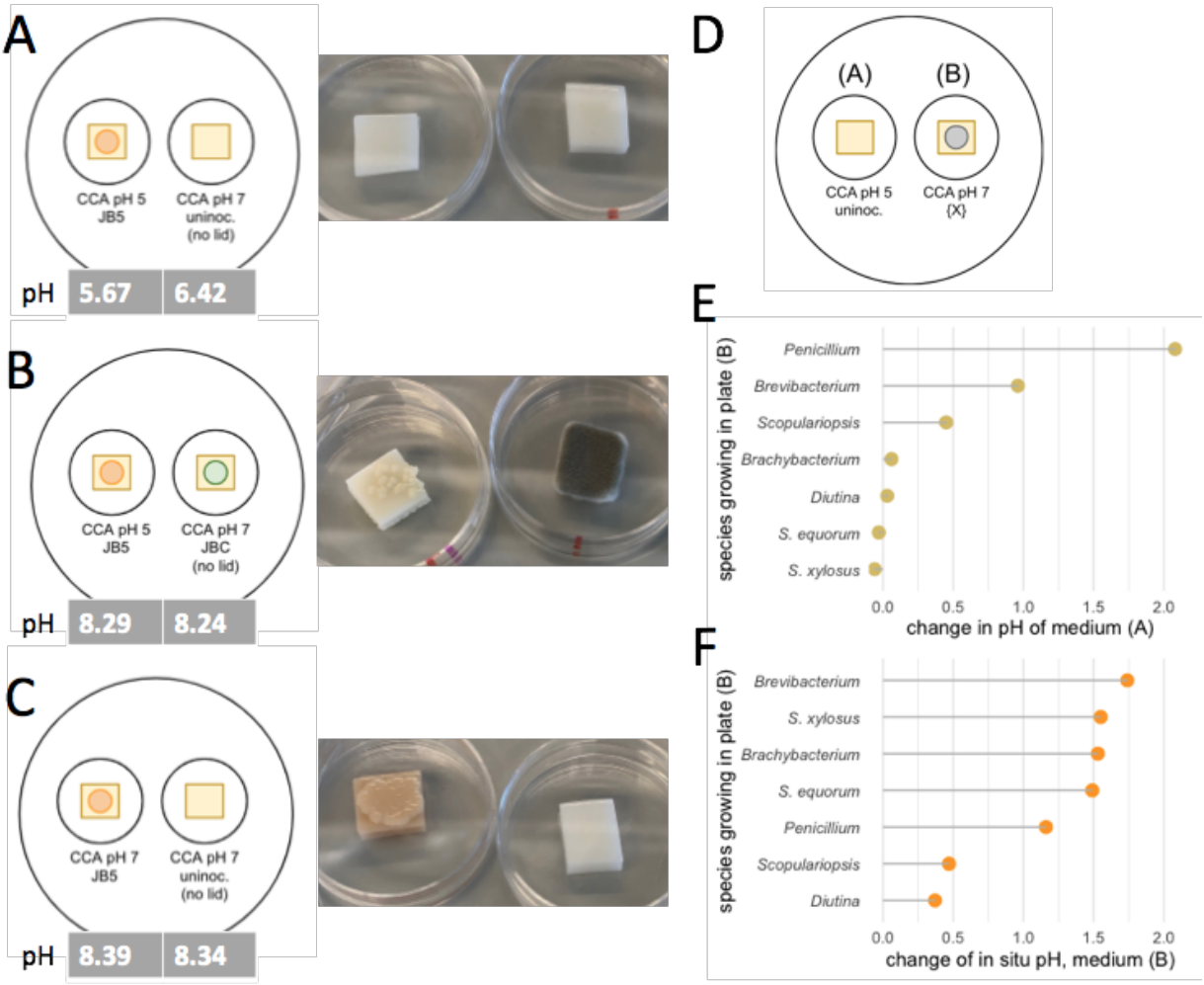

Figure 4.2-1. Deacidification through volatile compounds.
(A-B) Growth of *Brevibacterium* sp. strain JB5 on CCA pH 5, either sharing airspace with uninoculated CCA pH 7 (A) or CCA pH7 inoculated with *Penicillium* sp. strain JBC (B). "Uninoc." is short for "uninoculated." (C) Growth of *Brevibacterium* sp. strain JB5 on CCA pH 7, sharing airspace with uninoculated CCA pH 7. (D) Experimental schematic for (E-F). X marks the plate where a cheese rind-associated microbe is inoculated. (E) change in pH of CCA pH 5 medium through volatiles produced by species growing on neighboring CCA pH 7 for 5 days. (F) In situ change in pH of CCA pH 7 after 5 days of species growth.

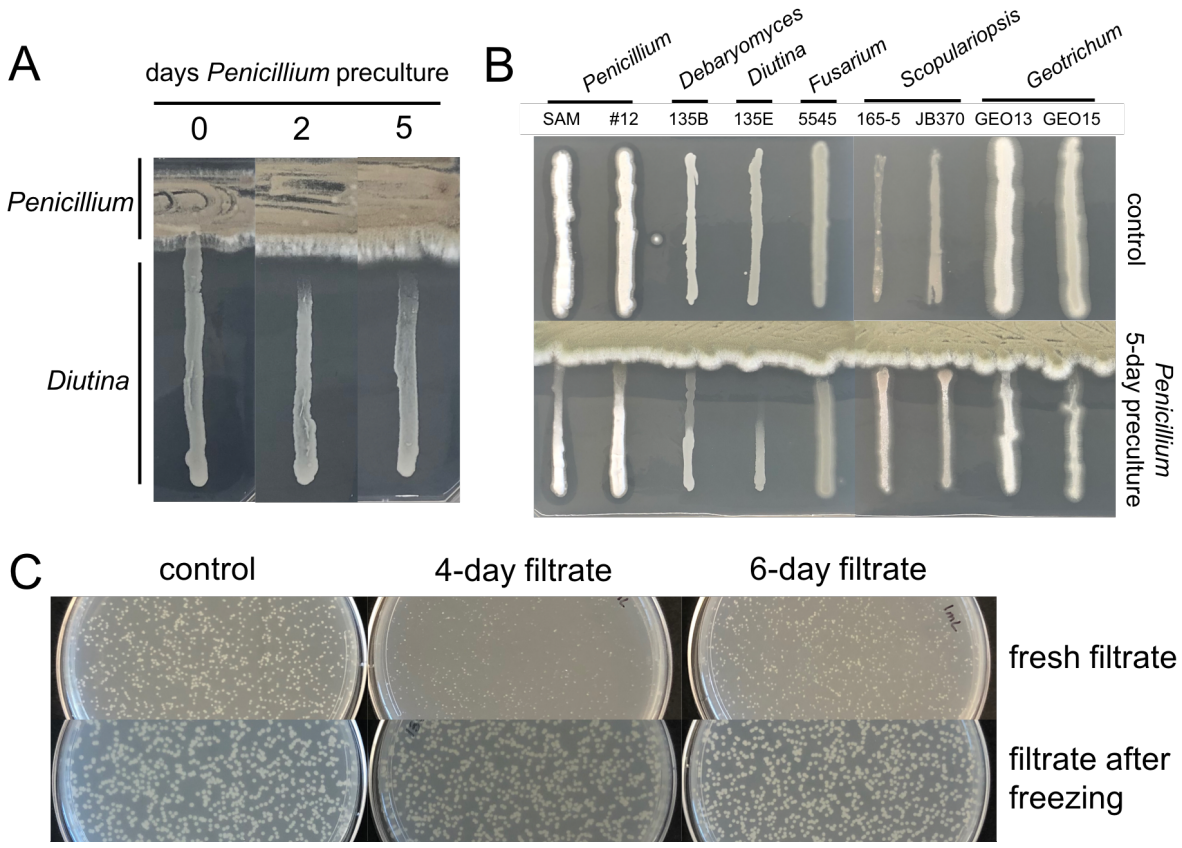

Figure 4.2-2. Susceptibility to inhibition by *Penicillium* sp. strain JBC.
(A-B) Screen of target species against *Penicillium* sp. strain JBC precultured to different ages (A) or for 5 days (B) before plating target species. (C) Effect of 1 mL *Penicillium* culture filtrate on colony size of *Diutina catenulata* 135E, filtrates from liquid cultures of *Penicillium* grown for 4 days or 6 days. Control = no filtrate added.

Supplemental Figures

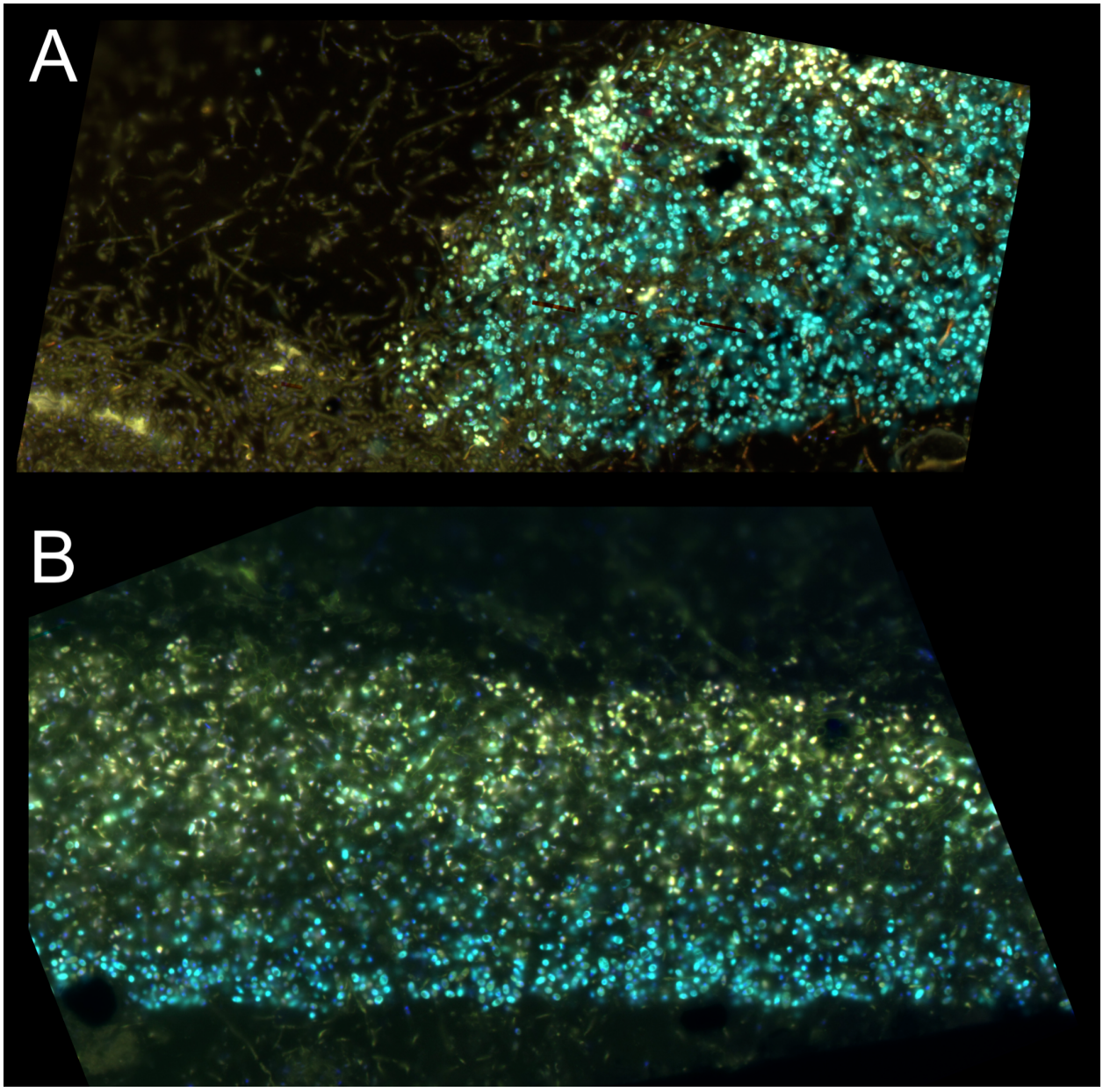

Supplemental Figure 4.2-1. Biofilm structure of cocultures containing *Penicillium* sp. strain JBC and *Diutina catenulata* strain 135E.
Vertical cross-sections of *in vitro* rind biofilms that were inoculated on CCA pH 5 with 200 CFUs of each fungal strain and cultured for 10 days (A) or for 21 days (B) before harvest and processing (see methods in section 4.3). Biofilm cross-sections are oriented so the cheese medium is at bottom and the air interface of the biofilm is at the top in each panel. *Diutina* cells were hybridized *in situ* with a fluorophore-labeled DNA probe (Ccat1344-Cy5, see Table 4.3.3) targeting a unique section of the 18S rRNA subunit (cyan channel). Fungal cell wall matter autofluorescence is shown in the yellow and red channels.

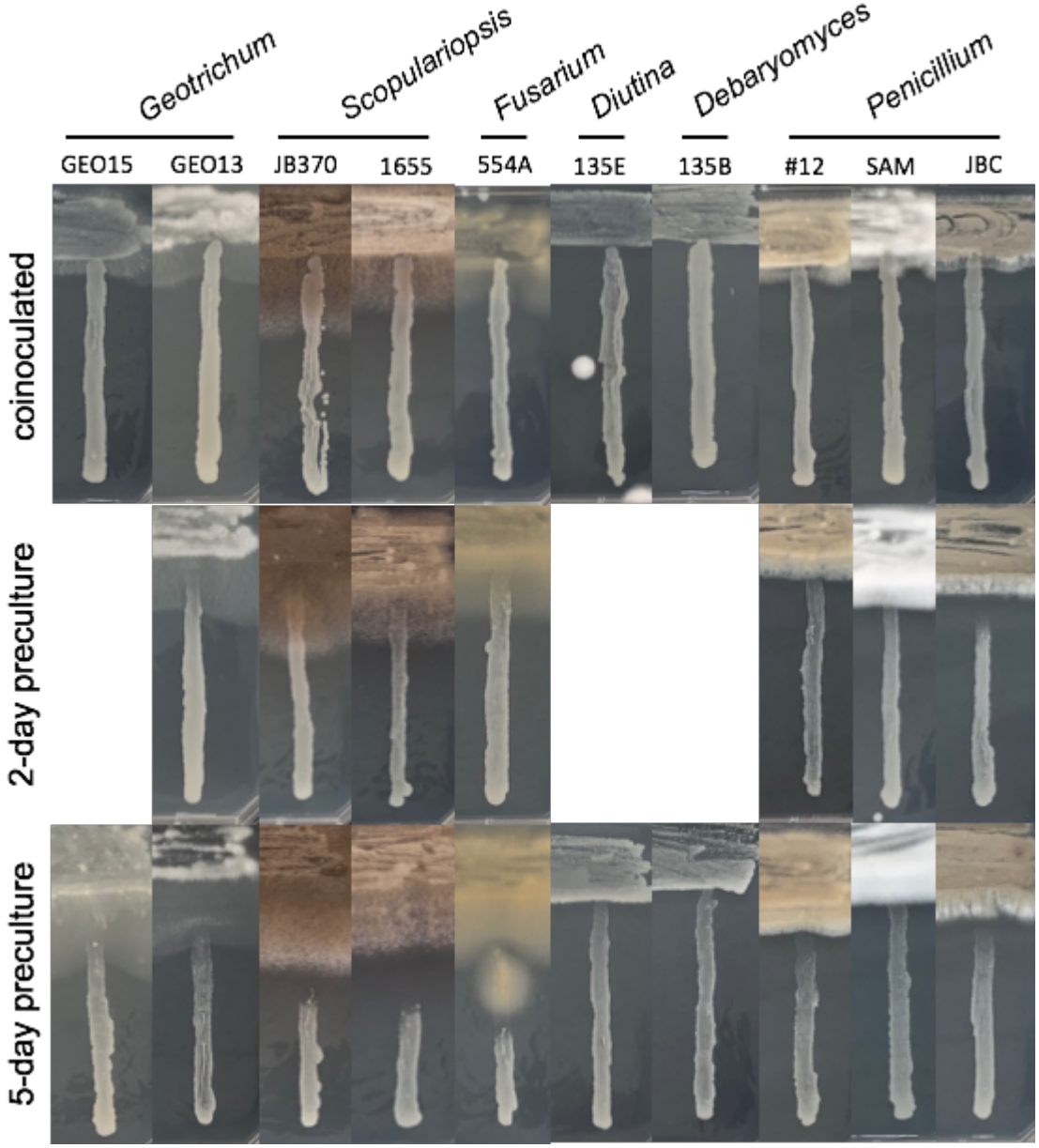

Supplemental Figure 4.2-2. Fungal effects on *Diutina catenulata* 135E.
Growth of vertical *Diutina* streaks tested against source fungal strains marked at top. Source strains were inoculated at the same time as *Diuitna* ("coinoculated", top) or they were precultured for 2 or 5 days before inoculating target *Diutina* streaks.

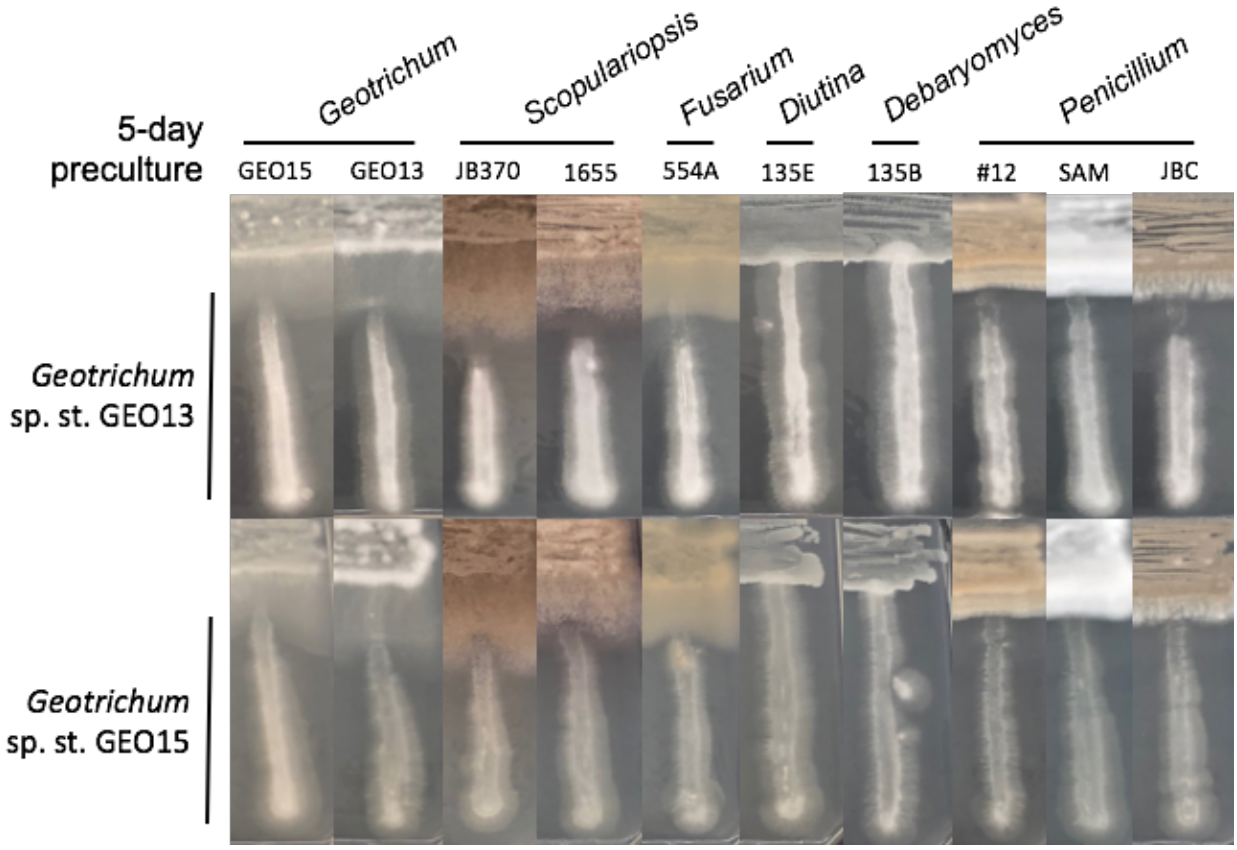

Supplemental Figure 4.2-3. Fungal effects on *Geotrichum* strains.
Growth of vertical *Geotrichum* streaks tested against source fungal strains marked at top. Source strains were precultured for 5 days before inoculating target *Geotrichum* streaks.

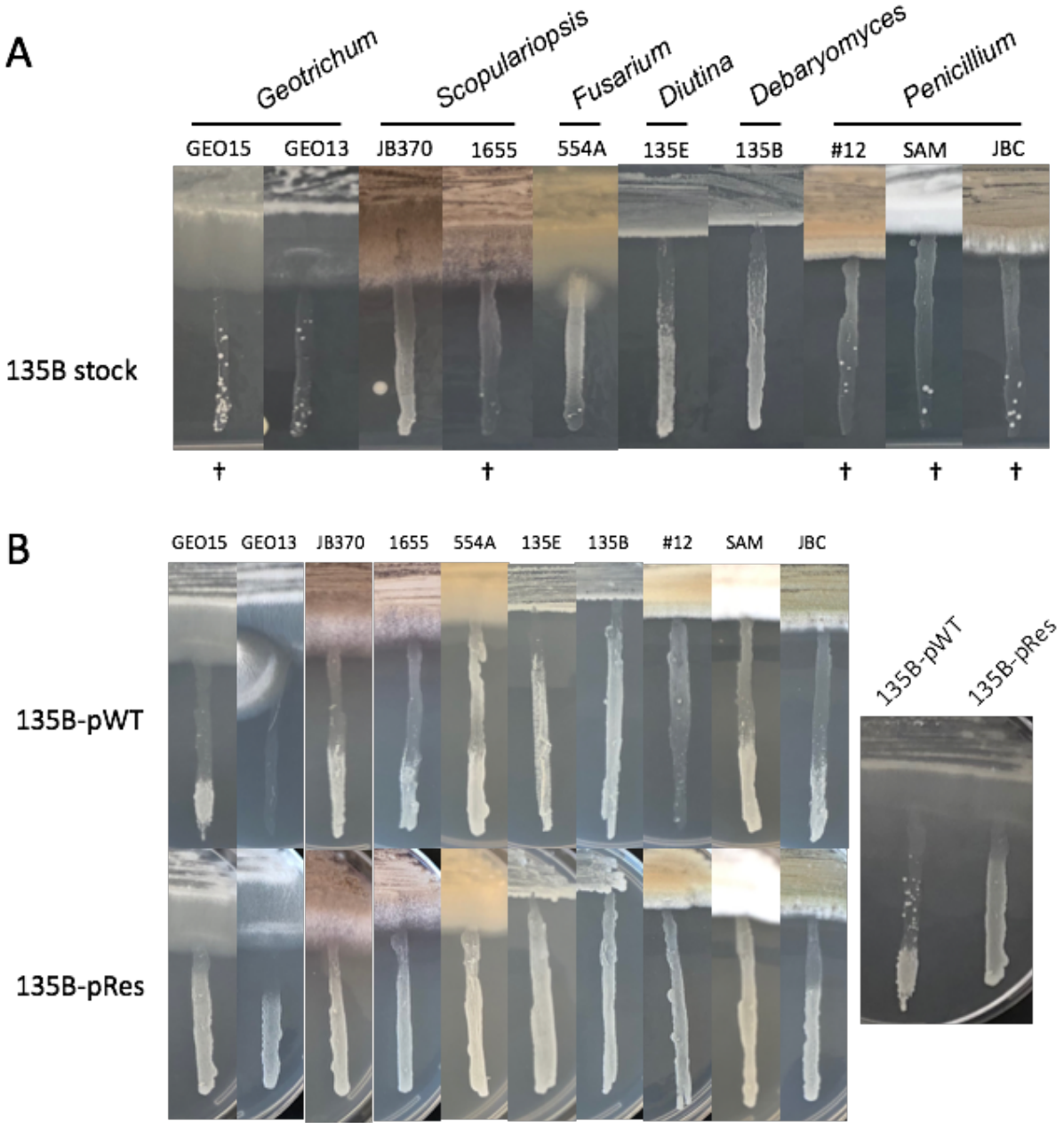

Supplemental Figure 4.2-4. Fungal effects on *Debaryomyces* sp. strain 135B.
Growth of vertical *Debaryomyces* streaks, from frozen stock of the yeast (A) or from single colonies isolated from a streak in panel A (B), tested against source fungal strains marked at top. Source strains were precultured for 5 days before inoculating target *Debaryomyces* streaks. (A) Pictures show four-day growth of *Debaryomyces.* Crosses mark combinations in which resistant colonies have been observed previously. (B) The pWT isolate was taken from a lawning portion of a streak, and the pRes isolate was picked from a fatter, "resistant" colony. Complete panel pictures were taken two days after streaking the target *Debaryomyces*. Right panel shows the development of resistant colonies against source strain GEO15, picture taken 19 days after target streak inoculation.

4.3 Spatial organization of a cheese rind biofilm

Introduction

Many relevant biofilms, including those involved in medicine, that exist in the environment, or are developed for industries, live in a spatially organized structure. We know that these structures may be layered according to the physicochemical needs of the biofilm species, such as in the case of a Winogradsky column or microbial mats (Krumbein et al., 2003). As microscopy techniques have advanced, microbiologists have taken a closer look at multi-cellular spatial structures. Use of fluorescent genetic markers has revealed that the organization of microbial biofilms also reflects the interactions between microorganisms, such as competition (spatial segregation) or cooperation (spatial intermixing) (Estrela and Brown, 2013; Momeni et al., 2013; Nadell et al., 2010; Venters et al., 2017).

A complex biofilm community is likely to show spatial phenotypes characteristic of both physiochemical needs of the community and species interactions. This is evident in the spatial structure of human dental plaque which, through the use of microbe-specific fluorescent probes, shows zones of layering that can be attributed to niche chemical requirements in addition to regions of close association between co-aggregating species (Mark Welch et al., 2016). Spatial structure can also in turn interfere with interactions between pairs of microbes in a community, through imposing higher-order interactions or providing physical protection (Estrela and Brown, 2018; Harcombe et al., 2014; Testa et al., 2019). It is evident that understanding spatial organization is important for contextualizing microbial interactions within multi-species communities.

In this Chapter, we use the *in vitro* model community studied in Chapter 2 to build protocols for uniquely identifying each bacterial and fungal isolate within the spatial context of a lab-grown multi-species biofilm and we suggest future avenues for using these techniques.

Results

Alternate protocols for fluorescently labeling bacteria and fungi. Fluorescent *in situ* hybridization (FISH) protocols were optimized for each isolate bacteria and fungi making up the *in vitro* rind community model. In brief, FISH protocols follow a process where microbial cells are chemically fixed, enzymatically permeabilized as necessary, dehydrated, then incubated with nucleotide-based probes that hybridize to specific sequences in the cell. For fluorescence-based microbial taxonomic identification, unique regions of the small subunit ribosomal RNA are targeted with a complementary DNA probe conjugated to a fluorescent molecule.

Universal prokaryotic and eukaryotic probes were used to optimize FISH protocol parameters, including pre-hybridization treatments and hybridization conditions (Table 4.3.1). Pure cultures of each species, ideally at mid-log stage to maximize ribosomal content, were prepared to optimize parameters for all bacteria and fungi. The ultimate goal was to build a protocol that will simultaneously allow the labeling of all bacteria and fungi in the community, for combinatorial labeling and spectral imaging (CLASI-FISH) of multi-species biofilms (Valm et al., 2012).

The bacteria making up the studied model community are all gram positive species: two *Staphylococcus* species and two Actinobacterial species of genera *Brevibacterium* and *Brachybacterium*. Since the thick peptidoglycan layer of gram-positive species can impede probe entry into cells, lysozyme permeabilization is a valuable enzymatic pre-treatment. This was effective for the Actinobacteria tested, but since many *Staphylococcus* species are well-known for having lysozyme-resistant cell walls (Bera et al., 2005), a staphylolysin treatment was tested. For *S. xylosus* strain BC10 and *S. equorum* strain BC9, no enzymatic treatment was found to improve

the fluorescent signal, while *S. succinus* strain BC15 was resistant to any labeling regardless of fixation or enzymatic permeabilization treatment.

For increased fungal signal, a chitinase pre-treatment was found to be particularly beneficial for increasing permeabilization of and probe binding to *Diutina*, and as an added feature it was found to significantly decrease autofluorescence of *Scopulariopsis*, a phenomenon that has been documented before (Baschien et al., 2001). When performing FISH on both bacteria and fungi at the same time, the order of enzymatic pre-treatments before hybridization was found to matter: treating bacterial cells with lysozyme before chitinase treatment, but not chitinase before lysozyme, resulted in lysed cells, suggesting that permeabilization with lysozyme rendered bacterial cells sensitive to the chitinase solution.

Filamentous fungi are particularly difficult to label using fluorescent probes that bind to ribosomal RNA sequences. One problem is the minimal effectiveness of using DNA-based probes. Multiple studies have found that peptide nucleic acid (PNA) probes, which contain a peptide backbone in place of a phosphate backbone for binding sequences of nucleosides, have had wider success in labeling fungi (Shinozaki et al., 2011; Teertstra et al., 2004). This may be because mold cell walls can have high lipid contents, with (Rogers et al., 1980) reporting *Penicillium charlesii* as having up to 37.5% lipid content in its cell wall. While PNA probes more successfully hybridize to small subunit ribosomal RNA sequences in filamentous fungi, they reveal inconsistent labeling throughout filaments. These inconsistencies take two forms: one seems to be related to whether filamentous are truly whole or alive, in that both nuclear staining and FISH fluorescence is correlated with visible cytoplasm (Lee, 2011); the second inconsistency is intracellular, wherein probe signal is punctate or fades along the length of a filament moving away from the growing tip,

suggesting that ribosomes are located specifically within fungal filaments (Supplemental Figure 4.3-1).

Since the ultimate goal was to develop a single protocol for simultaneous labeling of all bacteria and fungi, the fungal-specific and bacterial-specific protocols were strategically combined to create a "universal protocol." By systematically swapping protocol-specific parameters and measuring average fluorescence of labeled pure cultures, optimal universal conditions for hybridization could be achieved (Table 4.3.2).

Stabilizing structure of cheese rind biofilms. While chemical fixation of pure cultures is fairly straightforward, fixation of *in vitro* rind biofilms proved to be a challenge. Biofilms without filamentous fungi were not adhered to the surface of cheese curd-based agar, and as a result cells would diffuse away from the biofilm into the aqueous fixative. Agarose also failed to adhere to the medium and so attempts to embed in agarose disrupted the biofilm. When biofilms included filamentous fungi, the biofilm adhered to the medium, but since filaments tend to be hydrophobic, formaldehyde solution cannot evenly enter these biofilms for fixation. Formaldehyde vapor fixation is a technique that has been used previously for preserving the conidial structure of filamentous fungi for scanning electron microscopy (Kim, 2008). Using this simple method, the structure of biofilms without molds was maintained and biofilms with molds were evenly more evenly fixed and spore layers maintained.

To look inside of biofilms, sections are sliced for fluorescent imaging on slides. Traditional methods of sectioning samples (paraffin wax for microtomy, optimal cutting temperature fluid for cryosectioning) were found to be unsuitable as the porous structure of rind biofilms (particularly those including molds) lead to crumbling sections. I turned to polymerizing resins which were used for visualizing dental plaque samples (Mark Welch et al., 2016). Glycol methacrylate (GMA)

is allowed to infiltrate a fixed biofilm sample before a polymerizing agent is added to solidify the sample for sectioning. These hard resin samples can be successfully sectioned using an ultramicrotome equipped with a sharp glass edge, though samples thicker than those that this sectioning technology can produce (>4 μm) may be desirable for 3-dimensional rind structure. After sectioning, sections mounted onto slides are submitted to enzymatic permeabilization and FISH as described before.

Spatial structure of in vitro cheese rind biofilms. *In vitro* cheese rind biofilms are characterized by a thick mat of bacterial and yeast cells that build up to approximately 150 μm above the cheese surface, with mold hyphae growing into the cheese medium, through the mat of yeast and bacterial cells, and then above this mat or at least another 150 μm, where they sporulate. We hypothesized that fungal filaments might be able to transport medium nutrients further from the cheese surface and so biofilms containing molds might build up a taller mat of bacteria and yeast. However, biofilms consistently grew to be 120-150 μm tall, with no measurable difference between communities containing or lacking mold species (Figures 4.3.1, Figure 4.3.2).

Low initial inoculation density (200 CFUs of each species across a 96-well plate agar surface) leads to clusters of bacteria connected by yeast (Figures 4.3.1, Figure 4.3.2, Figure 4.3.4). These clusters, particularly at the surface of the cheese, suggest the formation of microcolonies that run up against each other. If biofilms are grown from an initially dense inoculation (2 million CFUs of each species across a 96-well plate agar surface), this microcolony-like structure is no longer visible; instead, we observe a more layered structure (Figure 4.3.4). The order of layering reflects the temporal pattern of succession of this community, shown in Figure 2.2.1, with early-colonizing *Staphlyococcus* species and *Diutina* at the bottom and late-colonizing *Brachybacterium* and filamentous fungi at the top.

Discussion

The presented protocol in this section allows for fluorescent identification of specific bacterial and fungal species from a cheese rind. This technique provides valuable context for microbiome interactions. Preliminary results indicate that bacterial species in particular are spatially segregated, either as microcolonies or in layers, with limited opportunities for direct interspecies bacterial interactions. This may contribute to the findings in Chapter 2 that successional dynamics of this *in vitro* community are primarily driven by fungal members of the community. Increased physical contact between fungi and bacteria, or fungi and other fungi, may contribute to their dominant role in affecting community growth.

Methods and Protocols

Preparation of pure cultures for FISH protocol testing. 2-mL liquid cultures in LB should be grown up with aeration. Once grown to mid-log, cells should be pelleted and washed with 1X phosphate buffered saline (PBS). For filamentous fungi, frozen spore stock is spread across a PCAMS plate and left to grow at room temp in the dark for 5 days. Filaments are gently removed from the plate using 1X PBS and a cell scraper, then filaments should be pelleted using slow centrifugation, and PBS removed. For any bacteria or fungi, then suspend cells in 1 mL 4 °C 4% paraformaldehyde (PFA) from a fresh ampule. Leave cells to fix in PFA for 8 hours. Pellet cells in centrifuge pre-cooled to 4 °C then wash twice using 4 °C 1X PBS. Resuspend cells in -20 °C 50% EtOH (v/v) and store cells at -20 °C for use.

Optimal bacterial FISH protocol for gram-positive cheese rind isolates. The optimal protocol for bacterial FISH is modified from (Pernthaler et al., 2001). Samples dried onto slides should first be subject to enzymatic pre-treatment: 2 mg/mL lysozyme (stored at -20 °C then thawed) should be applied over the sample (e.g., 25 uL lysozyme solution over a 1uL spot of fixed

cells) let to incubate at 37 °C for 10 minutes. All incubations done at temperatures higher than room temperature should be done in a lidded container made humid with a kimwipe or paper towel moistened with water. Wash off the lysozyme solution using cold 50% ethanol, then immediately proceed to a cold ethanol dehydration series: immerse slides in cold 50%, then 80%, then 100% ethanol for 3 minutes each. Let slides dry before continuing on to hybridization. Freshly prepare hybridization buffer (final 20% formamide, 900 mM NaCl, 0.01% sodium dodecyl sulfate (SDS), 20 mM Tris-HCl pH 7.5). 1 uL of probe (5 uM working concentration) should be added for every 100 uL hybridization buffer. Cover sample with well-mixed hybridization solution (e.g., 25 uL hybridization solution over a 1uL spot of fixed cells) and incubate in humid box for 3 hours at 46 °C. During hybridization, prewarm wash buffer (225 mM NaCl, 20 mM Tris-HCl pH 7.5, 1/100 volume 5 mM EDTA) to 46 °C. After 3 hours of hybridization, use wash buffer to rinse probes off slides (into formamide waste) and then cover samples with fresh wash buffer. Incubate samples in wash buffer at 46 °C for 15 minutes, then repeat washing process, including incubation. Slides should be protected by mounting in VECTASHIELD Antifade Mounting Medium and sealing coverslips with nail polish.

Optimal bacterial FISH protocol for gram-positive cheese rind isolates. The optimal protocol for fungal FISH is modified from (Teertstra et al., 2004). Samples dried onto slides should first be subject to enzymatic permeabilization: 2 mg/mL lysozyme (stored at -20 °C then thawed) should be applied over the sample (e.g., 25 uL lysozyme solution over a 1uL spot of fixed cells) let to incubate at 37 °C for 10 minutes. All incubations done at temperatures higher than room temperature should be done in a lidded container made humid with a kimwipe or paper towel moistened with water. Wash off the lysozyme solution using cold 50% ethanol, then let slides dry. Then incubate samples similarly with chitinase (1 mg/mL in 1% SDS - 1X PBS, adjusted to pH

5.5) at 30 °C for 10 minutes. Wash off the chitinase solution with cold 50% ethanol then immediately proceed to a cold ethanol dehydration series: immerse slides in cold 50%, then 80%, then 100% ethanol for 3 minutes each. Let slides dry before continuing on to hybridization. Freshly prepare hybridization buffer (100 mM NaCl, 0.5% sodium dodecyl sulfate (SDS), 25 mM Tris-HCl pH 9). 1 uL of probe (5 uM working concentration) should be added for every 100 uL hybridization buffer. Cover sample with well-mixed hybridization solution (e.g., 25 uL hybridization solution over a 1uL spot of fixed cells) and incubate in humid box for 1 hour at 54 °C. During hybridization, prewarm TE buffer (10 mM Tris-HCl pH 9.0, 1 mM EDTA) to 46 °C. After hybridization, use the wash buffer to rinse probes off slides and then cover samples with fresh wash buffer. Incubate samples in wash buffer at 54 °C for 20 minutes, then repeat washing process, including incubation two times more. Slides should be protected by mounting in VECTASHIELD Antifade Mounting Medium (Vector Labs) and sealing coverslips with nail polish.

Probe design for cheese rind isolates. Bacterial 16S rDNA sequences were acquired by colony PCR (27f and 1492r primers) and sanger sequencing. Fungal 18S rDNA sequences were acquired by extracting DNA using the PowerSoil DNA Isolation Kit (QIAGEN), then amplifying two regions of the 18S sequence (NS1 & NS4 primer pair, NS3 & NS8 primer pair) and submitting for sanger sequencing and assembling the two PCR-amplified regions into a single sequence using Geneious 10.2.6 (https://www.geneious.com). Bacterial strain-specific probe sequences were designed at sites with at least two mismatches along 18- to 22-nucleotide lengths of the 16S rDNA sequence. *In silico* probe hybridization and specificity for target versus off-target community 16S sequences was tested using mathFISH (Yilmaz et al., 2011). Fungal strain-specific probe sequences were taken from positions along the 18S rDNA sequence where fungal species-specific

probes had already been designed. Of two probes designed to bind at different rDNA sites, the most specific (not hybridizing to pure cultures of other species) or brighter-fluorescing of two probes was used going forward (Table 4.3.3). It should be noted that, if hybridization is specific, both probes can be used to nearly double the fluorescent signal from cells. While DNA-based probes work well for all bacteria and for the yeast *Diutina*, they were minimally effective at labeling filamentous fungal species. Instead, peptide nucleic acid (PNA) probes were ordered for labeling *Penicillium* and *Scopulariopsis*.

In vitro cheese biofilm culturing. Strains selected for *in vitro* model biofilms were the same as used in Chapter 2. Stocks were grown up in LB, washed, aliquoted, and stored at -80 °C in PBS-20% glycerol or, for molds, scraped up from a CCA plate then aliquoted and stored at -80 °C in PBS-20% glycerol. Cell stocks were quantified through stock dilution and colony counting. For inoculation, stocks were diluted to 200 CFUs / 1 µL then 1 µL of each species for a community mixed together. Cell mixes were inoculated on CCA pH 5 in 96 well plates. Cell mixtures should be additionally diluted if necessary and plated on 90-mm petri dishes to count the inoculation size of each species. Plates were lidded and left to dry overnight at room temperature. On day 1 plates were sealed with an Aeraseal film and placed in a bag with a damp paper towel to maintain moisture. On day 2 bags containing plates were moved to 15 °C and grown in the dark.

Biofilm processing for spatial analysis. If measuring community composition, replicate biofilms should be harvested and plated for colony forming units as described in Section 2.2, "Methods." After harvesting biofilms to use for cell counts, the 96-well plate is flipped upside-down over an OmniTray base containing 10 mL 4% PFA from a fresh ampule. Apply parafilm around the two plates to seal them, then tightly tape down the connected plates to the chemical fume hood surface to ensure the seal. Samples are vapor-fixed for at least 3 hours, then biofilms

with their cheese agar plug are carefully removed using an appropriately curved tool, e.g. we use a cuticle pusher. Excess cheese is removed using an Exacto knife, leaving 1-2 mm agar under the biofilm. Transferred samples to individual microcentrifuge tubes containing 1 mL cold 50% ethanol, then store at 4 degC at least overnight.

For embedding, fixed samples are first trimmed to fit into resin molds (approximately 2-3 mm wide and 5-7 mm long). Samples are then subject to dehydration by transferring samples into cold 80% ethanol then cold 100% ethanol for ~2 hours each at 4 °C. Then, samples are transferred to Technovit 8100 infiltration solution and incubated at 4 °C for 6-8 hours. Mold should be pre-cooled to 4 °C, and all next work should be done on a cold surface (we use Lab Armor Beads cooled to 4 degC). Infiltrated samples are transferred into mold wells and then polymerization solution is mixed up, pipetted into wells to cover samples, and quickly covered with small polyethylene sheets for a hermetic seal. The mold is wrapped with a paper towel to soak up any condensation, and samples in the mold are left at 4 °C overnight to polymerize. After polymerizing, samples should be stored hermetically at room temperature, or at 4 °C in the presence of a dehydrating substance.

Figures

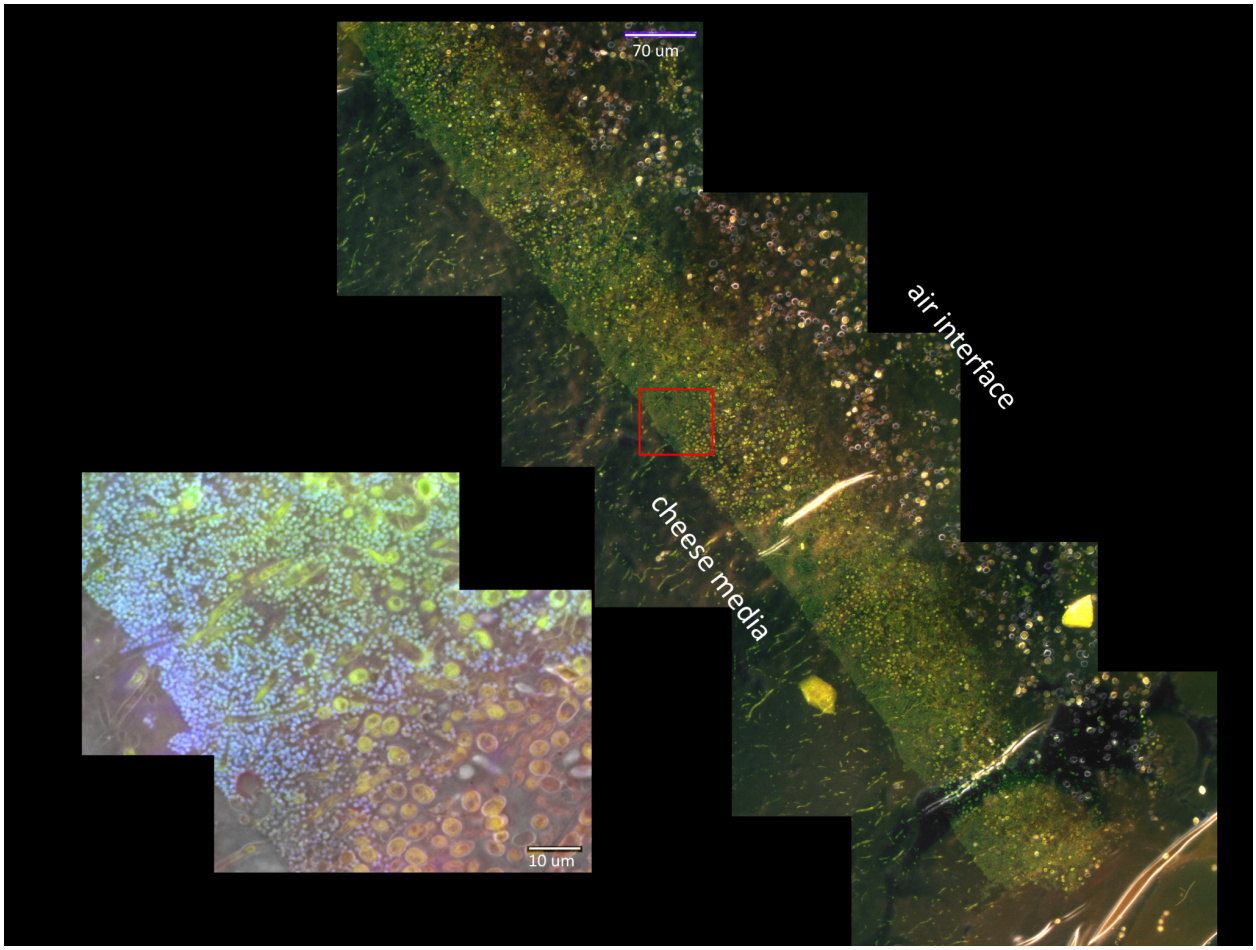

Figure 4.3-1. Biofilm structure of *in vitro* cheese rind.
Biofilms were grown for 12 days on CCA pH 5 before processing. Biofilm slice images are oriented according to labels. Large slice was imaged using green and red filters, illuminating autofluorescence of bacteria and fungi. Inset image, zooming in on the region outlined in red, shows bacteria nuclei stained with DAPI (blue channel), and autofluorescence of fungal cells in the green and red channels. Yeast are egg-shaped and molds look like empty tubes.

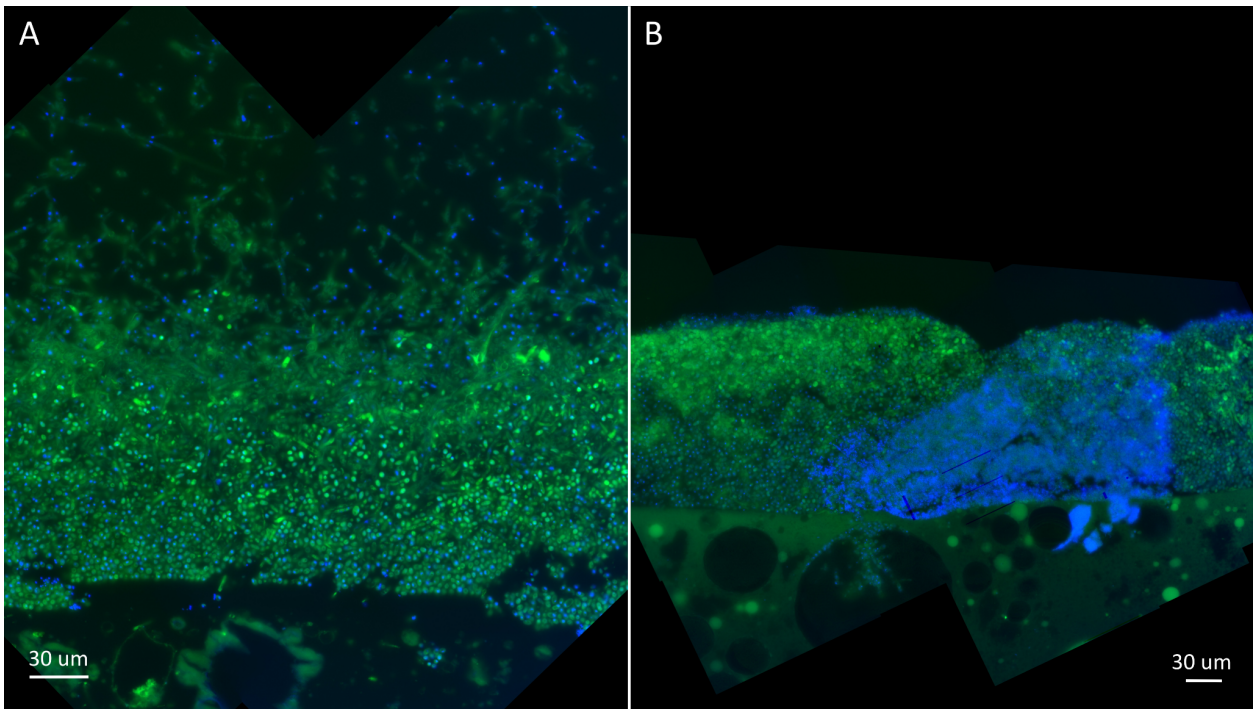

Figure 4.3-2. Biofilm structure of *in vitro* cheese rinds.
12-day old communities grown from an inoculation of ~200 CFUs each of 4 bacteria, 1 yeast, and two molds (full community) (A) or of just the 4 bacteria and 1 yeast (community without molds) (B). Biofilm slice images are oriented so that the cheese medium is at the bottom and the air interface of the biofilm is at the top. Green channel shows fungal autofluorescence, blue channel shows the nucleic acid stain DAPI. Dense DAPI staining indicates a cluster of bacterial cells.

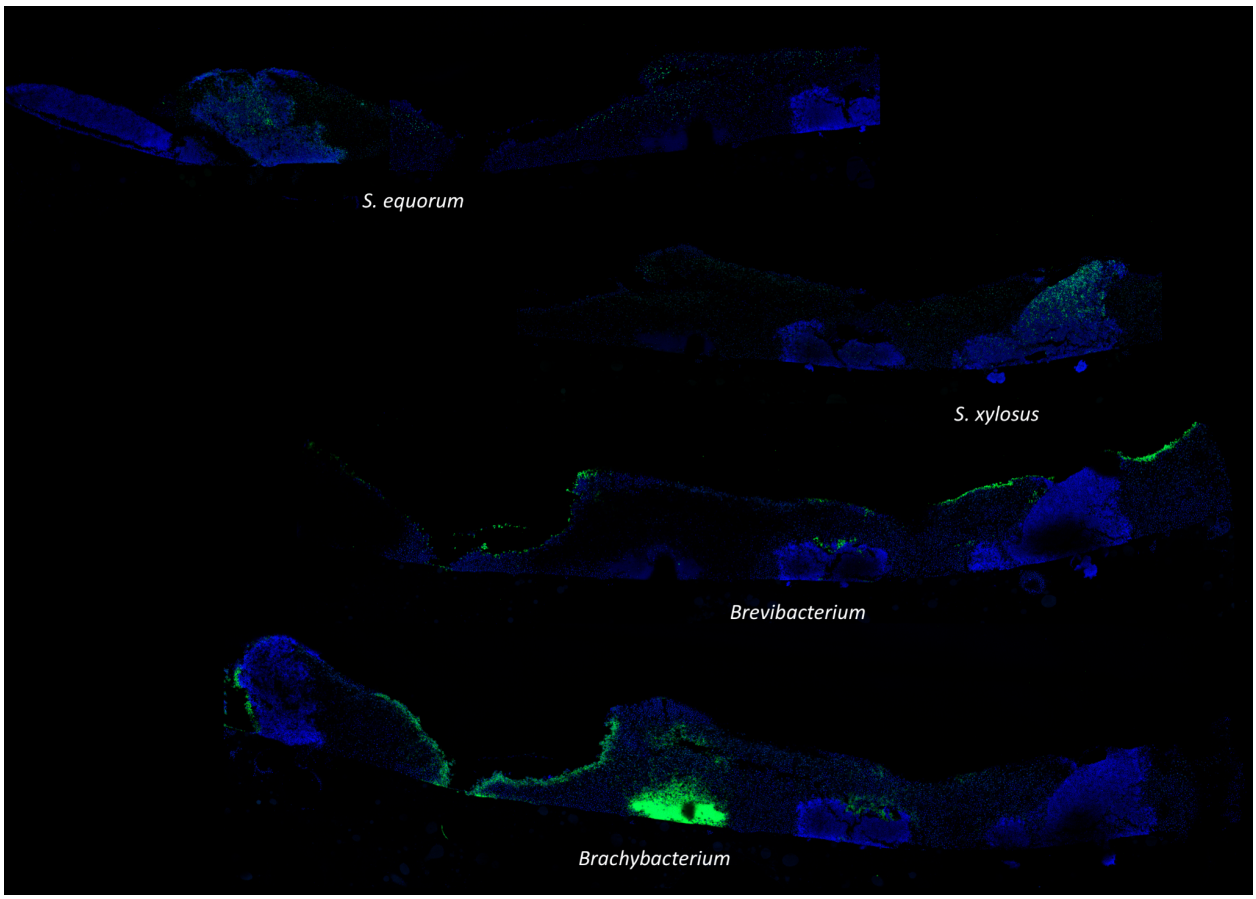

Figure 4.3-3. Biofilm structure and species-specific labeling of *in vitro* cheese rind without molds grown from a dilute initial inoculation.
Biofilms were grown for 12 days on CCA pH 5 before processing. Biofilm slice images are oriented so that the cheese medium is at the bottom and the air interface of the biofilm is at the top. Approximately sequential slices shown in the four biofilm images were each subject to FISH using a single species specific probe equipped with a Dy490 fluorophore (green channel). The target species for the probe is labeled under each slice. Blue channel shows DAPI nucleic acid dye. Dense DAPI staining indicates a cluster of bacterial cells.

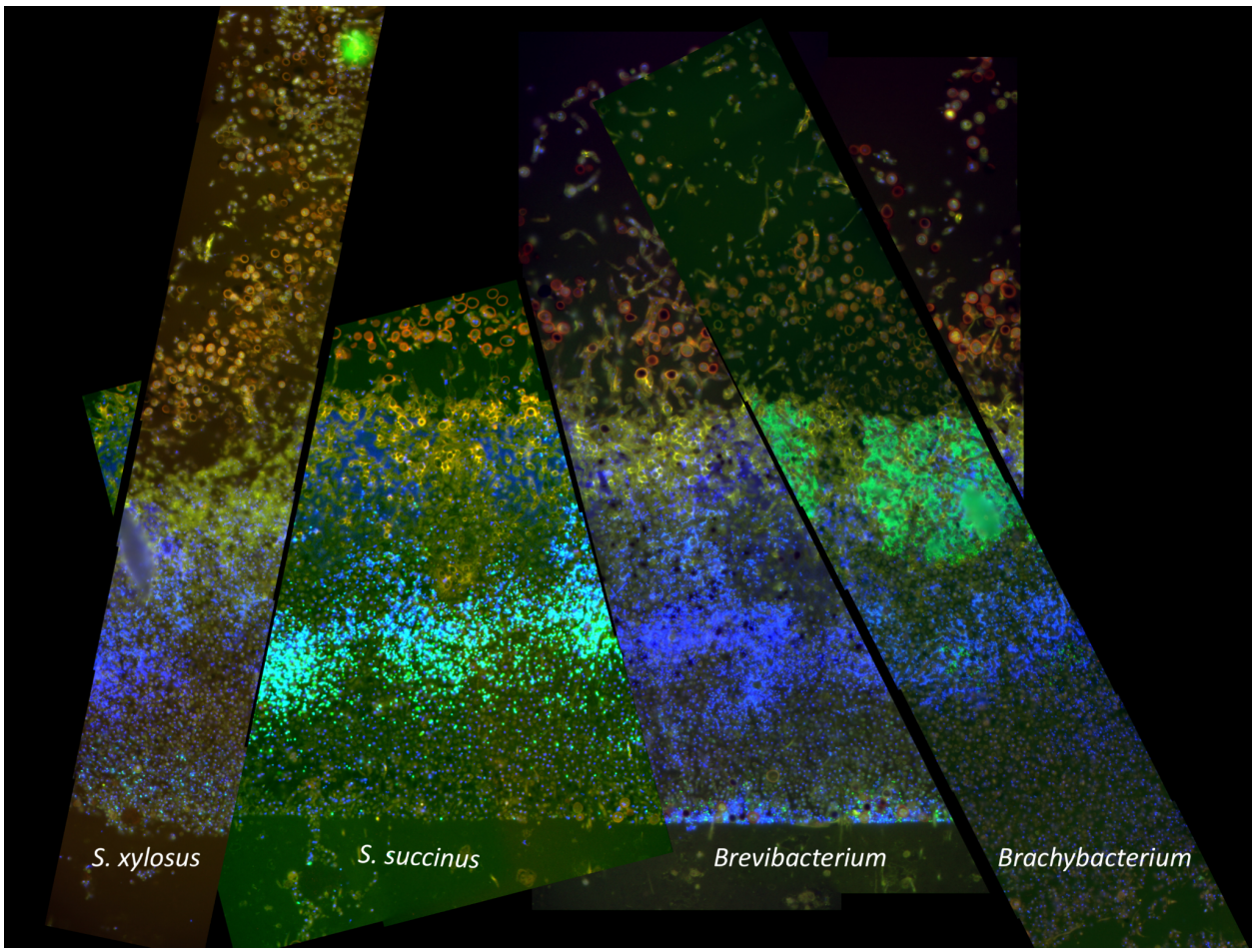

Figure 4.3-4. Biofilm structure and species-specific labeling of *in vitro* cheese rind grown from a dense initial inoculation.
Biofilms were grown for 10 days on CCA pH 5 before processing. Biofilm slice images are oriented so that the cheese medium is at the bottom and the air interface of the biofilm is at the top. Approximately sequential slices shown in the four panels were each subject to FISH using a single species specific probe equipped with a Dy490 fluorophore (green channel). Target species for the probe is labeled at the bottom of the panels. Red and yellow colors show autofluorescence of fungal species. Blue channel shows DAPI nucleic acid dye.

Supplemental Figure

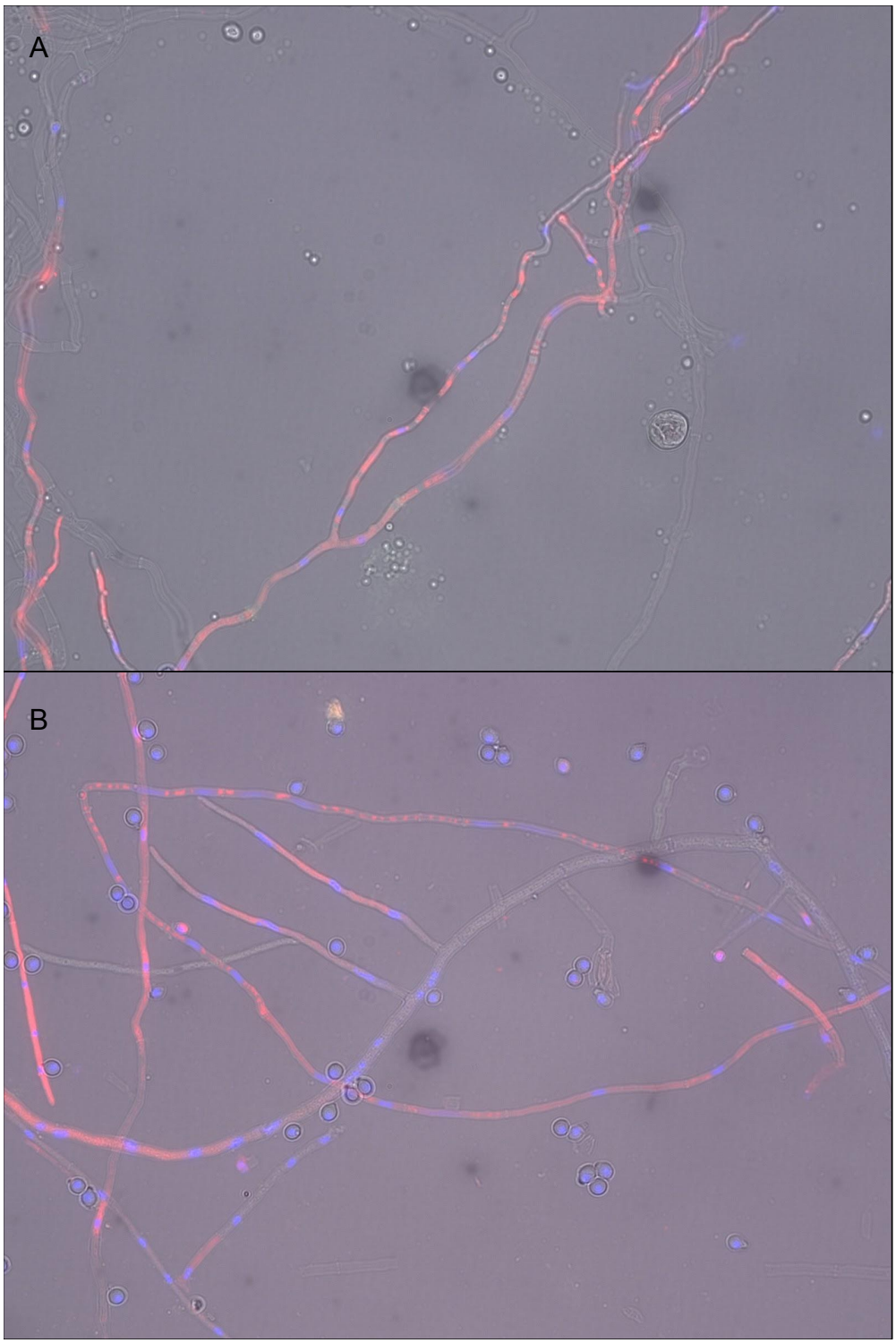

Supplemental Figure 4.3-1. Fluorescent labeling of filamentous fungal SSU ribosomal RNA. A universal eukaryote PNA probe EUK109, conjugated to the fluorophore TAMRA, was used to label *Scopulariopsis* sp. strain JB370 (A) and *Penicillium* sp. strain JBC (B), visible in the red channel. The nucleic acid stain DAPI highlights nuclei in blue. Brightfield microscopy shows the structure of fungal filaments and spores.

Tables

Table 4.3-1. Optimization of labeling protocols for bacteria or fungi.

Step to optimize	Parameters tested	Notes	Optimal for most bacteria	Optimal for most fungi	Universal Protocol
Pure culture growth stage	early-log				
	mid-log		X		X
	late-log/stationary				
Chemical Fixative	2% paraformaldehyde				
	4% paraformaldehyde	Fresh ampules recommended	X	X	X
	100% ethanol	Actinobacteria in particular fluoresced well following ethanol fixation	X		
	50% ethanol		X		X
Enzymatic Treatment	Lysozyme		X		X
	Stapholysin				
	Chitinase	chitinase only increases hybridization of fluorescent probes in Diutina, but has an added benefit of decreasing autofluorescence of Scopulariopsis		X	X
Ethanol dehydration series temperature	room temp				
	-20 degC		X		X
Hybiridization time	1-3 hours	must maintain humidity entire time to prevent much evaporation & concentration of hybridization solution	X	X	X
	O/N				
Probe concentration	.01 nM				
	.05 nM		X		X
	.1 nM				
Hybridization buffer adjuncts	sodium citrate (denaturant)				
	dextran sulfate (5%)	markedly increased yeast signal		X	

Table 4.3-2. Optimization of a universal protocol for simultaneous labeling of bacteria and fungi.

buffer component		success of hybridization variable in protocol: bacterial DNA probe protocol	fungal PNA probe protocol	notes
formamide	0%	–	+	
	20%	+	+	
NaCl	100 mM	–	+	
	900 mM	+	+	
SDS	0.01%	+	+	0.01% SDS retains better surface tension
	0.5%	+	+	
Tris buffer	20 mM, pH 7.5	+	–	
	25 mM, pH 9	+	+	
temperature	46 degC	+	–	
	54 degC	+	+	

cells highlighted in gray mark parameters used in universal protocol

Table 4.3-3. List of probe sequences tested in this study.

Target	Probe name	Probe sequence (5'-3')	better probe	probe aliases	position reference probe	Off-target hits?
Penicillium sp. st. JBC	JBC1342	AGGGCCGAGGTCTCGTTC	*		Baker, Brett J. et al. 2004	
Penicillium sp. st. JBC	JBC1070	ACGGGTCATTATAGAATCCCGT		pen-3	Wu, Zhihong et al. 2003	cross-hybridizes to Diutina
Scopulariopsis sp. st. JB370	Scop1342	GCAGGTTAAGGTCTCGTTC	*		Baker, Brett J. et al. 2004	
Scopulariopsis sp. st. JB370	Scop1070	ACGCGTCAAATAATAACATCGT	*		Wu, Zhihong et al. 2003	
Diutina catenulata st. 135E	Ccat1344	TAGCGGATAAGGTCTCGTTC	*		Baker, Brett J. et al. 2004	
Diutina catenulata st. 135E	Ccat1067	GGCCAAAGAGGTCCGCGCCCG	*		Wu, Zhihong et al. 2003	
Staphylococcus equorum st. BC9	StaphBC9-272	CGGCTACGTATCGTTGCCTT				
Staphylococcus equorum st. BC9	StaphBC9-375	CTCCGTCAGACTTTCGTCC	*			
Staphylococcus xylosus st. BC10	StaphBC15-377	CTCCGTCAGGCTTTCGC	*			
Brevibacterium sp. st. JB5	BRE845	TCTCTCTGTACCAGCCA	*		Kolloffel, Beat et al. 1997	
Brevibacterium sp. st. JB5	BreviJB5-600	AAGCGTTGCGTTTCCACAGC				
Brachybacterium sp. st. JB7	pB2023	TCACGAGGATGGGCCACTG	*	Bracb2	Kyselkova, Martina et al. 2008	
Brachybacterium sp. st. JB7	BrachyJB7-600	AGCCTCGGGTTTTCACGGC			Kyselkova, Martina et al. 2008	
all prokaryotes	EUB338	GCTGCCTCCCGTAGGAGT			Amann, R.I. et al. 1990	
all eukaryotes	EUK1209	GGGCATCACAGACCTG			Lim, E.L. et al. 1993	

4.4 Acknowledgements

Chapter 4 consists of unpublished material. The following individuals are also authors on this work: Section 4.2 - Rachel Dutton (UCSD); Section 4.3 - Jessica Mark-Welch (Marine Biological Laboratory), Rachel Dutton (UCSD). The dissertation author is the primary author of this material.

CHAPTER 5. Conclusion

5.1 Future Directions

Mechanisms of pH-mediated growth stimulation

Work towards investigating how environmental pH modulation affects community assembly shows that carbon sources (Ilhan et al., 2017; Ratzke et al., 2020), media buffering (Ilhan et al., 2017), and microbial metabolic capacity (Herschend et al., 2018; Ratzke and Gore, 2018) all contribute to determining pH dynamics and microbial community structure. During the cheese aging process, the change in rind pH, rising from pH 5 to almost pH 8, is thought to rely heavily on lactate-consuming species and is possible due to the nutrient environment of fresh curd consisting of high protein and low fermentable carbon. This neutralizing scenario increases diversity at the rind over time, as more microbes are adapted to a pH near neutral than to an extreme pH (Thompson et al., 2017; Tripathi et al., 2018).

Further investigation into mechanisms of deacidification reveal increased complexity in pH-related stimulation. For example, in Chapter 4.2 I identified volatile-based mechanisms of deacidification. Volatile compounds released by cheese microbes have been found to be only selectively stimulating of other cheese microbes (Cosetta et al., 2020). Whether the deacidifying volatiles produced by *Brevibacterium* sp. strain JB5, *Penicillium* sp. strain JBC, and *Scopulariopsis* sp. strain JB370, identified here, would instead generally stimulate acid-sensitive microbes through raising medium pH should be tested. Following up with headspace analysis might determine whether produced volatiles are the same for each identified producer, and whether these compounds are a more simple and general base (e.g. ammonia) or more complex (e.g. triethylamine as in (Jones et al., 2017)).

In the context of succession, it's unclear what the role of volatile-mediated stimulation might be. We showed in Chapter 2.2 that deacidification by *Diutina* early in community succession is particularly important for stimulating late-colonizing Actinobacterial species. As *Diutina* was not found to deacidify cheese medium through volatile production, an alternative mechanism of pH-related stimulation must occur. Preliminary work studying the stimulative interaction between *Diutina catenulata* strain 135E and *Brevibacterium* sp. strain JB5 suggests that *Brevibacterium* might be limited by amino acid acquisition under acidic conditions (data not shown), potentially due its encoded extracellular proteases being acid-sensitive (Tokita and Hosono, 1972). Follow-up studies performed on solid cheese medium, buffered at pH 5 and supplemented with amino acids, may reveal a more specific mechanism of stimulation for acid-sensitive cheese rind microbes.

Fungal antibiosis

Due to the potential of a bioactive molecule from *Penicillium* sp. strain JBC having specific activity against yeast, further work in assessing the scope of *Penicillium* sp. strain JBC inhibition against yeasts other than *Diutina* and *Debaryomyces*, such as taxonomically related *Candida* yeasts or skin-associated yeasts of the genus *Malassezia,* may point towards a novel anti-yeast molecule. Sequencing the genome or transcriptome of resistant *Debaryomyces* clones may help validate mechanisms of inhibition, though non-specific resistance to fungal competition in combination with a high rate of resistance mutation suggests a non-specific mutation mechanism such as chromosomal duplication (Petersen and Jespersen, 2004). Lastly, work is ongoing to extract and chemically characterize the active antifungal compound. With a lack of success in extracting the compound from spent medium, *in situ* approaches such as imaging mass spectrometry are underway.

Patterns of bacteriophage succession

Across three batches of developing cheese rinds, we found a clear and consistent pattern of bacteriophage succession that closely matched host bacterial succession. This suggests a prevalence of lysogenic phage within the cheese rind microbiome, though our coarse time course sampling may not be able to catch clear boom-bust cycles that are characteristic of a lytic phage infectious lifecycle. Further work to match more specific phage-host pairs, through the use of manual binning and CRISPR spacers, may provide more information about the potential role of bacterial strain selection through phage lysis. Future time-course studies of cheese phage would benefit from single-celled sequencing or chromosome capture techniques that can accurately assign phage to their infected bacterial hosts.

Initial investigation into phage succession dynamics at a sequence level showed potential successional patterns of dominant phage sequence variants. This may be due to selection for specific host-phage pairs over succession, or may be related to functional selection as the cheese rind environment changes over the aging process. Closer examination of the frequency of these variants over succession and their functional potential may reveal more understanding of the dynamics of microbiome succession. Incorporating similar sequences found in the mature rind sample that was sequenced 6 years, serving as an uncontrolled "passaging" of this community over a long period of time, may additionally contribute to understanding the selective pressures affecting cheese rind phage.

Development and characteristics of natural rind cheese biofilms

In Chapter 4.3, we presented a technical method for visualizing the distribution of bacteria and fungal cells in a cheese rind biofilm. We found that cell populations tended to be segregated, either in microcolonies if the cheese surface is initially colonized sparsely, or in layers if a dense

layer of cells is inoculated. Future applications of this technique may be used to assess how predictable is the spatial structure within a cheese rind, how spatial structure develops over time, and how comparable the spatial structure of an *in vitro* cheese rind is to the cave-aged cheese rind that the model is derived from. This technique can also be expanded to other cheese rind community models by designing new species-specific probes.

5.2 Concluding remarks

The presented dissertation set out to investigate drivers of community assembly in a model natural rind cheese microbiome. Contributing to this end, in Chapter 2 we presented a study revealing the key microbial interactions underlying the pattern of succession, using an *in vitro* model of this microbiome. We found that fungal members of the community in particular are influential in driving temporal dynamics of community formation, almost entirely through environmental modulation and antibiosis. In particular, this emphasizes the importance of including fungal species in other model microbial communities that represent microbiomes with medical, environmental, or industrial value. In Chapter 4.2, we followed up on mechanisms underlying these interactions that influence succession, and identified one of probably multiple mechanisms for media deacidification as well as a novel potential anti-yeast interaction.

While our *in vitro* model community was able to reveal factors that drive the overarching taxonomic pattern of succession, our simplified model lacks strain and, for the large part, even species-level resolution. Metagenomic studies of the native cheese rind from which the model was taken indicate considerable diversity within the dominant genera. An underexplored component of cheese rinds that is likely to contribute to strain- and species-level dynamics within the community are bacteriophage. To provide a foundation for future investigations of the role of phage in

directing the assembly of cheese rind microbiomes, in Chapter 3 we identified phage within previously-existing time course metagenomes spanning the rind development of the native cheese. We found that the phage community was highly reproducible between batches prepared within a short time frame, even among distinct phage strains, but that many very similar phage sequences could also be identified from the same style of cheese prepared many years later. This indicates that community assembly is fairly deterministic and selects for specific microbial members. Moreover, such findings could be useful for studying the evolution of phage-bacterial interactions in a semi-natural system.

Lastly, we recognize that our findings are occurring in a spatially-structured biofilm environment. One of the more difficult features of studying ecology in a microscopic system is the difficulty in discerning the "lay of the land." In Chapter 4.3, we adapted techniques previously used to visualize the spatial organization of microbes in dental plaque (Mark Welch et al., 2016) to our model natural rind cheese microbiome. While a protocol was identified for labeling fungi concurrently with bacteria, further work finding visible probe targets that are distributed across filaments is needed. Nonetheless, we found that microbes within cheese rind microbiomes tend to be spatially segregated, limiting the types of microbial interactions that may be occurring in a multi-species community. Further exploration of the spatial organization of the cheese rind biofilm may reveal trends that correlate with processes and patterns of community assembly.

CHAPTER 6. References

Abrego, N., Roslin, T., Huotari, T., Tack, A.J.M., Lindahl, B.D., Tikhonov, G., Somervuo, P., Schmidt, N.M., and Ovaskainen, O. (2020). Accounting for environmental variation in co-occurrence modelling reveals the importance of positive interactions in root-associated fungal communities. Mol. Ecol.

Akin, D.E., and Borneman, W.S. (1990). Role of rumen fungi in fiber degradation. J. Dairy Sci. *73*, 3023–3032.

Alneberg, J., Bjarnason, B.S., de Bruijn, I., Schirmer, M., Quick, J., Ijaz, U.Z., Lahti, L., Loman, N.J., Andersson, A.F., and Quince, C. (2014). Binning metagenomic contigs by coverage and composition. Nat. Methods *11*, 1144–1146.

Altschul, S.F., Gish, W., Miller, W., Myers, E.W., and Lipman, D.J. (1990). Basic local alignment search tool. J. Mol. Biol. *215*, 403–410.

Arkhipova, K., Skvortsov, T., Quinn, J.P., McGrath, J.W., Allen, C.C., Dutilh, B.E., McElarney, Y., and Kulakov, L.A. (2018). Temporal dynamics of uncultured viruses: a new dimension in viral diversity. ISME J. *12*, 199–211.

Bardgett, R.D., Freeman, C., and Ostle, N.J. (2008). Microbial contributions to climate change through carbon cycle feedbacks. ISME J. *2*, 805–814.

Baschien, C., Manz, W., Neu, T.R., and Szewzyk, U. (2001). Fluorescence in situ Hybridization of Freshwater Fungi. Int. Rev. Hydrobiol. *86*, 371–381.

Bera, A., Herbert, S., Jakob, A., Vollmer, W., and Götz, F. (2005). Why are pathogenic staphylococci so lysozyme resistant? The peptidoglycan O-acetyltransferase OatA is the major determinant for lysozyme resistance of Staphylococcus aureus. Mol. Microbiol. *55*, 778–787.

Bertuzzi, A.S., Walsh, A.M., Sheehan, J.J., Cotter, P.D., Crispie, F., McSweeney, P.L.H., Kilcawley, K.N., and Rea, M.C. (2018). Omics-Based Insights into Flavor Development and Microbial Succession within Surface-Ripened Cheese. mSystems *3*.

Bintsis, T. (2018). Lactic acid bacteria as starter cultures: An update in their metabolism and genetics. AIMS Microbiol *4*, 665–684.

Blin, K., Shaw, S., Steinke, K., Villebro, R., Ziemert, N., Lee, S.Y., Medema, M.H., and Weber, T. (2019). antiSMASH 5.0: updates to the secondary metabolite genome mining pipeline. Nucleic Acids Res. *47*, W81–W87.

Bolger, A.M., Lohse, M., and Usadel, B. (2014). Trimmomatic: a flexible trimmer for Illumina sequence data. Bioinformatics *30*, 2114–2120.

Bonaïti, C., Leclercq-Perlat, M.-N., Latrille, E., and Corrieu, G. (2004). Deacidification by Debaryomyces hansenii of smear soft cheeses ripened under controlled conditions: relative humidity and temperature influences. J. Dairy Sci. *87*, 3976–3988.

Brislawn, C.J., Graham, E.B., Dana, K., Ihardt, P., Fansler, S.J., Chrisler, W.B., Cliff, J.B., Stegen, J.C., Moran, J.J., and Bernstein, H.C. (2019). Forfeiting the priority effect: turnover defines biofilm community succession. ISME J. *13*, 1865–1877.

Burns, A.R., Stephens, W.Z., Stagaman, K., Wong, S., Rawls, J.F., Guillemin, K., and Bohannan, B.J. (2016). Contribution of neutral processes to the assembly of gut microbial communities in the zebrafish over host development. ISME J. *10*, 655–664.

Cadotte, M.W., Drake, J.A., and Fukami, T. (2005). Constructing Nature: Laboratory Models as Necessary Tools for Investigating Complex Ecological Communities. In Advances in Ecological Research, (Academic Press), pp. 333–353.

Calvo, A.M., Wilson, R.A., Bok, J.W., and Keller, N.P. (2002). Relationship between secondary metabolism and fungal development. Microbiol. Mol. Biol. Rev. *66*, 447–459, table of contents.

Capouya, R., Mitchell, T., Clark, D.I., Clark, D.L., and Bass, P. (2020). A survey of microbial communities on dry-aged beef in commercial meat processing facilities. Meat Muscle Biol. *4*.

Chapin, F.S., Walker, L.R., Fastie, C.L., and Sharman, L.C. (1994). Mechanisms of Primary Succession Following Deglaciation at Glacier Bay, Alaska. Ecol. Monogr. *64*, 149–175.

Chapin, F.S., Walker, L.R., Fastie, C.L., and Sharman, L.C. (1994). Mechanisms of Primary Succession Following Deglaciation at Glacier Bay, Alaska. Ecol. Monogr. 64, 149–175.

Chow, C.-E.T., and Fuhrman, J.A. (2012). Seasonality and monthly dynamics of marine myovirus communities. Environ. Microbiol. *14*, 2171–2183.

Cooper, W.S. (1923). The Recent Ecological History of Glacier Bay, Alaska: The Present Vegetation Cycle. Ecology *4*, 223–246.

Cosetta, C.M., and Wolfe, B.E. (2020). Deconstructing and Reconstructing Cheese Rind Microbiomes for Experiments in Microbial Ecology and Evolution. Curr. Protoc. Microbiol. *56*, e95.

Cosetta, C.M., Kfoury, N., Robbat, A., and Wolfe, B.E. (2020). Fungal volatiles mediate cheese rind microbiome assembly. Environ. Microbiol. *22*, 4745–4760.

Cuenca-Estrella, M., Gomez-Lopez, A., Mellado, E., Buitrago, M.J., Monzón, A., and Rodriguez-Tudela, J.L. (2003). Scopulariopsis brevicaulis, a fungal pathogen resistant to broad-spectrum antifungal agents. Antimicrob. Agents Chemother. *47*, 2339–2341.

Curtin, Á.C., and McSweeney, P.L.H. (2004). Catabolism of Amino Acids in Cheese during Ripening. In Cheese: Chemistry, Physics and Microbiology, P.F. Fox, P.L.H. McSweeney, T.M. Cogan, and T.P. Guinee, eds. (Academic Press), pp. 435–454.

De Smet, J., Zimmermann, M., Kogadeeva, M., Ceyssens, P.-J., Vermaelen, W., Blasdel, B., Bin Jang, H., Sauer, U., and Lavigne, R. (2016). High coverage metabolomics analysis reveals phage-specific alterations to Pseudomonas aeruginosa physiology during infection. ISME J. *10*, 1823–1835.

Dick, G.J. (2019). The microbiomes of deep-sea hydrothermal vents: distributed globally, shaped locally. Nat. Rev. Microbiol. *17*, 271–283.

Dinno, A. (2015). Nonparametric Pairwise Multiple Comparisons in Independent Groups using Dunn's Test. Stata J. *15*, 292–300.

Dordet-Frisoni, E., Dorchies, G., De Araujo, C., Talon, R., and Leroy, S. (2007). Genomic diversity in Staphylococcus xylosus. Appl. Environ. Microbiol. *73*, 7199–7209.

Draper, L.A., Ryan, F.J., Smith, M.K., Jalanka, J., Mattila, E., Arkkila, P.A., Ross, R.P., Satokari, R., and Hill, C. (2018). Long-term colonisation with donor bacteriophages following successful faecal microbial transplantation. Microbiome *6*, 220.

Dugat-Bony, E., Lossouarn, J., De Paepe, M., Sarthou, A.-S., Fedala, Y., Petit, M.-A., and Chaillou, S. (2020). Viral metagenomic analysis of the cheese surface: A comparative study of rapid procedures for extracting viral particles. Food Microbiol. *85*, 103278.

Dutton, M.V., and Evans, C.S. (1996). Oxalate production by fungi: its role in pathogenicity and ecology in the soil environment. Can. J. Microbiol. *42*, 881–895.

Emerson, J.B., Thomas, B.C., Andrade, K., Allen, E.E., Heidelberg, K.B., and Banfield, J.F. (2012). Dynamic viral populations in hypersaline systems as revealed by metagenomic assembly. Appl. Environ. Microbiol. *78*, 6309–6320.

Enke, T.N., Datta, M.S., Schwartzman, J., Cermak, N., Schmitz, D., Barrere, J., Pascual-García, A., and Cordero, O.X. (2019). Modular Assembly of Polysaccharide-Degrading Marine Microbial Communities. Curr. Biol. *29*, 1528–1535.e6.

Ercolini, D., Pontonio, E., De Filippis, F., Minervini, F., La Storia, A., Gobbetti, M., and Di Cagno, R. (2013). Microbial ecology dynamics during rye and wheat sourdough preparation. Appl. Environ. Microbiol. *79*, 7827–7836.

Estrela, S., and Brown, S.P. (2013). Metabolic and demographic feedbacks shape the emergent spatial structure and function of microbial communities. PLoS Comput. Biol. *9*, e1003398.

Estrela, S., and Brown, S.P. (2018). Community interactions and spatial structure shape selection on antibiotic resistant lineages. PLoS Comput. Biol. *14*, e1006179.

Feiner, R., Argov, T., Rabinovich, L., Sigal, N., Borovok, I., and Herskovits, A.A. (2015). A new perspective on lysogeny: prophages as active regulatory switches of bacteria. Nat. Rev. Microbiol. *13*, 641–650.

Filion, M., St-Arnaud, M., and Fortin, J.A. (1999). Direct interaction between the arbuscular mycorrhizal fungus Glomus intraradices and different rhizosphere microorganisms. New Phytol. *141*, 525–533.

Fox, P.F., and Wallace, J.M. (1997). Formation of Flavor Compounds in Cheese. In Advances in Applied Microbiology, S.L. Neidleman, and A.I. Laskin, eds. (Academic Press), pp. 17–85.

Fox, P.F., Lucey, J.A., and Cogan, T.M. (1990). Glycolysis and related reactions during cheese manufacture and ripening. Crit. Rev. Food Sci. Nutr. *29*, 237–253.

Fröhlich-Wyder, M.-T., Arias-Roth, E., and Jakob, E. (2019). Cheese yeasts. Yeast *36*, 129–141.

Fuchsman, C.A., Palevsky, H.I., Widner, B., Duffy, M., Carlson, M.C.G., Neibauer, J.A., Mulholland, M.R., Keil, R.G., Devol, A.H., and Rocap, G. (2019). Cyanobacteria and cyanophage contributions to carbon and nitrogen cycling in an oligotrophic oxygen-deficient zone. ISME J. *13*, 2714–2726.

Gao, C.-H., Cao, H., Cai, P., and Sørensen, S.J. (2021). The initial inoculation ratio regulates bacterial coculture interactions and metabolic capacity. ISME J. *15*, 29–40.

Gilbert, J.A., Steele, J.A., Caporaso, J.G., Steinbrück, L., Reeder, J., Temperton, B., Huse, S., McHardy, A.C., Knight, R., Joint, I., et al. (2012). Defining seasonal marine microbial community dynamics. ISME J. *6*, 298–308.

Gorka, S., Dietrich, M., Mayerhofer, W., Gabriel, R., Wiesenbauer, J., Martin, V., Zheng, Q., Imai, B., Prommer, J., Weidinger, M., et al. (2019). Rapid Transfer of Plant Photosynthates to Soil Bacteria via Ectomycorrhizal Hyphae and Its Interaction With Nitrogen Availability. Front. Microbiol. *10*, 168.

Grice, E.A., and Segre, J.A. (2011). The skin microbiome. Nat. Rev. Microbiol. *9*, 244–253.

Guo, J., Bolduc, B., Zayed, A.A., Varsani, A., Dominguez-Huerta, G., Delmont, T.O., Pratama, A.A., Gazitúa, M.C., Vik, D., Sullivan, M.B., et al. (2021a). VirSorter2: a multi-classifier, expert-guided approach to detect diverse DNA and RNA viruses. Microbiome *9*, 37.

Guo, J., Vik, D., Adjie, A., Roux, S., and Sullivan, M. (2021b). Viral sequence identification SOP with VirSorter2 v2 (ZappyLab, Inc.).

Gurney, J., Brown, S.P., Kaltz, O., and Hochberg, M.E. (2020). Steering Phages to Combat Bacterial Pathogens. Trends Microbiol. *28*, 85–94.

Hampton, H.G., Watson, B.N.J., and Fineran, P.C. (2020). The arms race between bacteria and their phage foes. Nature *577*, 327–336.

Harcombe, W.R., Riehl, W.J., Dukovski, I., Granger, B.R., Betts, A., Lang, A.H., Bonilla, G., Kar, A., Leiby, N., Mehta, P., et al. (2014). Metabolic resource allocation in individual microbes determines ecosystem interactions and spatial dynamics. Cell Rep. *7*, 1104–1115.

Hendrix, H., Kogadeeva, M., Zimmermann, M., Sauer, U., De Smet, J., Muchez, L., Lissens, M., Staes, I., Voet, M., Wagemans, J., et al. (2019). Host metabolic reprogramming of Pseudomonas aeruginosa by phage-based quorum sensing modulation.

Herrera, C.M., García, I.M., and Pérez, R. (2008). Invisible floral larcenies: microbial communities degrade floral nectar of bumble bee-pollinated plants. Ecology *89*, 2369–2376.

Herschend, J., Koren, K., Røder, H.L., Brejnrod, A., Kühl, M., and Burmølle, M. (2018). In Vitro Community Synergy between Bacterial Soil Isolates Can Be Facilitated by pH Stabilization of the Environment. Appl. Environ. Microbiol. *84*.

Hoek, T.A., Axelrod, K., Biancalani, T., Yurtsev, E.A., Liu, J., and Gore, J. (2016). Resource Availability Modulates the Cooperative and Competitive Nature of a Microbial Cross-Feeding Mutualism. PLoS Biol. *14*, e1002540.

Howard-Varona, C., Lindback, M.M., Bastien, G.E., Solonenko, N., Zayed, A.A., Jang, H., Andreopoulos, B., Brewer, H.M., Glavina Del Rio, T., Adkins, J.N., et al. (2020). Phage-specific metabolic reprogramming of virocells. ISME J. *14*, 881–895.

Ilhan, Z.E., Marcus, A.K., Kang, D.-W., Rittmann, B.E., and Krajmalnik-Brown, R. (2017). pH-Mediated Microbial and Metabolic Interactions in Fecal Enrichment Cultures. mSphere *2*.

Jackrel, S.L., Yang, J.W., Schmidt, K.C., and Denef, V.J. (2020). Host specificity of microbiome assembly and its fitness effects in phytoplankton. ISME J.

Jones, S.E., Ho, L., Rees, C.A., Hill, J.E., Nodwell, J.R., and Elliot, M.A. (2017). Streptomyces exploration is triggered by fungal interactions and volatile signals. Elife *6*.

Kaiser, C., Kilburn, M.R., Clode, P.L., Fuchslueger, L., Koranda, M., Cliff, J.B., Solaiman, Z.M., and Murphy, D.V. (2015). Exploring the transfer of recent plant photosynthates to soil microbes: mycorrhizal pathway vs direct root exudation. New Phytol. *205*, 1537–1551.

Karahadian, C., and Lindsay, R.C. (1987). Integrated Roles of Lactate, Ammonia, and Calcium in Texture Development of Mold Surface-Ripened Cheese1. J. Dairy Sci. *70*, 909–918.

Kastman, E.K., Kamelamela, N., Norville, J.W., Cosetta, C.M., Dutton, R.J., and Wolfe, B.E. (2016). Biotic Interactions Shape the Ecological Distributions of Staphylococcus Species. MBio *7*.

Katoh, K., and Standley, D.M. (2013). MAFFT multiple sequence alignment software version 7: improvements in performance and usability. Mol. Biol. Evol. *30*, 772–780.

Kavagutti, V.S., Andrei, A.-Ş., Mehrshad, M., Salcher, M.M., and Ghai, R. (2019). Phage-centric ecological interactions in aquatic ecosystems revealed through ultra-deep metagenomics. Microbiome *7*, 135.

Keller, N.P. (2019). Fungal secondary metabolism: regulation, function and drug discovery. Nat. Rev. Microbiol. *17*, 167–180.

Kieft, K., and Anantharaman, K. (2021). Deciphering active prophages from metagenomes.

Kieft, K., Zhou, Z., and Anantharaman, K. (2020). VIBRANT: automated recovery, annotation and curation of microbial viruses, and evaluation of viral community function from genomic sequences. Microbiome *8*, 90.

Kim, K.W. (2008). Vapor Fixation of Intractable Fungal Cells for Simple and Versatile Scanning Electron Microscopy. Journal of Phytopathology *156*, 125–128.

Kim, J.E., and Kim, H.S. (2019). Microbiome of the Skin and Gut in Atopic Dermatitis (AD): Understanding the Pathophysiology and Finding Novel Management Strategies. J. Clin. Med. Res. *8*.

Knowles, B., Silveira, C.B., Bailey, B.A., Barott, K., Cantu, V.A., Cobián-Güemes, A.G., Coutinho, F.H., Dinsdale, E.A., Felts, B., Furby, K.A., et al. (2016). Lytic to temperate switching of viral communities. Nature *531*, 466–470.

Koenig, J.E., Spor, A., Scalfone, N., Fricker, A.D., Stombaugh, J., Knight, R., Angenent, L.T., and Ley, R.E. (2011). Succession of microbial consortia in the developing infant gut microbiome. Proc. Natl. Acad. Sci. U. S. A. *108 Suppl 1*, 4578–4585.

Koren, S., Walenz, B.P., Berlin, K., Miller, J.R., Bergman, N.H., and Phillippy, A.M. (2017). Canu: scalable and accurate long-read assembly via adaptive k-mer weighting and repeat separation. Genome Res. *27*, 722–736.

Kortright, K.E., Chan, B.K., Koff, J.L., and Turner, P.E. (2019). Phage Therapy: A Renewed Approach to Combat Antibiotic-Resistant Bacteria. Cell Host Microbe *25*, 219–232.

Kosalková, K., García-Estrada, C., Ullán, R.V., Godio, R.P., Feltrer, R., Teijeira, F., Mauriz, E., and Martín, J.F. (2009). The global regulator LaeA controls penicillin biosynthesis, pigmentation and sporulation, but not roquefortine C synthesis in Penicillium chrysogenum. Biochimie *91*, 214–225.

Kramer, S., Dibbern, D., Moll, J., Huenninghaus, M., Koller, R., Krueger, D., Marhan, S., Urich, T., Wubet, T., Bonkowski, M., et al. (2016). Resource Partitioning between Bacteria, Fungi, and Protists in the Detritusphere of an Agricultural Soil. Front. Microbiol. *7*, 1524.

Krumbein, W.E., Brehm, U., Gerdes, G., Gorbushina, A.A., Levit, G., and Palinska, K.A. (2003). Biofilm, Biodictyon, Biomat Microbialites, Oolites, Stromatolites Geophysiology, Global Mechanism, Parahistology. In Fossil and Recent Biofilms, (Springer, Dordrecht), pp. 1–27.

Kumar, A., Asthana, M., Gupta, A., Nigam, D., and Mahajan, S. (2018). Chapter 3 - Secondary Metabolism and Antimicrobial Metabolites of Penicillium. In New and Future Developments in Microbial Biotechnology and Bioengineering, V.K. Gupta, and S. Rodriguez-Couto, eds. (Amsterdam: Elsevier), pp. 47–68.

Labonté, J.M., Swan, B.K., Poulos, B., Luo, H., Koren, S., Hallam, S.J., Sullivan, M.B., Woyke, T., Wommack, K.E., and Stepanauskas, R. (2015). Single-cell genomics-based analysis of virus-host interactions in marine surface bacterioplankton. ISME J. *9*, 2386–2399.

Labrie, S.J., and Moineau, S. (2007). Abortive infection mechanisms and prophage sequences significantly influence the genetic makeup of emerging lytic lactococcal phages. J. Bacteriol. *189*, 1482–1487.

Langmead, B., and Salzberg, S.L. (2012). Fast gapped-read alignment with Bowtie 2. Nat. Methods *9*, 357–359.

Lee, J. (2011). The Distribution of Cytoplasm and Nuclei within the Extra-radical Mycelia in Glomus intraradices, a Species of Arbuscular Mycorrhizal Fungi. Mycobiology *39*, 79–84.

Li, H. (2011). A statistical framework for SNP calling, mutation discovery, association mapping and population genetical parameter estimation from sequencing data. Bioinformatics *27*, 2987–2993.

Liu, J., Zhu, S., Liu, X., Yao, P., Ge, T., and Zhang, X.-H. (2020). Spatiotemporal dynamics of the archaeal community in coastal sediments: assembly process and co-occurrence relationship. ISME J. *14*, 1463–1478.

Lozupone, C.A., Stombaugh, J.I., Gordon, J.I., Jansson, J.K., and Knight, R. (2012). Diversity, stability and resilience of the human gut microbiota. Nature *489*, 220–230.

Luciano-Rosario, D., Keller, N.P., and Jurick, W.M., 2nd (2020). Penicillium expansum: biology, omics, and management tools for a global postharvest pathogen causing blue mould of pome fruit. Mol. Plant Pathol. *21*, 1391–1404.

Luo, E., Aylward, F.O., Mende, D.R., and DeLong, E.F. (2017). Bacteriophage Distributions and Temporal Variability in the Ocean's Interior. MBio *8*.

Marcellino, S.N., and Benson, D.R. (1992). Scanning electron and light microscopic study of microbial succession on bethlehem st. Nectaire cheese. Appl. Environ. Microbiol. *58*, 3448–3454.

Mark Welch, J.L., Rossetti, B.J., Rieken, C.W., Dewhirst, F.E., and Borisy, G.G. (2016). Biogeography of a human oral microbiome at the micron scale. Proc. Natl. Acad. Sci. U. S. A. *113*, E791–E800.

McSweeney, P.L.H. (2004). Biochemistry of Cheese Ripening: Introduction and Overview. In Cheese: Chemistry, Physics and Microbiology, P.F. Fox, P.L.H. McSweeney, T.M. Cogan, and T.P. Guinee, eds. (Academic Press), pp. 347–360.

de Melo, A.G., Rousseau, G.M., Tremblay, D.M., Labrie, S.J., and Moineau, S. (2020). DNA tandem repeats contribute to the genetic diversity of Brevibacterium aurantiacum phages. Environ. Microbiol. *22*, 3413–3428.

Menouni, R., Hutinet, G., Petit, M.-A., and Ansaldi, M. (2015). Bacterial genome remodeling through bacteriophage recombination. FEMS Microbiol. Lett. *362*, 1–10.

Ming, C., Huang, J., Wang, Y., Lv, Q., Zhou, B., Liu, T., Cao, Y., Gerrits van den Ende, B., Al-Hatmi, A.M.S., Ahmed, S.A., et al. (2019). Revision of the medically relevant species of the yeast genus Diutina. Med. Mycol. *57*, 226–233.

Momeni, B., Brileya, K.A., Fields, M.W., and Shou, W. (2013). Strong inter-population cooperation leads to partner intermixing in microbial communities. Elife *2*, e00230.

Mönnich, J., Tebben, J., Bergemann, J., Case, R., Wohlrab, S., and Harder, T. (2020). Niche-based assembly of bacterial consortia on the diatom Thalassiosira rotula is stable and reproducible. ISME J. *14*, 1614–1625.

Morel, G., Sterck, L., Swennen, D., Marcet-Houben, M., Onesime, D., Levasseur, A., Jacques, N., Mallet, S., Couloux, A., Labadie, K., et al. (2015). Differential gene retention as an evolutionary mechanism to generate biodiversity and adaptation in yeasts. Sci. Rep. *5*, 11571.

Morin, M., Pierce, E.C., and Dutton, R.J. (2018). Changes in the genetic requirements for microbial interactions with increasing community complexity. Elife *7*.

Morris, M.M., Frixione, N.J., Burkert, A.C., Dinsdale, E.A., and Vannette, R.L. (2020). Microbial abundance, composition, and function in nectar are shaped by flower visitor identity. FEMS Microbiol. Ecol. *96*.

Mounier, J., Monnet, C., Vallaeys, T., Arditi, R., Sarthou, A.-S., Hélias, A., and Irlinger, F. (2008). Microbial interactions within a cheese microbial community. Appl. Environ. Microbiol. *74*, 172–181.

Murat Eren, A., Esen, Ö.C., Quince, C., Vineis, J.H., Morrison, H.G., Sogin, M.L., and Delmont, T.O. (2015). Anvi'o: an advanced analysis and visualization platform for 'omics data. PeerJ *3*, e1319.

Nadell, C.D., Foster, K.R., and Xavier, J.B. (2010). Emergence of spatial structure in cell groups and the evolution of cooperation. PLoS Comput. Biol. *6*, e1000716.

Nayfach, S., Camargo, A.P., Schulz, F., Eloe-Fadrosh, E., Roux, S., and Kyrpides, N.C. (2021). CheckV assesses the quality and completeness of metagenome-assembled viral genomes. Nat. Biotechnol. *39*, 578–585.

Nurk, S., Meleshko, D., Korobeynikov, A., and Pevzner, P.A. (2017). metaSPAdes: a new versatile metagenomic assembler. Genome Res. *27*, 824–834.

Olejarz, J., Iwasa, Y., Knoll, A.H., and Nowak, M.A. (2021). The Great Oxygenation Event as a consequence of ecological dynamics modulated by planetary change. Nat. Commun. *12*, 3985.

Oppong-Danquah, E., Passaretti, C., Chianese, O., Blümel, M., and Tasdemir, D. (2020). Mining the Metabolome and the Agricultural and Pharmaceutical Potential of Sea Foam-Derived Fungi. Mar. Drugs *18*.

Pacheco, A.R., Moel, M., and Segrè, D. (2019). Costless metabolic secretions as drivers of interspecies interactions in microbial ecosystems. Nat. Commun. *10*, 103.

Pernthaler, J., Glöckner, F.-O., Schönhuber, W., and Amann, R. (2001). Fluorescence in situ hybridization (FISH) with rRNA-targeted oligonucleotide probes. Methods in Microbiology *30*, 207–226.

Petersen, K.M., and Jespersen, L. (2004). Genetic diversity of the species Debaryomyces hansenii and the use of chromosome polymorphism for typing of strains isolated from surface-ripened cheeses. J. Appl. Microbiol. *97*, 205–213.

Petersen, K.M., Westall, S., and Jespersen, L. (2002). Microbial succession of Debaryomyces hansenii strains during the production of Danish surfaced-ripened cheeses. J. Dairy Sci. *85*, 478–486.

Pierce, E.C., Morin, M., Little, J.C., Liu, R.B., Tannous, J., Keller, N.P., Pogliano, K., Wolfe, B.E., Sanchez, L.M., and Dutton, R.J. (2021). Bacterial-fungal interactions revealed by genome-wide analysis of bacterial mutant fitness. Nat Microbiol *6*, 87–102.

Pozo, M.I., Lachance, M.-A., and Herrera, C.M. (2012). Nectar yeasts of two southern Spanish plants: the roles of immigration and physiological traits in community assembly. FEMS Microbiol. Ecol. *80*, 281–293.

Purko, M., Nelson, W.O., and Wood, W.A. (1951). The Associative Action Between Certain Yeasts and Bacterium Linens. J. Dairy Sci. *34*, 699–705.

Rao, C., Coyte, K.Z., Bainter, W., Geha, R.S., Martin, C.R., and Rakoff-Nahoum, S. (2021). Multi-kingdom ecological drivers of microbiota assembly in preterm infants. Nature.

Ratzke, C., and Gore, J. (2018). Modifying and reacting to the environmental pH can drive bacterial interactions. PLoS Biol. *16*, e2004248.

Ratzke, C., Barrere, J., and Gore, J. (2020). Strength of species interactions determines biodiversity and stability in microbial communities. Nat Ecol Evol *4*, 376–383.

Rea, M.C., Görges, S., Gelsomino, R., Brennan, N.M., Mounier, J., Vancanneyt, M., Scherer, S., Swings, J., and Cogan, T.M. (2007). Stability of the biodiversity of the surface consortia of Gubbeen, a red-smear cheese. J. Dairy Sci. *90*, 2200–2210.

Redford, A.J., and Fierer, N. (2009). Bacterial succession on the leaf surface: a novel system for studying successional dynamics. Microb. Ecol. *58*, 189–198.

Rogers, H.J., Perkins, H.R., and Ward, J.B. (1980). Cell walls of filamentous fungi. In Microbial Cell Walls and Membranes, (Springer, Dordrecht), pp. 469–477.

Shannon, P., Markiel, A., Ozier, O., Baliga, N.S., Wang, J.T., Ramage, D., Amin, N., Schwikowski, B., and Ideker, T. (2003). Cytoscape: a software environment for integrated models of biomolecular interaction networks. Genome Res. *13*, 2498–2504.

Shinozaki, M., Okubo, Y., Sasai, D., Nakayama, H., Murayama, S.Y., Ide, T., Wakayama, M., Hiruta, N., and Shibuya, K. (2011). Identification of Fusarium species in formalin-fixed and paraffin-embedded sections by in situ hybridization using peptide nucleic acid probes. J. Clin. Microbiol. *49*, 808–813.

Shkoporov, A.N., Clooney, A.G., Sutton, T.D.S., Ryan, F.J., Daly, K.M., Nolan, J.A., McDonnell, S.A., Khokhlova, E.V., Draper, L.A., Forde, A., et al. (2019). The Human Gut Virome Is Highly Diverse, Stable, and Individual Specific. Cell Host Microbe *26*, 527–541.e5.

Somerville, V., Lutz, S., Schmid, M., Frei, D., Moser, A., Irmler, S., Frey, J.E., and Ahrens, C.H. (2019). Long-read based de novo assembly of low-complexity metagenome samples results in finished genomes and reveals insights into strain diversity and an active phage system. BMC Microbiol. *19*, 143.

Spitaels, F., Wieme, A.D., Janssens, M., Aerts, M., Daniel, H.-M., Van Landschoot, A., De Vuyst, L., and Vandamme, P. (2014). The microbial diversity of traditional spontaneously fermented lambic beer. PLoS One *9*, e95384.

Teertstra, W.R., Lugones, L.G., and Wösten, H.A.B. (2004). In situ hybridisation in filamentous fungi using peptide nucleic acid probes. Fungal Genet. Biol. *41*, 1099–1103.

Testa, S., Berger, S., Piccardi, P., Oechslin, F., Resch, G., and Mitri, S. (2019). Spatial structure affects phage efficacy in infecting dual-strain biofilms of Pseudomonas aeruginosa. Commun Biol *2*, 405.

Thompson, L.R., Sanders, J.G., McDonald, D., Amir, A., Ladau, J., Locey, K.J., Prill, R.J., Tripathi, A., Gibbons, S.M., Ackermann, G., et al. (2017). A communal catalogue reveals Earth's multiscale microbial diversity. Nature *551*, 457–463.

Toju, H., Vannette, R.L., Gauthier, M.-P.L., Dhami, M.K., and Fukami, T. (2018). Priority effects can persist across floral generations in nectar microbial metacommunities. Oikos *127*, 345–352.

Tokita, F., and Hosono, A. (1972). Studies on the extracellular protease produced by *Brevibacterium linens*. Anim. Sci. J. *43*, 39–48.

Tredennick, A.T., Hooker, G., Ellner, S.P., and Adler, P.B. (2021). A practical guide to selecting models for exploration, inference, and prediction in ecology. Ecology *102*, e03336.

Tripathi, B.M., Stegen, J.C., Kim, M., Dong, K., Adams, J.M., and Lee, Y.K. (2018). Soil pH mediates the balance between stochastic and deterministic assembly of bacteria. ISME J. *12*, 1072–1083.

Tucker, C.M., and Fukami, T. (2014). Environmental variability counteracts priority effects to facilitate species coexistence: evidence from nectar microbes. Proc. Biol. Sci. *281*, 20132637.

Valm, A.M., Mark Welch, J.L., and Borisy, G.G. (2012). CLASI-FISH: principles of combinatorial labeling and spectral imaging. Syst. Appl. Microbiol. *35*, 496–502.

Vannier, N., Agler, M., and Hacquard, S. (2019). Microbiota-mediated disease resistance in plants. PLoS Pathog. *15*, e1007740.

Vass, M., Székely, A.J., Lindström, E.S., and Langenheder, S. (2020). Using null models to compare bacterial and microeukaryotic metacommunity assembly under shifting environmental conditions. Sci. Rep. *10*, 2455.

Venters, M., Carlson, R.P., Gedeon, T., and Heys, J.J. (2017). Effects of Spatial Localization on Microbial Consortia Growth. PLoS One *12*, e0168592.

Vylkova, S., Carman, A.J., Danhof, H.A., Collette, J.R., Zhou, H., and Lorenz, M.C. (2011). The fungal pathogen Candida albicans autoinduces hyphal morphogenesis by raising extracellular pH. MBio *2*, e00055–11.

Walsh, A.M., Crispie, F., Kilcawley, K., O'Sullivan, O., O'Sullivan, M.G., Claesson, M.J., and Cotter, P.D. (2016). Microbial Succession and Flavor Production in the Fermented Dairy Beverage Kefir. mSystems *1*.

Whiteside, M.D., Werner, G.D.A., Caldas, V.E.A., Van't Padje, A., Dupin, S.E., Elbers, B., Bakker, M., Wyatt, G.A.K., Klein, M., Hink, M.A., et al. (2019). Mycorrhizal Fungi Respond to Resource Inequality by Moving Phosphorus from Rich to Poor Patches across Networks. Curr. Biol. *29*, 2043–2050.e8.

Wolfe, B.E., Button, J.E., Santarelli, M., and Dutton, R.J. (2014). Cheese rind communities provide tractable systems for in situ and in vitro studies of microbial diversity. Cell *158*, 422–433.

Wood, D.E., Lu, J., and Langmead, B. (2019). Improved metagenomic analysis with Kraken 2. Genome Biol. *20*, 257.

Worrich, A., Stryhanyuk, H., Musat, N., König, S., Banitz, T., Centler, F., Frank, K., Thullner, M., Harms, H., Richnow, H.-H., et al. (2017). Mycelium-mediated transfer of water and nutrients stimulates bacterial activity in dry and oligotrophic environments. Nat. Commun. *8*, 15472.

Xu, Y., Vinas, M., Alsarrag, A., Su, L., Pfohl, K., Rohlfs, M., Schäfer, W., Chen, W., and Karlovsky, P. (2019). Bis-naphthopyrone pigments protect filamentous ascomycetes from a wide range of predators. Nat. Commun. *10*, 3579.

Xu, Y., Tandon, R., Ancheta, C., Arroyo, P., Gilbert, J.A., Stephens, B., and Kelley, S.T. (2021). Quantitative profiling of built environment bacterial and fungal communities reveals dynamic material dependent growth patterns and microbial interactions. Indoor Air *31*, 188–205.

Yilmaz, L.S., Parnerkar, S., and Noguera, D.R. (2011). mathFISH, a web tool that uses thermodynamics-based mathematical models for in silico evaluation of oligonucleotide probes for fluorescence in situ hybridization. Appl. Environ. Microbiol. *77*, 1118–1122.

Zeidner, G., Bielawski, J.P., Shmoish, M., Scanlan, D.J., Sabehi, G., and Béjà, O. (2005). Potential photosynthesis gene recombination between Prochlorococcus and Synechococcus via viral intermediates. Environ. Microbiol. *7*, 1505–1513.

Zhang, Y., Kastman, E.K., Guasto, J.S., and Wolfe, B.E. (2018). Fungal networks shape dynamics of bacterial dispersal and community assembly in cheese rind microbiomes. Nat. Commun. *9*, 336.

(2010). R: A Language and Environment for Statistical Computing : Reference Index (R Foundation for Statistical Computing).